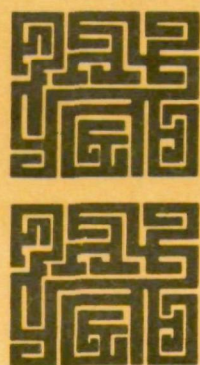
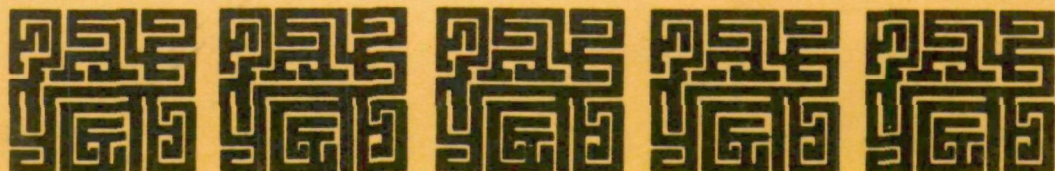
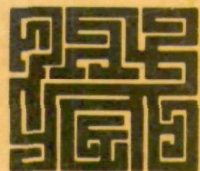
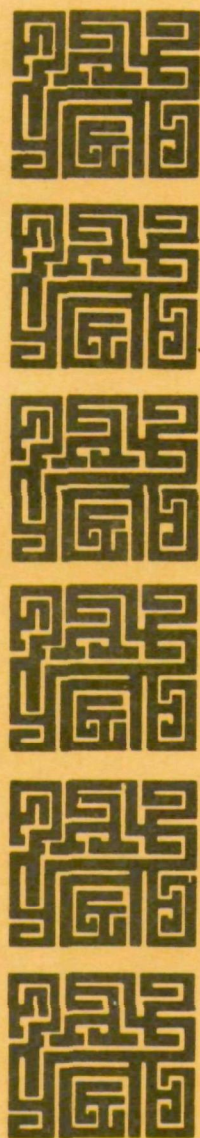


**EPA 340/1-76-005  
JUNE 1976**

**Stationary Source Enforcement Series**

**APPLICATION OF  
REMOTE TECHNIQUES IN  
STATIONARY SOURCE  
AIR EMISSION MONITORING**



**U.S. ENVIRONMENTAL PROTECTION AGENCY  
Office of Enforcement  
Office of General Enforcement  
Washington, D. C. 20460**

# **APPLICATION OF REMOTE TECHNIQUES IN STATIONARY SOURCE AIR EMISSION MONITORING**

by

**C. B. Ludwig and M. Griggs  
SCIENCE APPLICATIONS, INC.  
La Jolla, California 92037**

**Contract No. EPA 68-03-2137**

**Project Officers: Dr. F. J. Biros  
Office of Enforcement**

**Dr. S. H. Melfi  
Environmental Monitoring and  
Support Laboratory/Las Vegas**

**Prepared for:**

**U. S. Environmental Protection Agency  
Washington, D. C. 20460**

**June 1976**



## **EPA REVIEW NOTICE**

**This report has been reviewed by the Environmental Protection Agency and approved for publication with some modification. Approval does not signify that the contents necessarily reflect the views and policies of the Agency, nor does mention of trade names or commercial products constitute endorsement or recommendation for use.**

**The Stationary Source Enforcement series of reports is issued by the Office of Enforcement, Environmental Protection Agency, to assist the Regional Offices in activities related to enforcement of implementation plans, new source emission standards, and hazardous emission standards to be developed under the Clean Air Act. Copies of Stationary Source Enforcement reports are available—as supplies permit—from Air Pollution Technical Information Center, Environmental Protection Agency, Research Triangle Park, North Carolina 27711, or may be obtained, for a nominal cost, from the National Technical Information Service, 5285 Port Royal Road, Springfield, Virginia 22161.**

## FOREWORD

This report documents the work performed under Contract No. EPA 68-03-2137 between September 1974 and March 1975, and updated during April/May 1976. The work was sponsored by the Environmental Protection Agency, Office of Enforcement. The objective of this program was to assess the application of remote techniques to monitor stationary source air emissions.

---

The authors wish to thank the many researchers who have provided valuable information about on-going programs, practical experience in the field and have given freely their opinions about the role of remote monitoring techniques. The authors are also indebted to their co-workers at Science Applications, Inc., W. Malkmus, J. Myer, E. R. Bartle, L. Acton and G. Hall for contributions in the different topics, and to J. Wang for many calculations. In particular we wish to thank K. Arnone for her dedication in preparing the manuscript.



## CONTENTS

		<u>Page</u>
1	EXECUTIVE SUMMARY	1
1.1	Background and Scope	1
1.2	Performance Specifications for Remote Monitoring	3
1.3	Present Development and Analysis of Remote Monitoring Techniques	4
1.4	Advantages and Disadvantages	7
1.5	Major Conclusion and Recommendations	9
2	INTRODUCTION	11
3	OVERVIEW OF THE REQUIREMENTS FOR THE PER- FORMANCE SPECIFICATIONS OF REMOTE MONITORS	15
3.1	Standards of Performance for New Stationary Sources	16
3.2	National Emission Standards for Hazardous Air Pollutants	25
3.3	National Ambient Air Quality Standards	26
3.4	Outline of Performance and Test Procedures for the Use of Remote Monitors	34
4	PRESENT DEVELOPMENT OF REMOTE MONITORING TECHNIQUES	39
4.1	Overview	39
4.2	Theory	43
4.2.1	CW Infrared System	43
4.2.2	Pulsed Laser Systems	48
4.2.3	Perimeter Monitoring	53
4.3	Review of Active Systems	54
4.3.1	Differential Absorption	54
4.3.2	Raman Scattering	57
4.3.3	Resonance Raman	61

4.3.4	Fluorescence	63
4.3.5	Lidar	64
4.3.6	Intercomparison of Measurements of Gases	68
4.3.7	Stack Effluent Velocity Measurements	70
4.4	Review of Passive Systems	71
4.4.1	Passive Opacity Techniques	72
4.4.2	Matched-Filter Spectrometer	74
4.4.3	Gas Filter Correlation	77
4.4.4	Medium Resolution Dispersive Spectrometer System	81
4.4.5	Interferometer-Spectrometer	83
4.4.6	Filter Wheel Sensor	89
4.4.7	Laser Heterodyne Technique	89
4.4.8	Dispersive Hadamard Transform Spectrometer	95
4.4.9	Passive Vidicon Instrumentation	97
4.5	Area Surveys	97
4.6	On-Going and Planned Research Programs	101
5	PRACTICAL CONSIDERATIONS	105
5.1	Overview	105
5.2	Eye Safety Hazards from Laser Systems	106
5.2.1	The Maximum Permissible Exposure and Minimum Safety Range	107
5.2.2	Required Modifications	108
5.2.3	Final System Parameters	109
5.3	Error Analysis of Active Systems	111
5.3.1	DAS Systems	111
5.3.2	Raman Systems	114
5.3.3	Lidar Systems	116
5.3.4	Intercomparison of Laser Techniques	118
5.4	Error Analysis of Passive Infrared Systems	126
5.4.1	Source Strength	126
5.4.2	The Measurements of Signal Differences	129
5.4.3	Perimeter Monitoring Data Analysis (Infrared)	134

6	ADVANTAGES AND DISADVANTAGES OF REMOTE MONITORING TECHNIQUES	135
6.1	Overview	135
6.2	Cost Effectiveness	136
6.2.1	Opacity	137
6.2.2	Gas Concentration	138
6.3	Measurements of Mass Emission Rates	139
6.4	Unannounced and Non-Interfering Monitoring	139
6.5	Survey of Wide Geographical Areas	140
6.6	Rapid Response in Pollution Episodes	141
6.7	Limitation Under Certain Atmospheric Conditions	143
6.8	Increased Requirements in Calibration	143
6.9	Safety Hazard	143
7	CONCLUSIONS AND RECOMMENDATIONS	145
7.1	General Conclusions	145
7.2	Recommendations	149
8	REFERENCES	165



# 1

## EXECUTIVE SUMMARY

### 1.1 BACKGROUND AND SCOPE

The Clean Air Act of 1967 authorized the development of measurement methods to meet the requirements of reducing air pollution to levels considered safe for human health and welfare. During the last decade, many of the required techniques for measuring stack emissions and ambient air quality were developed by Federal agencies and private industry. The techniques were based on many methodologies, such as manual, automatic, extractive, point or integrated sampling, and remote (visual observations). The purpose of the present study is to evaluate the status of remote monitoring instruments (i. e., not visual observations) and to provide a working document for the different regional offices and laboratories of EPA and state agencies. The intent is that this document may serve as a guide for the application of remote monitoring techniques in the following areas:

- Surveillance and compliance monitoring of smoke-stacks and extended sources;
- Monitoring to support EPA's research studies for the evaluation of control equipment and development of performance standards;
- Surveys of emissions for validation of dispersion models;
- Surveys to determine the representativeness of ambient air point measurements and to assist in developing optimum contact monitoring networks; and
- Quick response in air pollution episodes.

In the present study remote monitoring is defined as sensing, by an electro-optical technique, specific chemical and/or physical parameters of the environment where the monitoring instrument and the parameter under investigation are separated by a distance. At present, EPA, NASA, NOAA, DOT and other federal agencies are sponsoring the development of instruments and/or techniques to remotely monitor the environment, utilizing active or passive systems. Active systems consist of two basic units: a transmitter and a receiver, while passive systems consist only of a receiver. The transmitter in an active system emits a beam of energy, which interacts with the plume/atmosphere by scattering, absorption and/or stimulated emission, which is subsequently observed by the receiver. In the passive system, the receiver merely observes the radiation from the plume/atmosphere, which may be emitted thermal radiation, or scattered solar radiation.

Several modes in the application of remote monitoring were addressed (see Figure 1-1): direct observation of the plume by passive or active monitors, perimeter monitoring by uplooking from van-based platforms

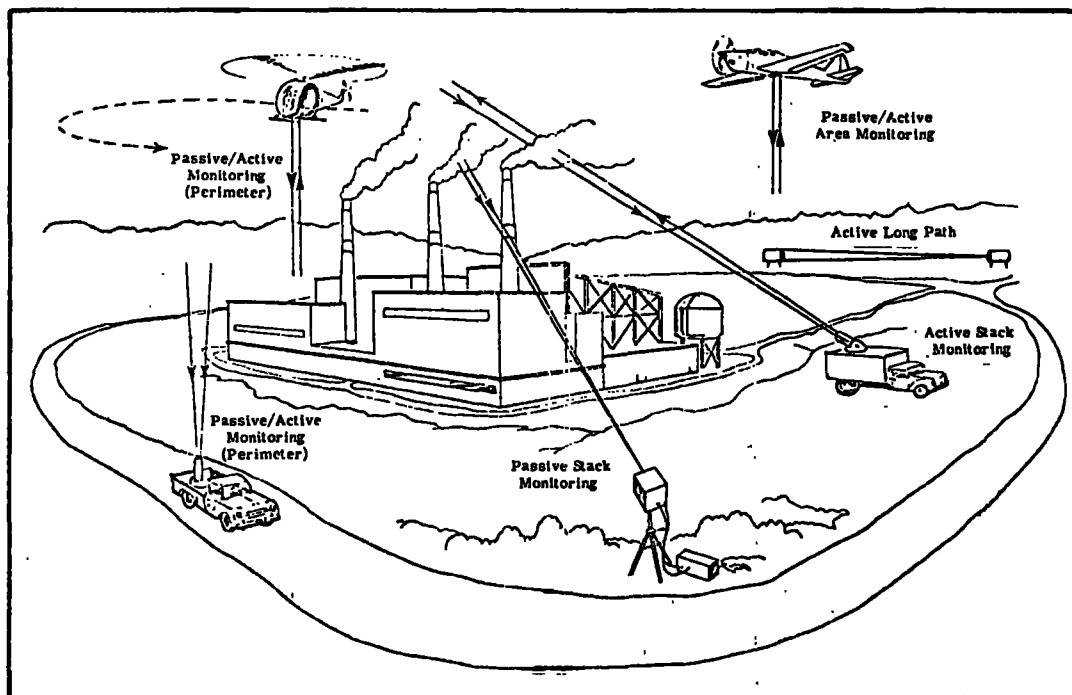


Figure 1-1. Modes of active and passive remote techniques in monitoring emissions from stationary sources: Direct observation of stack plume, perimeter monitoring (ground and airborne) and area monitoring.

or down-looking from airborne platforms, and horizontally by active long-path systems, although the latter application is limited to cases where the horizontal long-path is representative of a given situation (Section 4.5). In addition, area monitoring using an aircraft, can be used in surveillance. These surveys of wider geographical areas can also assist in the determination of environmental quality degradation, plant site selection, the design of contact monitoring networks, and the tracking of plumes to study atmospheric dispersion, diffusion and fate of pollutants.

## 1.2 PERFORMANCE SPECIFICATIONS FOR REMOTE MONITORING

The introduction of remote monitors as tools in EPA's enforcement programs requires the adaptation of performance specifications and test procedures for these instruments. We have reviewed the codified reference methods, test methods, measurement principles and performance specifications as listed in the appendices of Parts 50, 51, 53, 60 and 61 of Title 40 of the Code of Federal Regulations, as to their adaptability to remote monitors (Section 3.0). We concluded that the performance specifications as presently given in the Appendices A and B of Part 60 for the continuous monitors can be adapted to the remote monitors, but that the calibration test procedures require major revisions. This is so because the interferences of the intervening atmosphere and of the sky background are significant, and provisions during calibration testing must be made to simulate different meteorological conditions. This simulation is judged to be important since the different remote monitors react differently to changes in meteorological conditions. Some of the provisions could probably be patterned after those contained in Reference Method 9 for the visual determinations of the opacity of emissions from stationary sources.



### 1.3 PRESENT DEVELOPMENT AND ANALYSIS OF REMOTE MONITORING TECHNIQUES

A review of the recent development of remote monitors sponsored by Federal and other agencies, as well as by private industry, both in the U. S. A. and other countries, revealed that several active and passive techniques were worthy of further analysis. The active techniques include the pulsed laser systems that involve differential absorption, Raman, resonance Raman, fluorescence, and lidar, as well as the continuous wave (CW) systems that utilize laser, dispersive and non-dispersive components (Section 4.3). The passive techniques include dispersive and non-dispersive correlation systems, spectrometers, interferometer-spectrometers, radiometers, heterodyne radiometers, photography and vidicons (Section 4.4). Overviews of these techniques and their main characteristics are given in Tables 1-1 and 1-2, together with their present status. It can be seen that for all the remote techniques judged to be useful for monitoring stack emissions, only two actual systems are commercially available and even they have limited applications.

In general, we conclude that the active systems have been demonstrated to be more sensitive than the passive systems. In addition, the passive systems are more influenced by interfering parameters, such as background radiation. On the other hand, passive systems are less expensive than the active systems and can be made into cost-effective tools for compliance monitoring, as long as the measured deviation from the standard in pollutant concentration is larger than the instrument errors.

The air pollutants (previously identified as important to monitor) that are judged to be amenable to remote monitoring in the near-term include particles/opacity,  $\text{SO}_2$ ,  $\text{NO}_2$ ,  $\text{CO}$ , light hydrocarbons,  $\text{HCl}$ ,  $\text{HF}$ ,  $\text{NH}_3$ ,  $\text{NO}_x$ ,  $\text{H}_2\text{S}$ ,  $\text{HNO}_3$ ,  $\text{O}_3$  and vinyl chloride; and in the long-term include heavy hydrocarbons, oxides of sulfur, certain specific trace elements (asbestos, beryllium, mercury), and chlorinated hydrocarbons. In addition, many newly identified pollutants of interest can probably be monitored by remote monitors, after their spectral characteristics are identified.

TABLE 1-1. Overview of Active Systems Under Development

Technique/ Instrument	Spectral Region	Species/ Parameter	Mode	Development Status	Remarks
Differential Absorption	Vis/UV	SO <sub>2</sub> , NO <sub>2</sub> , O <sub>3</sub>	Stack/Area	Prototype Field Tested	Ground-based - Present instrumentation as used not eye-safe (Section 4.3.1)
		SO <sub>2</sub> , NO <sub>2</sub> , O <sub>3</sub>	Perimeter/ Area	Prototype Field Tested	Has been done for SO <sub>2</sub> (Section 4.3.1)
	IR	Many Gases	Stack	Prototype Under Development	Development is primarily for ambient air (see Table 4-15)
			Perimeter/ Area	Under Development for Aircraft Application	See Table 4-15, at present for ozone
Lidar	Vis	Opacity	Stack	Prototype Field Tested	Not eye safe yet, (Section 4.3.5) eye- safe system being developed
		Particles	Area	Prototype on Air- craft Field Tested	Gives 3-dimensional mapping of relative concentrations (Section 4.5)
Laser Doppler Velocimeter	IR	Velocity	Stack/ Perimeter	Advanced Prototype Field Tested	Necessary for some emission standards (Section 4.3.7 and Table 3-1)
		Mass Flow	Stack	Demonstrated in Field Tests	Relates opacity and mass concentration (Section 4.3.7)
Long-Path	Vis/UV /IR	Many Gases	Area	Several Techniques Field Tested, Some Prototypes Developed; COSPEC Commer- cially Available	Using remote transmitter or retro- reflector; can be laser, dispersive or non-dispersive systems (Table 3-16); useful mainly for ambient air monitoring
Raman	Vis/UV	SO <sub>2</sub>	Stack	Field Tests Not Encouraging	Limited in range, especially during day (Sections 4.3.2 and 5.3.2)
		Many Gases	Stack/ Area	Theoretical	Usefulness limited (Section 4.3.2 and 5.3.2)
Resonance Raman	Vis/UV	Many Gases	Stack/ Area	Laboratory Study	Needs to be demonstrated in field; possible interference due to fluorescence by gases and other species (Section 4.3.3)
Fluorescence	Vis/UV	Many Gases	Stack/ Area	Laboratory Study	Looks doubtful in terms of sensitivity and specificity; (Section 4.3.4)
Fabry-Perot Raman	Vis/UV	Some Gases	Stack/ Area	Laboratory Study	Provides increased sensitivity over vibrational Raman; still limited in range, especially during day (Section 4.3.2)

TABLE 1-2. Overview of Passive Systems Under Development

Technique/ Instrument	Spectral Region	Species/ Parameter	Mode	Development Status	Remarks
Matched Filter Correlation	UV/Vis	SO <sub>2</sub> , NO <sub>2</sub>	Stack/ Perimeter	COSPEC Commercially Available, Field Tested, Not Encouraging for Stacks; Main Emphasis on Perimeter Monitoring	Quantitative interpretation difficult due to varying aerosols (Section 4.4.2 and 4.5)
Gas Filter Correlation	IR	SO <sub>2</sub>	Stack	JRB Sensor Commercially Available, Being Field Tested	Limited in concentration and tempera- ture range (Section 4.4.3), but tem- perature effect reduced
		CO	Perimeter	Prototype Field Tested	No quantitative data reported as yet (Section 4.5)
		SO <sub>2</sub>	Perimeter	Prototype Under Development	See Table 4-14
Photography	Vis	Opacity	Stack	Being Field Tested on Ground and From Aircraft	Needs further development for quantita- tive analysis; nighttime observations feasible with image intensifier (Section 4.4.1)
Vidicon	UV	SO <sub>2</sub>	Stack	Prototype Field Tested	Quantitative interpretation difficult due to varying aerosols; has potential as a velocimeter (Section 4.4.9)
	IR	SO <sub>2</sub>	Stack	Prototype Field Tested	Independent knowledge of plume tempera- ture required for quantitative analysis; has potential as a velocimeter (Section 4.4.9)
Heterodyne Radiometer	IR	Many Gases	Stack/ Perimeter/ Area	Laboratory Study and Aircraft Based Proto- type Under Develop- ment	Achieves high specificity; has yet to be demonstrated in field (Section 4.4.7)
Dispersive Spectrometer	IR	Many Gases	Stack	Several Techniques Field Tested, Some Prototypes Developed	Includes scanning spectrometer and in- terferometer-spectrometer; requires high spectral resolution for specificity and requires knowledge of plume tem- perature (Section 4.4.4 and 4.4.5)



## **1.4 ADVANTAGES AND DISADVANTAGES**

Based upon the review of the remote monitoring techniques, we have identified the following advantages which apply in varying degrees to the different enforcement and research and development programs.

- **Cost Effectiveness**

Although the initial capital costs are higher for remote instruments than for point samplers, the operational costs are less because of their mobility allowing rapid coverage of more sources and areas. Our estimate is that for some remote monitoring applications the operational costs are less by as much as about a factor of 10.

Remote techniques provide also a cost-effective method to monitor and survey wide geographical areas for the purpose of assisting in the determination of environmental quality degradation, plant site selection, design of contact monitoring networks, and in tracking plumes.

- **Measurements of Mass Emission Rates**

The signals of the laser Doppler velocimeter (LDV) are not only related to the particle velocity, but also to the opacity of the plume. When the relationship between the opacity and mass loading for each type of source has been established, the LDV will provide the particulate mass emission rate from a source.

- **Unannounced and Non-Interfering Monitoring**

The remote technique provides a most effective tool for compliance monitoring, even at night, without requiring entry into the facility premises. In addition, remote monitoring does not interfere with the normal plant operations.

- **Rapid Response**

In cases of air pollution episodes, the highly mobile and flexible remote monitors can be used to assess the extent, trend, and required response to counteractions more rapidly than the stationary in-situ sensors.

The following disadvantages have been identified:

- **Possible High Initial Capital Costs**

At the present time, the purchase price of all remote instruments are more expensive than the extractive or in-situ devices. The active systems are more so than the passive systems. However, as more and more instruments are built, one can assume that the purchase price will come down.

- **Limited Applications Under Certain Conditions**

Adverse weather conditions such as fog, heavy rain or extremely high particulate content in the atmosphere can affect the measurement capability of the remote techniques.

- **Calibration Procedures More Complicated**

Indications are that the remote techniques will be more difficult to calibrate than the extractive or in-situ devices because of the atmospheric influence. It is anticipated that—similar to the calibrated smokestack used in smoke schools—a test range with a remote stack source must be provided in which several atmospheric conditions can be reliably simulated.

- **Possible Eye Safety Hazard**

Caution must be exercised in using lasers so that they comply with the Federal Regulations. Thus, some of the laser applications which demand an increase in emitted power in order to meet the sensitivity and range requirements, had to be eliminated from the list of useful systems.

## 1.5 MAJOR CONCLUSION AND RECOMMENDATIONS

Based upon our review and analysis of the remote techniques being developed, our major conclusion is that remote monitoring can play a significant role in EPA's enforcement and R&D activities. However, our interaction with the private sector has led us to the conclusion that adequate incentives do not exist for the instrument companies to develop many of the promising remote monitors any further, since the costs to achieve a production field instrument are too high and the potential market is too small. Thus, it is necessary for EPA to provide increased funding for the development of field instruments for use by the regional offices and state agencies.

Our analysis shows that not all techniques/instruments presently developed are equally well suited for monitoring of smokestack emissions. For direct observation of hot plumes and indirect observation of complex sources through perimeter monitoring, the less expensive passive systems will suffice, while the direct observation of cool plumes will require the application of the more expensive active laser systems. The laser systems that are most promising for near-term operational use are differential absorption, lidar and laser Doppler velocimeter. The most promising passive systems are correlation instruments, vidicons and aircraft photographic techniques. For area surveys, both active and passive systems (ground-based and airborne) have application.

Based upon the above conclusion, we make the following recommendations:

- Increase the support for the development of remote techniques. In particular, the following tasks are judged to be of about equal priority:
  - make the most promising active systems (differential absorption, Lidar and laser Doppler velocimeter) operational for van-based and airborne applications for the gaseous pollutants  $\text{SO}_2$  and  $\text{NO}_2$ , and particulate pollutants,
  - make the most promising passive systems (correlation instruments, and vidicons) operational for smokestack monitoring for the gaseous pollutants  $\text{SO}_2$  and  $\text{NO}_2$ ,
  - continue to develop the aircraft photographic technique for opacity measurements,
  - extend the active differential absorption techniques to other species, including hazardous air pollutants utilizing the UV and IR spectra,
  - continue the development of heterodyne radiometry,
  - extend the passive correlation instruments to other species,
  - continue passive perimeter monitoring;



- Continue—with somewhat less priority than the above—the development of techniques whose practical applications have yet to be demonstrated, in particular, resonance Raman and fluorescence;
- Consider the establishment of one or more test ranges, in which remote monitors can be calibrated;
- Adapt existing performance specifications of continuous monitors to remote monitoring application and initiate the formulation of additional test procedures required in the application of remote monitors.

# 2

## INTRODUCTION

Presently, EPA, NASA, NOAA and other federal agencies are sponsoring the development of remote monitoring instruments for sensing air quality. Remote monitoring, for the purpose of this document, is defined as sensing a specific chemical and/or physical parameter of the environment where the monitoring instrument and the parameter under investigation are separated by a distance. Some of these instruments have been developed to the point where they are presently useful to EPA in its monitoring program; other instruments have not been developed to this stage.

The purpose of the present study is to evaluate the status of remote monitoring techniques and to provide a working document for the different offices and laboratories of EPA and state agencies. It is the intent that this document may serve as a guide for the application of remote monitoring techniques in (1) surveillance and compliance monitoring of smokestacks and extended sources; (2) monitoring to support EPA's research studies for the evaluation of control equipment and development of performance standards; (3) surveys of emissions for input to dispersion models and their validation; (4) surveys to determine the representativeness of ambient air point measurements and to assist in developing optimum contact monitoring networks; and (5) quick response in air pollution episodes.

The Clean Air Act (42 U. S. C. 1857) of 1963 encouraged state, regional and local regulatory control programs by providing matching funds for research and technical assistance, and at the same time, gave authority to the Federal Government to intervene in enforcing the abatement of air pollution in interstate problem areas. The specific abatement procedures included--a) conference with the cognizant official agencies, b) public hearing, and c) court action. These procedures could take up several years, involving complex procedures to prove non-compliance.

The Clean Air Act was amended in 1967 to establish air quality control regions for the purpose of setting ambient air quality standards, based upon criteria that reflect the latest scientific and medical knowledge of effects of air contaminants on health and welfare. It also called for the development and issuance of information on recommended pollution control techniques, and the initiation of joint government-industry research to develop and demonstrate improved emission control technology to the degree required to prevent and abate air pollution. It is clear that monitoring devices had to be available for control assist.

The Clean Air Act as amended in 1970 extended the geographical coverage of the Federal program for the prevention, control and abatement of air pollution from both stationary and moving sources. In particular, emission regulations for environmental control were established. It was also established that research and development for measurement techniques of the following air pollutants should be conducted as listed in Table 2-1.

TABLE 2-1. Pollutants to be Monitored (Ellison 1974)

1. Oxides of sulfur (SO <sub>2</sub> , SO <sub>3</sub> , H <sub>2</sub> SO <sub>4</sub> )	19. Hydrogen fluoride
2. Oxides of nitrogen (NO <sub>x</sub> , NO, NO <sub>2</sub> , HNO <sub>3</sub> )	20. Hydrogen sulfide
3. Particulate matter (size distribution chemical composition)	21. Mercaptans
4. Asbestos	22. Ammonia and amines
5. Mercury	23. Organic acids
6. Beryllium	24. Aldehydes
7. Carbon monoxide	25. Odor
8. Nonmethane hydrocarbons	26. Photochemical oxidants
9. Certain specific hydrocarbons	27. Copper
10. Polychlorinated biphenyls	28. Zinc
11. Polynuclear organic matter	29. Boron
12. Reactive hydrocarbons	30. Tin
13. Hydrogen chloride	31. Lithium
14. Manganese	32. Chromium
15. Selenium	33. Vanadium
16. Arsenic	34. Cadmium
17. Phosphoric acid	35. Lead
18. Chlorine	36. Aeroallergens

Basically, two regulatory parameters for each of these pollutants need be established: an emission standard and a measurement method. EPA is proceeding along these lines and standards and measurement methods have been established for some of the above pollutants. A progress report about the status of these developments was written by Ellison (1974). In the same report, a brief statement about the remote measurement of air pollutants was made. Ellison states that "...the potential effectiveness of air pollution measurement and monitoring by means of these techniques justifies a reasonable effort to investigate their usefulness."

The earliest method of remote sensing of smokestack plumes was by way of visual observations, comparing the blackness of the plume with a chart of graduated shades of blackness (Ringelmann method). This method was extended to non-black plumes by training observers to determine the plume opacity. The opacity method was adopted by EPA and was promulgated as a reference method. The present study is not concerned with visual observations of plumes, however.

The present study is concerned with remote sensing and monitoring by means of instruments. One of the earliest instruments for monitoring the atmosphere remotely was a modified searchlight as pioneered by Hulburt (1946) and refined by Elterman (1966). By observing the back-scattered signal, the concentration distribution of the particles could be determined up to altitudes as high as 35 km. This system was double-ended and not readily applicable to the monitoring of smokestack plumes. However, with the advent of laser systems that could produce pulses of short duration, the single-ended probing of plumes became feasible. The method of using lidar (light detection and ranging) to determine plume opacity was first developed at SRI (Evans 1967). About the same time, the utilization of the movement of the particles for the measurement of the velocity was realized (Foreman et al. 1965) and the development of the LDV (Laser Doppler Velocimeter) was begun.

Efforts to measure gaseous constituents in the plume were initially restricted to passive methods. The thermal emission of hot plumes provides a distinct source that can be observed by infrared sensors against the cold sky background (Low and Clancy 1967). The major problem with the passive method is the fact that the emission is a function of both the gaseous concentration as well as the plume temperature. The difficulty in remotely determining the plume temperature has prevented the early application of the passive methods, and only now it appears that through the application of various ratioing techniques, eliminating the temperature dependency, has it become feasible to measure gaseous pollutants.

The application of active systems to the measurement of gaseous species in plumes was slow in developing. Although the theoretical feasibility of utilizing scattering methods (Raman, resonant Raman and fluorescence) was recognized rather early, the experimental demonstration was much more difficult than anticipated. The reasons for this are the small Raman cross sections and/or the interference effects for the resonant scattering methods. Many attempts have been made to overcome the difficulties. The avenue of using more powerful lasers to overcome the weak Raman signals has been restricted by stringent eye safety rules, and the elimination of the interference effects (broad-band fluorescence by the aerosols and some commonly occurring gaseous pollutants such as nitrogen dioxide and hydrocarbons) has not been achieved as yet.

In general, molecular absorption techniques do not have these limitations; DAS (Differential Absorption by Scattering) systems are being widely developed for several species in the visible and infrared. The absorption cross sections are large, and the narrow band width of laser lines minimizes the interference effects.

A discussion of the theory and state-of-the-art of the above-mentioned active and passive methods is presented in this report, together with an overview of the New Source Performance Standards (NSPS), the National Emission Standards for Hazardous Air Pollutants (NESHAPS) and the National Ambient Air Quality Standards (NAAQS).

# 3

## OVERVIEW OF THE REQUIREMENTS FOR THE PERFORMANCE SPECIFICATIONS OF REMOTE MONITORS

In this section, we review the basis for the performance specification and operating parameter for the use of remote monitors. For the application to stack compliance monitoring, the specifications can be based upon the ones proposed or promulgated by EPA for the continuous emission monitors of stationary sources. For the application of monitoring the ambient air quality, the specifications must be consistent with the ones promulgated for the ambient air monitors.

In December 1971, the standards of performance for new stationary sources were codified (40 CFR Part 60) for five industries together with several reference test methods to be used during the performance tests to demonstrate compliance with the standards. The reference methods may be altered if it can be demonstrated that the alteration does not affect the results significantly. These methods fall into the category of alternative methods. No equivalent methods have yet been specified. The reference methods are for the in-stack measurements of sample and velocity traverses, gas velocity and volumetric flow rate, CO<sub>2</sub> and excess air, moisture, particles, SO<sub>2</sub>, NO<sub>x</sub>, sulfuric acid mist and for the remote visual observations of the opacity of emissions. Since that time, standards of performance for nineteen more industries have been promulgated, together with additional reference methods that apply to the in-stack measurements of CO, H<sub>2</sub>S, SO<sub>2</sub>, and total fluorides.

EPA has promulgated in 1975 provisions for the continuous compliance monitoring of some gases and opacity, together with performance specifications and specification test procedures of instruments that monitor those gases.

National Ambient Air Quality Standards were promulgated in 1971 (40 CFR Part 50). Subsequently, the requirements for the preparation, adoption and submittal of implementation plans, including the requirements for emission monitoring of stationary sources (40 CFR Part 51) and the approval and promulgation of the implementation plans (40 CFR Part 52) were codified.

In 1973, national emission standards for some hazardous air pollutants were promulgated, together with several reference methods, for the determination of emissions from stationary sources (40 CFR 61). In February 1975, rules and regulations for ambient air monitoring reference methods and equivalent methods were promulgated (40 CFR Part 53).

These rules establish the concept of measurement principle and calibration procedure for continuous/automated analyzers that measure certain air pollutants. Except for the visual observations of emissions, no test methods for remote sensing techniques have yet been proposed for either the emissions from stationary sources or the ambient air quality.

In the following subsections, we give first an overview of the new source performance standards, including the performance specifications for continuous monitors (Section 3.1), the emission standards for hazardous air pollutants (Section 3.2), and the national primary and secondary ambient air quality standards including the test procedures that establish reference and equivalent methods (Section 3.3). Finally in Section 3.4 we outline a set of general requirements for the use of remote monitors in stack compliance monitoring.

### 3.1 STANDARDS OF PERFORMANCE FOR NEW STATIONARY SOURCES

In order to assess the sensitivity remote monitoring instruments must have, we have listed the new source performance standards of 24 industrial plants in Table 3-1. It can be seen that the performance standards for the opacity can be lower than 10 percent, and for the concentrations of SO<sub>2</sub> and CO lower than 650 ppm and 550 ppm by volume, respectively. All other standards are given in pounds per fuel or in pounds per product, a measure which requires additional information

**TABLE 3-1. New Source Performance Standards**

Plant	Status*	Ref.	Standards
(1) Fossil fueled steam generators	Pm	40CFR60 (Subpart D)	Opacity: 20%, 40% max. for 2 min. in any hour SO <sub>2</sub> : 0.8 lb/10 <sup>6</sup> BTU (liquid fuel) 1.2 lb/10 <sup>6</sup> BTU (solid fuel) NO <sub>x</sub> : 0.2 lb/10 <sup>6</sup> BTU (gas fuel) 0.3 lb/10 <sup>6</sup> BTU (liquid fuel) 0.7 lb/10 <sup>6</sup> BTU (solid fuel)
(2) Incinerators	Pm	40CFR60 (Subpart E)	Particle: 0.18 g/m <sup>3</sup> (corr. to 12% CO <sub>2</sub> )
(3) Portland Cement Plants	Pm	40CFR60 (Subpart F)	Opacity: 20% (kiln) 10% opacity
(4) Nitric Acid Plants	Pm	40CFR60 (Subpart G)	NO <sub>x</sub> : 3 lb/ton acid produced 10% opacity
(5) Sulfuric Acid Plants	Pm	40CFR60 (Subpart H)	Acid Mist: 0.15 lb/ton acid product 10% opacity
(6) Asphalt Concrete Plants	Pm	40CFR60 (Subpart I)	Opacity: ≤ 20%
(7) Petroleum Refineries	Pm	40CFR60 (Subpart J)	Opacity: ≤ 30%, except for 3 min. in any hour CO: ≤ 500 ppm H <sub>2</sub> S: ≤ 230 mg/dscm in fuel gas SO <sub>2</sub> : alternate method equivalent to H <sub>2</sub> S standard
(8) Storage Vessels for Petroleum Liquids	Pm	40CFR60 (Subpart K)	Hydrocarbons: If p > 78 torr, vapor recovery system required
(9) Secondary Lead Smelters	Pm	40CFR60 (Subpart L)	Opacity: ≤ 20% (blast furnace) ≤ 10% (pot furnace)
(10) Secondary Brass and Bronze Ingot Production Plant	Pm	40CFR60 (Subpart M)	Opacity: ≤ 20% (reveratory furnace) ≤ 10% (blast or electric furnace) (excluding uncombined water)
(11) Iron and Steel Plant	Pm	40CFR60 (Subpart N)	Particles: ≤ 50 mg/dscm
(12) Sewage Treatment Plant	Pm	40CFR60 (Subpart O)	Opacity: ≤ 20% (except for uncombined water)
(13) Primary Copper Smelters	Pm	41 FR 2338 (Subpart P)	Opacity: ≤ 20% SO <sub>2</sub> : ≤ 650 ppm v
(14) Primary Zinc Smelters	Pm	41 FR 2340 (Subpart Q)	Opacity: ≤ 20% SO <sub>2</sub> : ≤ 650 ppm v
(15) Primary Lead Smelters	Pm	41 FR 2340 (Subpart R)	Opacity: ≤ 20% SO <sub>2</sub> : ≤ 650 ppm v



Plant	Status*	Ref.	Standards
(16) Steel Plant: Electric Arc Furnaces	Pm	40 FR 43853 (Subpart AA)	Opacity: $\leq 3\%$ (exit from a control device) $\leq 0\%$ (exit from the shop) $\leq 20\%$ (exit from the shop during charging a furnace) $\leq 40\%$ (exit from the shop during tapping a furnace) $\leq 10\%$ (from dust handling equipment)
(17) Ferro-alloy Production Facilities	Pm	40 FR 18501 (Subpart Z)	Opacity: $\leq 0\%$ (except for $0\%$ from control system) $\leq 0\%$ from control system (after tapping at least 60% of each tapping period) $\leq 10\%$ (from dust handling equipment) CO: $\leq 200,000$ ppm v
(18) Primary Aluminum Reduction Plants	Pm	41 FR 3828 (Subpart S)	Total fluorides: $\leq 1$ kg/ton of aluminum produced Opacity: $\leq 10\%$ (from pot room) $\leq 20\%$ (from anode bake plant)
(19) Coal Preparation Plants	Pm	41 FR 2234 (Subpart Y)	Opacity: $\leq 20\%$ from any thermal dryer gases $\leq 10\%$ from any pneumatic coal cleaning equipment gases $\leq 20\%$ from any coal processing and conveying equipment, coal storage systems, or coal transfer and loading systems gases.
(20) Phosphate Fertilizer Industry Wet Process Phosphoric Acid Plants	Pm	40 FR 33154 (Subpart T)	Total Fluorides: $\leq 10$ g/ton of equivalent $P_2O_5$ feed
(21) Phosphate Fertilizer Industry: Super- phosphoric Acid Plants	Pm	40 FR 33155 (Subpart U)	Total Fluorides: $\leq 5$ g/ton
(22) Phosphate Fertilizer Industry Diammonium Phosphate Plants	Pm	40 FR 33155 (Subpart V)	Total Fluorides: $\leq 30$ g/ton
(23) Phosphate Fertilizer Industry Triple Super- phosphate Plants	Pm	40 FR 33156 (Subpart W)	Total Fluorides: $\leq 100$ g/ton
(24) Phosphate Fertilizer Industry: Granular Triple Superphosphate Storage Facilities	Pm	40 FR 33156 (Subpart X)	Total Fluorides: $\leq 0.25$ g/hr/ton of equivalent $P_2O_5$ stored

\* Pm means promulgated and Pp means proposed.

to determine compliance. We find that the units "pounds per product" or "pounds per fuel" pose problems in relating directly the quantities obtained by remote sensors to the standards.

As a basis for the formulation of performance specifications of the remote techniques for enforcement monitoring, we have reviewed the continuous emission monitoring requirements and performance testing methods codified in 40CFR60.

EPA has promulgated or proposed standards of performance for twenty-four source categories. These standards include emission standards for

- particulate matter
- sulfur dioxide
- nitrogen oxides
- sulfuric acid mist
- carbon monoxide
- hydrocarbons
- fluorides

They also include test methods and procedures, using reference methods as given in Appendix A of 40CFR60. These reference methods include

- |          |   |   |
|----------|---|---|
| Method 1 | - | Sample and Velocity Traverses for Stationary Sources                                      |
| 2        | - | Determination of Stack Gas Velocity and Volumetric Flow Rate                              |
| 3        | - | Gas Analyzers for CO <sub>2</sub> , Excess Air and Dry Molecular Weight                   |
| 4        | - | Determination of Moisture in Stack Gases  |
| 5        | - | Determination of Particulate Emissions for Stationary Sources                             |
| 6        | - | Determination of SO <sub>2</sub> Emissions from Stationary Sources                        |
| 7        | - | Determination of NO <sub>x</sub> Emissions from Stationary Sources                        |
| 8        | - | Determination of Sulfuric Acid Mist and SO <sub>2</sub> Emissions from Stationary Sources |

- |      |   |   |
|------|---|---|
| 9    | - | Visual Determination of the Opacity of Emissions from Stationary Sources                          |
| 10   | - | Determination of CO Emissions from Stationary Sources   |
| 11   | - | Determination of H <sub>2</sub> S Emissions from Stationary Sources                               |
| 12   | - | Reserved  |
| 13 A | - | Determination of Total Fluoride Emissions from Stationary Sources - SPADNS Zirconium Lake Method  |
| 13 B | - | Determination of Total Fluoride Emissions from Stationary Sources - Specific Ion Electrode Method |
| 14   | - | Determination of Fluoride Emissions of Primary Aluminum Plants                                    |

In order that sources which have demonstrated compliance with applicable standards during the initial performance tests remain in compliance, provisions were included in 40CFR60 that require the installation of continuous monitors.

Initially EPA intended that the selection and use of continuous instruments be in the form of instrument specifications and calibration procedures, i. e. , a formal EPA instrumentation certification program. Once certified, an instrument from a particular product line of a given instrument vendor could be installed in fulfillment of the monitoring requirements for that source.

However, the "product line certification" approach was soon considered undesirable because an instrument so certified may not perform properly at the source due to

- unexpected or disregarded interferences
- improper installation
- undetected damages from handling.

It was realized that no one instrument model would be expected to provide accurate results for each of the wide variety of (new) sources. Therefore, a different approach has been adopted which requires the

source owner to demonstrate at each source the capability of continuous monitoring systems to meet the performance specifications for systems which monitor

1. Opacity
2. SO<sub>2</sub> and NO<sub>x</sub>
3. O<sub>2</sub>

Specifications for systems which monitor

H<sub>2</sub>S

CO

will be proposed by EPA at a later date. The validity of these specifications for the above systems has been evaluated in depth by extensive testing programs at steam generating facilities. The technical support for these specifications are contained in the report "Performance Specifications for Stationary Source Monitoring Systems for Gases and Visible Emissions" (EPA-650/2-74-013, January 1974).

The provisions specifying general continuous emission monitoring requirements (40CFR60, §60.13 and App. B) have been promulgated in Oct. 1975 (40FR46254). These include the performance specifications and specification test procedures (1) for transmissometer systems for continuous measurement of the opacity of stack effluents, (2) for monitors of SO<sub>2</sub> and NO<sub>x</sub> from stationary sources, and (3) for monitors of O<sub>2</sub> and CO<sub>2</sub> from stationary sources. The provisions for (2) and (3) are generally broken down into

Principle and Applicability  
Apparatus  
Definitions  
Installation Specification  
Continuous Monitoring System  
Performance Specifications  
Performance Specification Test Procedures  
Calculations, Data Analysis and Reporting  
References

Additional provisions for (1) are given for the installation, optional design specifications and determination of conformance with design specifications. It is noteworthy that provisions for (3) are made

to include alternative procedures due to the variation of existing analyzers. The provisions state that any such alternative procedures must fulfill the same purpose (verify response, drift and accuracy) as the given performance specifications and test procedures.

As an illustration of the proposed performance specifications, the requirements for the transmissometer (1), the SO<sub>2</sub> and NO<sub>x</sub> monitors (2) and the CO<sub>2</sub> and NO<sub>2</sub> (3) are summarized in Tables 3-2 through 3-4, respectively.

A report of all emission monitoring and a summary of excess emissions must be given quarterly by the owner or operator of the stationary source, to be used by the Administrator to determine whether acceptable operating and maintenance procedures are being used. The continuous monitors are required on affected facilities where

- they can assist in minimizing pollutant emissions,
- the technical feasibility exists using currently available continuous monitoring technology,
- the cost of the monitors is reasonable.

Initially, only a limited amount of cost data was available. In the meantime, more cost data have been accumulated. In the promulgation of the continuous emission monitoring requirements, EPA is quoting the following values. For opacity monitoring alone, investment costs including data reduction equipment and performance tests are approximately \$20,000, and annual operating costs are approximately \$8,500. For power plants that are required to install opacity, nitrogen oxides, sulfur dioxide, and diluent (O<sub>2</sub> or CO<sub>2</sub>) monitoring systems, the investment cost is approximately \$55,000, and the operating cost is approximately \$30,000. EPA states that "These are significant costs but are not unreasonable in comparison to the approximately seven million dollar investment cost for the smallest steam generation facility affected by these regulations." (40 FR 46254).

The parameters listed in the Tables 3-2 through 3-4 with an asterisk are expressed as the sum of the absolute mean value plus 95 percent confidence interval of a series of tests, according to

$$\bar{x} = \frac{1}{n} \sum_{i=1}^n x_i$$

where  $x_i$  are the individual values,  $\Sigma$  is the sum of the individual values,  $\bar{x}$  is the mean value, and  $n$  are the number of data points. The 95 percent confidence interval (two-sided) is calculated according to

**TABLE 3-2. Performance Specifications for Transmissometer**

Parameter	Specifications
Calibration error	$\leq 3\%$ of test filter value*
Zero drift (24 hour)	$\leq 2\%$ of emission standard*
Calibration drift (24 hour)	$\leq 2\%$ of emission standard*
Response time	10 seconds (maximum)
Operational period	168 hours

**TABLE 3-3. Performance Specifications for SO<sub>2</sub> and NO<sub>x</sub> Monitors**

Parameter	Specifications
Accuracy	$\leq 20\%$ of reference mean value
Calibration error*	$\leq 5\%$ of each (50%, 90%) calibration gas mixture value
Zero drift (2 hours)*	$\leq 2\%$ of span
Zero drift (24 hour)*	$\leq 2\%$ of span
Calibration drift (2 hour)*	$\leq 2\%$ of span
Calibration drift (24 hour)*	$\leq 2.5\%$ of span
Response time	15 minutes maximum
Operational period	168 hours minimum

**TABLE 3-4. Performance Specifications for CO<sub>2</sub> and O<sub>2</sub> Monitors**

Parameter	Specifications
Zero drift (2 hour)*	$\leq 0.4\%$ O <sub>2</sub> or CO <sub>2</sub>
Zero drift (24 hour)*	$\leq 0.5\%$ O <sub>2</sub> or CO <sub>2</sub>
Calibration drift (2 hour)*	$\leq 0.4\%$ O <sub>2</sub> or CO <sub>2</sub>
Calibration drift (24 hour)*	$\leq 0.5\%$ O <sub>2</sub> or CO <sub>2</sub>
Operational period	168 hour minimum
Response time	10 minutes

$$C.I. .95 = \frac{t .975}{n\sqrt{n-1}} \sqrt{n(\sum x_i^2) - (\sum x_i)^2}$$

where  $\sum x_i$  is the sum of all data points,  $t .975 = t_{1-\alpha/2}$ , and C. I. .95 is the 95 percent confidence interval estimate of the average mean value.

VALUES FOR .975	
n	.975
2	12.706
3	4.303
4	3.182
5	2.776
6	2.571
7	2.447
8	2.386
9	2.306
10	2.262
11	2.228
12	2.201
13	2.179
14	2.160
15	2.145
16	2.131

The values in this table are already corrected for  $n-1$  degrees of freedom. Use  $n$  equal to the number of samples as data points.

The above provisions are not applicable to sources for which monitoring equipment has already been contracted for. However, this equipment must have the capability to monitor emission levels to within  $\pm 20$  percent with a confidence level of 95 percent. Compliance with the requirements is determined by subjecting the continuous monitoring system to evaluation with a variety of known opacity neutral density filters or a variety of known concentration calibration gases as applicable. In addition, owners or operators of all continuous monitoring systems are required to record the zero and span drift and to adjust them at least once daily, (or more often if prescribed by the instrument manufacturer), using zero and span gas introduced into the measurement system for extractive methods and certified calibration gas cells for non-extractive methods.

In addition, records must be maintained that include the occurrence and duration of any startup, shutdown, or malfunction of the facility as well as the air pollution control equipment. Also, files must be kept as to the results of any tests conducted in accordance with the procedures listed in the monitoring performance specifications.

### **3.2 NATIONAL EMISSION STANDARDS FOR HAZARDOUS AIR POLLUTANTS**

In addition to the regulations prescribing emission rates of air pollutants (SO<sub>2</sub>, NO<sub>x</sub>, particles, etc.) from new stationary sources, EPA has codified national emission standards in 40CFR61 for hazardous air pollutants, such as asbestos, beryllium, and mercury, and has proposed standards for vinyl chloride (40FR59532). Together with these standards; which are summarized in Table 3-5, test methods have been promulgated or proposed (App. B of 40CFR61). These include:

- Method 101: Reference method for determination of particulate and gaseous mercury emissions from stationary sources (air streams).
- Method 102: Reference method for determination of particulate and gaseous mercury emissions from stationary sources (hydrogen streams).
- Method 103: Beryllium screening method.
- Method 104: Reference method for determination of beryllium emissions from stationary sources.
- Method 105: Method for determination of mercury in wastewater treatment plant sewage sludges.
- Method 106: Determination of vinyl chloride from stationary sources.
- Method 107: Determination of vinyl chloride content of in-process wastewater samples, and vinyl chloride content of polyvinyl chloride resin, slurry, wet cake and latex samples.



TABLE 3-5. National Emission Standards for Hazardous Air Pollutants

Species	Status*	Ref.	Standards
Asbestos	Pm	40CFR61 (Subpart B)	No visible emission from asbestos mills, manufacturing (textile, cement, insulating material, friction products, paper, etc., floor tile, paints, etc., plastics and rubber materials chlorine), spraying. Roadway surfacing prohibited, precautions in demolition.
Beryllium	Pm	40CFR61 (Subpart C)	≤10g of beryllium over a 24 hour period from stationary sources; or ambient air limit of 0.01 g/m <sup>3</sup> averaged over a 30-day period; open burning of beryllium-containing waste (except propellants) is prohibited.
		40CFR61 (Subpart D)	≤75μg minutes/m <sup>3</sup> of air within the limits of 10 to 60 minutes for beryllium rocket motor firings.
Mercury	Pm	40CFR61 (Subpart E)	≤2,300g of mercury per 24 hour period from stationary sources.
Vinyl chloride	Pp	40FR59544 (Subpart F)	≤10ppm of vinyl chloride for vinyl chloride plants.
			≤10ppm of polyvinyl chloride for polyvinyl chloride plants; special requirements for reactor openings, strippers, holding containers, relief valves, etc.

Pm means promulgated  
Pp means proposed

### 3.3 NATIONAL AMBIENT AIR QUALITY STANDARDS

When the remote techniques are to be applied to establish the ambient air quality trends, the performance of the instruments must be consistent with the National Ambient Air Quality Standards, which have been codified in 40CFR50.

These standards are divided into primary and secondary standards. The primary ones are for the protection of human health, while the secondary ones are for the prevention of all other undesirable effects. In Table 3-6, the standards for six pollutants [CO, NO<sub>2</sub>, NMHC (non-methane hydrocarbons), particulate matter, SO<sub>2</sub>, and oxidants] are shown. Included in 40CFR 50 (Appendix A) are the following reference methods:

- A - Reference Method for SO<sub>2</sub> (pararosaniline method)
- B - Reference Method for Total Suspended Particles (high volume method)
- C - Measurement Principle and Calibration Procedure for CO (NDIR method)
- D - Measurement Principle and Calibration Procedure for Photochemical Oxidants
- E - Reference Method for Hydrocarbons
- F - Measurement Principle and Calibration Procedure for NO<sub>2</sub> (Gas Chemiluminescence)—(Proposed)

To implement these standards, the U. S. A. has been divided into some 240 Air Quality Control Regions (EPA, 1972.), the boundaries of which are based on considerations of urban-industrial distribution, topographical and meteorological factors, etc. In accordance with the provisions of Section 110 of the Clean Air Act, the States have submitted plans that provide for the implementation, maintenance, and enforcement of the National Air Quality Standards on a regional (air quality region) basis. The State Implementation Plan (SIP) for each region must provide for attainment of the primary standards in 3-5 years depending on whether an extension has been granted. The State plan is required to set forth the procedure for attaining the secondary standards within a reasonable amount of time. In the meantime, EPA has promulgated

TABLE 3-6. National Ambient Air Quality Standards

Pollutant	Standard Description
Carbon monoxide (Primary and secondary standards are the same)	<ul style="list-style-type: none"> <li>- 10 milligrams per cubic meter (9 ppm), maximum 8-hour concentration not to be exceeded more than once per year.</li> <li>- 40 milligrams per cubic meter (35 ppm), maximum 1-hour concentration not to be exceeded more than once per year.</li> </ul>
Nitrogen dioxide (Primary and secondary standards are the same)	<ul style="list-style-type: none"> <li>- 100 micrograms per cubic meter (0.05 ppm), annual arithmetic mean.</li> </ul>
Hydrocarbons (non-methane) (Primary and secondary standards are the same)	<ul style="list-style-type: none"> <li>- 160 micrograms per cubic meter (0.24 ppm), maximum 3-hour concentration (6-9 a.m.) not to be exceeded more than once per year. For use as a guide in devising implementation plans to meet the oxidant standards.</li> </ul>
Particulate matter Primary standard	<ul style="list-style-type: none"> <li>- 75 micrograms per cubic meter, annual geometric mean.</li> <li>- 260 micrograms per cubic meter, maximum 24-hour concentration not to be exceeded more than once per year.</li> </ul>
Secondary standard	<ul style="list-style-type: none"> <li>- 60 micrograms per cubic meter, annual geometric mean, as a guide to be used in assessing implementation plans to achieve the 24-hour standard.</li> <li>- 150 micrograms per cubic meter, maximum 24-hour concentration not to be exceeded more than once per year.</li> </ul>
Sulfur dioxide Primary standard	<ul style="list-style-type: none"> <li>- 80 micrograms per cubic meter, annual arithmetic mean.</li> <li>- 365 micrograms per cubic meter, maximum 24-hour concentration not to be exceeded more than once per year.</li> </ul>
Secondary standard	<ul style="list-style-type: none"> <li>- 1300 micrograms per cubic meter, maximum 3-hour concentration not to be exceeded more than once per year.</li> </ul>
Oxidant (Primary and secondary standards are the same)	<ul style="list-style-type: none"> <li>- 160 micrograms per cubic meter, maximum 1-hour concentration, not to be exceeded more than once per year.</li> </ul>

the requirements of emission monitoring of stationary sources to be included in the SIP's [40CFR51, §51.19(e) and Appendix P]. These requirements include the source categories to be affected and emission monitoring, recording, and reporting requirements for those sources. Performance specifications for accuracy, reliability, and durability of acceptable monitoring systems have to comply with the performance specifications 1, 2 and 3 as given in Appendix B of Part 60. Techniques to convert emission data to units of the applicable State emission standards must be given. Such data must be reported to the State as an indication of whether proper maintenance and operating procedures are being utilized by source operators to maintain emission levels at or below emission standards. Such data may be used directly or indirectly for compliance determination. Though the monitoring requirements are specified in detail, States are given some flexibility to resolve difficulties that may arise during the implementation of these regulations.

For monitoring the NAAQS, EPA has introduced the concepts of "reference methods" and "equivalent methods" to standardize measurement methodologies. Although not yet specified, remote monitors may eventually be included in these measurement methodologies. Originally, reference methods were specified for manual instruments that embodied a given technique (Appendices A through F of 40CFR 50). Subsequently, EPA has adopted a new concept for some of these pollutants, which is described in Part 53 of Title 40, Chapter I. Instead of specifying reference methods, measurement principles and calibration procedures are designated. For example, the NDIR becomes the measurement principle for CO. Any analyzer using the NDIR principle and calibration procedure and meeting the appropriate performance tests is designated as a reference method. As a consequence, there could be as many reference methods for CO as there are models of CO analyzers utilizing the NDIR measurement principle (Hoffman et al., 1975). Other methods, utilizing a different measurement principle, can be designated as equivalent method as long as equivalency to the reference methods can be demonstrated. In the case of CO, an equivalent method could be a manual or automatic flame ionization method or a remote long-path method.

Procedures for determining reference and equivalent methods were promulgated by EPA [49FR7042 (18 Feb. 1975)], affecting Parts 50 and 53 of Title 40 of the Code of Federal Regulations. An overview of the content of these rules is given in Table 3-7. How these rules apply to the pollutants is shown in Table 3-8.

There are three special cases in Table 3-8. The first two deal with reference methods that are specified both for total suspended particles (TSP) and SO<sub>2</sub>, instead of leaving them unspecified and the third case deals with the equivalent method for TSP. The reason for specifying reference methods for SO<sub>2</sub> and TSP is that the designated measurement principles are manual methods consisting of a series of operations to be performed by an operator. The reference method is defined by a series of explicit manual operations, and thus there can be only one reference method. An equivalent method for TSP is not possible since in this case the pollutant is defined as the material collected by the high-volume sampler during the sample-collection phase of the reference method.

In any application of designating a candidate method as reference or equivalent determination, the following information must be supplied: A clear identification of the candidate method which will distinguish it from all other methods and by which it may be referred to unambiguously. A detailed description of the candidate method. The measurement principle, manufacturer, name, model number, and other forms of identification; a listing of the significant components; schematic diagrams; and a detailed description of the apparatus and measurement procedures. A comprehensive operation or instruction manual providing a complete and detailed description of the operational and calibration procedures prescribed for field use of the candidate method and all instruments utilized as part of that method, adequate warning of potential safety hazards that may result from normal use, or (if the method is automated) from normal use or malfunction of the method and a description of necessary safety precaution, a clear description of installation and operation procedures and of necessary periodic maintenance, as well as comprehensive trouble-shooting and corrective maintenance procedures and parts identification diagrams. A statement that the candidate method has been tested in accordance with the procedures described in Subpart B and/or Subpart C of Part 53, as applicable, including test data, records calculations, and test results as specified. A statement to the effect that the method or analysis tested is representative and that a quality control program will be followed.

**TABLE 3-7. Applicability of 40CFR50 and 53 (40FR7042)**

	Reference Method	Equivalent Method
Manual	Those methods as given in the Appendices to Part 50, except at present, App. C (for CO) and App. D (for oxidants)	Any method that satisfies the requirements in Subpart C of Part 53.
Automatic	Those methods whose "measurement principles and calibration procedures" are specified in the Appendices of Part 50 (namely App. C and D at present).	Any method that satisfies the requirements in Subparts B and C of Part 53.

**TABLE 3-8. Summary of Reference and Equivalent Methods (Hoffman et al., 1975)**

Pollutant	Measurement principle or method	Reference method	Equivalent methods
TSP	High-volume sampler (manual method)	High-volume sampler	None possible
SO <sub>2</sub>	Pararosaniline (manual method)	Pararosaniline	Manual or continuous
CO	Nondispersive infrared	•	Manual or continuous
O <sub>3</sub>	Chemiluminescence	•	Manual or continuous
NO <sub>2</sub>	Chemiluminescence **	•	Manual or continuous

\*None specified. Manufacturer must submit data documenting that the analyzer meets performance specifications.

\*\* Proposed, 41FR11258 (17 March 1976)

Subpart B (40CFR53) contains the performance specifications, which are summarized in Table 3-9 and 3-10 (41FR 11252 - 11266).

TABLE 3-9. Performance Specifications For Automated Methods

Performance parameter	Units <sup>1</sup>	Sulfur dioxide	Photochemical oxidants	Carbon monoxide	Nitrogen dioxide	Definitions and test procedures
1. Range.....	Parts per million:	0-0.5	0-0.5	0-50	0-0.5	Sec. 53.23(a).
2. Noise.....	do.....	.005	.005	.50	.005	Sec. 53.23(b).
3. Lower detectable limit.....	do.....	.01	.01	1.0	.01	Sec. 53.23(c).
4. Interference equivalent.....	do.....					Sec. 53.23(d).
Each interferant.....	do.....	±.02	±.02	±1.0	±0.2	
Total interferant.....	do.....	.06	.06	1.5	.04	
5. Zero drift, 12 and 24 hour.....	do.....	±.02	±.02	±1.0	±.02	Sec. 53.23(e).
6. Span drift, 24 hour.....	do.....					Do.
20 percent of upper range limit.....	Percent.....	±20.0	±20.0	±10.0	±20.0	
80 percent of upper range limit.....	do.....	±5.0	±5.0	±2.5	±5.0	
7. Lag time.....	Minutes.....	20	20	10	20	Do.
8. Rise time.....	do.....	15	15	5	15	Do.
9. Fall time.....	do.....	15	15	5	15	Do.
10. Precision.....	do.....					Do.
20 percent of upper range limit.....	Parts per million:	.01	.01	.5	.02	
80 percent of upper range limit.....	do.....	.015	.01	.5	.03	

<sup>1</sup> To convert from parts per million to  $\mu\text{g}/\text{m}^3$  at 25°C and 760 mm Hg, multiply by  $M/0.02447$ , where  $M$  is the molecular weight of the gas.

Subpart C contains the procedures for determining a consistent relationship between candidate methods and reference methods. Equivalency is shown when the differences between measurements made by a candidate manual or automatic method and made simultaneously by a reference method are less than or equal to the value specified in the last column of Table 3-11.

So far, notices have been published in the Federal Register in which EPA has designated several SO<sub>2</sub> monitors as equivalent methods (40FR3893, 27 Jan. 1976) and ozone and CO monitors as reference methods (41FR5144, 4 Feb. 1976, and 41FR7450, 18 Feb. 1976).

TABLE 3-10. Interferant Test Concentration,<sup>1</sup>  
Parts Per Million

Pollutant	Analyzer type <sup>2</sup>	Hydrochloric acid	Ammonia	Hydrogen sulfide	Sulfur dioxide	Nitrogen dioxide	Nitric oxide	Carbon dioxide	Ethylene	Ozone	M-Xylene	Water vapor	Carbon monoxide	Methane	Ethane
SO <sub>2</sub>	Flame photometric (FPD)			0.1	0.14			750				20,000	50		
SO <sub>2</sub>	Gas chromatography (FPD)			.1	.14			750				20,000	50		
SO <sub>2</sub>	Spectrophotometric-wet chemical (pararosaniline reaction)	0.2	0.1	.1	.14	0.5		750		0.5					
SO <sub>2</sub>	Electrochemical	.2	.1	.1	.14	.5	0.5		0.2	.5		20,000			
SO <sub>2</sub>	Conductivity	.2	.1		.14	.5		750							
SO <sub>2</sub>	Spectrophotometric-gas phase				.14	.5	.5			.5	0.2				
O <sub>3</sub>	Chemiluminescent			.1				750		4.08		20,000			
O <sub>3</sub>	Electrochemical		.1		.5	.5				4.08		20,000			
O <sub>3</sub>	Spectrophotometric-wet chemical (potassium iodide reaction)		.1		.5	.5	.5			4.08		20,000			
O <sub>3</sub>	Spectrophotometric-gas phase				.5	.5	.5			4.08					
CO	Infrared							750				20,000	10		
CO	Gas chromatography with flame ionization detector											20,000	10		0.5
CO	Electrochemical						.5		.2			20,000	10		
CO	Catalytic combustion-thermal detection		.1					750	.2			20,000	10	5.0	.5
CO	IR fluorescence							750				20,000	10		.5
CO	Mercury replacement-UV photometric								.2			20,000	10		.5
NO <sub>2</sub>	Chemiluminescent		.1		.5	.1	.5					20,000			
NO <sub>2</sub>	Spectrophotometric-wet chemical (azo-dye reaction)				.5	.1	.5			.5					
NO <sub>2</sub>	Electrochemical		.1		.5	.1	.5			.5		20,000	50		
NO <sub>2</sub>	Spectrophotometric-gas phase		.1		.5	.1	.5			.5		20,000	50		

<sup>1</sup> Concentrations of interferant listed must be prepared and controlled to  $\pm 10$  percent of the state value.

<sup>2</sup> Analyzer types not listed will be considered by the administrator as special cases.

<sup>3</sup> Do not mix with pollutant.

<sup>4</sup> Concentration of pollutant used for test. These pollutant concentrations must be prepared to  $\pm 10$  percent of the stated value.

TABLE 3-11. Test Concentration Ranges, Number Of Measurements Required, and Maximum Discrepancy Specification

Pollutant	Concentration range, parts per million	Simultaneous measurements required				Maximum discrepancy specification, parts per million
		1-hr		24-hr		
		First set	Second set	First set	Second set	
Oxidants	Low 0.06 to 0.10	5	6			0.02
	Med 0.15 to 0.25	3	6			.03
	High 0.35 to 0.45	1	6			.04
	Total	14	18			
Carbon monoxide	Low 7 to 11	5	6			1.5
	Med 20 to 30	5	6			2.0
	High 35 to 45	1	6			3.0
	Total	14	18			
Sulfur dioxide	Low 0.02 to 0.05			3	3	0.02
	Med 0.10 to 0.15			3	3	.03
	High 0.30 to 0.60	7	8	2	2	.04
	Total	7	8	7	8	
Nitrogen dioxide	Low 0.02 to 0.08			3	3	0.02
	Med 0.10 to 0.20			2	3	.02
	High 0.25 to 0.35			2	2	.03
	Total			7	8	



### **3.4 OUTLINE OF PERFORMANCE AND TEST PROCEDURES FOR THE USE OF REMOTE MONITORS**

The generalized performance specifications and specification test procedures outlined here for the use of remote monitors in enforcement monitoring follow the format given in 40CFR60, App. B. ; Nader (1975) has suggested that the present specifications can be worded such as to apply not only to the extractive and in-situ instruments, but also to the remote monitors. Nader states that an evaluation of present specifications may result in some modifications but preferably after the regulation is appropriately modified. It appears that, in many paragraphs of the Performance Specifications, this can be accomplished without great difficulty. On the other hand, the calibration procedures required for a remote monitor are quite different and the regulations would require—in our opinion—significant modifications. In the following we briefly discuss the suggested performance specifications and parameters that would apply to remote sensors.

#### **(1) Principle and Applicability**

Must include statements to the effect that opacity and/or gases are sampled remotely, that specifications are given in terms of performance specifications and that test procedures are given to determine the capability of the remote monitors to conform to the performance specifications prior to approving the system for evidentiary monitoring in case developments.

#### **(2) Apparatus**

Must include a listing of all auxiliary equipment needed to perform the test procedures to determine conformance with the performance specification and to perform the field measurements.

#### **(3) Definitions**

All definitions for the measurements of the opacity and gases are essentially applicable, as given in 40CFR60, App. A and B.

Definitions of subsystems must include receiver, transmitter and/or remote reflector units, where appropriate. Maximum output of measurement system must take account the specific source, stack diameter, and source temperatures. Reference must be made to the performance standards for laser products (DHEW 1975).

#### (4) Measurement System Performance Specifications

Statement needed to the effect that the measurement system (remote monitor) must meet certain performance specifications to be considered acceptable under this method. These performance specifications can be patterned after the ones proposed in 40CFR60 App. A and B., giving considerations to the performance standards for laser products in terms of eye and skin safety. However, since the measurements are influenced by the interfering atmosphere, these performance specifications are only valid under a specified set of conditions given in the performance specification test procedures as outlined below. For field measurements made under conditions significantly different from the ones given in the performance specification test procedures, well described and documented "field measurements procedures" must be developed.

#### (5) Performance Specification Test Procedures

These procedures involve the calibration tests, field tests for accuracy (relative), drift and response time.

Some of the calibration tests may be conducted in the laboratory. Relatively large calibration cells will be required whose wall effects on the pollutant concentration and on the light transmission (reflections) must be either negligible or accountable. For passive remote monitors, the cells must be heated to simulate the stack emission at elevated temperatures. The self emission of the windows must be accounted for. The simulation of atmospheric interference and sky background is very difficult, and, in the case of water vapor interference, impracticable. In the case of opacity measurements, special "neutral density filters" simulating specific particulate emission must be used; some simulation of field conditions must be made such as illumination by direct or indirect sunlight.

All tests that cannot be simulated in the laboratory must be performed during the field tests conducted for accuracy, drift and response time. The procedures should follow the certification procedures developed by EPA for Reference Method 9 (visual

determination of the opacity of emissions for stationary sources). In these procedures, the candidate remote monitor must be tested and demonstrate the ability to measure the opacity and/or pollutant gas concentrations under different conditions in the plume, intervening atmosphere, and sky background. Similarly, as in Reference Method 9, a "stack emission generator" must be specified; it must be equipped with in-situ meters for smoke and gases that can be related to reference methods. In addition to the specification of a "stack emission generator," the sky background and the atmosphere slant path between the stack and the candidate remote monitor must be specified. This can be accomplished by monitoring the atmosphere and sky background by ambient air monitors that include measurements of interfering species ( $\text{H}_2\text{O}$ ,  $\text{CO}_2$ ,  $\text{CO}$ ,  $\text{CH}_4$ ,  $\text{N}_2\text{O}$ , particles, etc.) and meteorological parameters (temperature, wind, clouds, etc.)

Instead of using a "stack emission generator," it may be possible to utilize well-instrumented actual smoke stacks, whose behavior under different fuel and load conditions are known. Of course, certain tests such as the one for response time, may be impractical to conduct with an actual smokestack.

In addition to the above special requirements for the use of remote monitors, the performance specification test procedures must include provisions to account for the expected change in sky background and intervening atmospheric conditions between the "test range" and the field. These additional provisions must include the determination of the effect of interference by "normal" and/or additional atmospheric species present at the time of the observation. This interference arises not only from the path between source and sensor, but also from the sky background. In the UV and visible spectrum, scattering of sunlight presents an interference, while the thermal radiation from the sky and/or clouds (total or partial cover) cause an interference in the infrared. For active systems, narrow band optical filtering minimizes the background effects, and for passive methods, measurements adjacent to the target plume provides the necessary information about the background radiation, although care must be taken that the background is uniform for these two measurements.

#### (6) Calculations, Data Analysis and Reporting

In addition to the procedures for determination of mean values

and confidence intervals, analysis of accuracy (relative), calibration error, zero drift, calibration drift, response time and operational test period, as required for extractive or in-situ continuous monitors, field records must be kept which indicate the

time

observer location (distance, direction, height)

background description

sky conditions (cloud cover, sun position)

weather conditions (wind direction and speed, temperature)

plume description (if visible).

#### (7) References

Adequate references must be provided to document the consistent relationship of remote monitors with in-situ or extractive devices, as well as the consistent relationship of remotely measured pollution levels during the performance specification tests and the field applications.

# 4

## PRESENT DEVELOPMENT OF REMOTE MONITORING TECHNIQUES

### 4.1 OVERVIEW

Considerable work has been done in recent years on the development of active and passive systems to remotely measure gaseous and particulate pollutants in emissions from stationary sources, around the perimeter of multiple stationary sources, and in the ambient air. Some developments are still in the theoretical feasibility stage; others have been demonstrated in the laboratory, and some have been used in the field.

Passive techniques for gases rely on measurements of infrared, visible or ultraviolet radiation containing the absorption or emission spectrum of the gas of interest. In the UV/visible region the radiation is either scattered sunlight or direct sunlight; in the infrared the radiation is emitted by the gas itself and its background. For particulate measurements, visible observations of sunlight scattered by the particles are made by trained visual observers or instruments. Infrared techniques have the great advantage of working during both day and night, whereas, in general, the UV/visible techniques are useful only during the day. An exception to this latter statement could occur for opacity measurements if low-light-level image enhancement instrumentation is used, or if the stack plume is artificially illuminated for visual observation.

For gaseous measurements the techniques generally require high spectral resolution to distinguish the spectral characteristics of the gas of interest from those of interfering species. This high resolution may presently be achieved by high resolution interferometer spectrometers, by conventional spectrometers, by gas filter correlation, or by laser heterodyne detection. Other methods, not relying on high resolution, utilize the matched-filter technique or several narrow band filters together with a computer for interpretation of the data. Other techniques

which appear not to have been applied to remote sensing of air pollution include derivative spectroscopy and Hadamard spectroscopy.

The main problem with passive techniques is the data interpretation. In the infrared there is generally spectral interference from gases in the source of pollution and in the atmosphere. This spectral overlap together with the dependence of the radiant intensity on the temperature of the source and of the intervening atmosphere makes the inversion of the radiative transfer equation to obtain the pollutant concentration very difficult. In the UV/visible the data interpretation for gases is complex due to scattering by atmospheric aerosols and particles in the source of pollution. The scattering depends on the particle type, number, size distribution and spatial distribution, all of which are generally unknown, and on the sun angle. For observations of particles, in a plume or in the ambient air, the same problems due to the complexities of scattering apply.

The techniques presently being investigated for active laser systems are Raman scattering, resonance Raman scattering, fluorescence scattering, and differential absorption, for gaseous pollutants; and elastic backscattering for particulate pollutants. All methods involve the projection of laser pulses into the atmosphere, and measurement of an inelastic or elastic backscattered signal from the pollutant, and, in theory, are capable of giving range resolution, and hence the spatial distribution of the pollutants.

In Raman scattering the laser radiation is changed in frequency when it is scattered by the molecule; this shift is characteristic of the molecule, and the amplitude of the scattered signal is related to the number density of that molecule. This technique has been demonstrated in the field, in both stack emissions and ambient air. However, its applicability is restricted in concentration range and/or distance.

Increased sensitivity may be obtained by using resonance Raman scattering, in which the laser frequency is chosen to be close to an absorption line of the molecule. The theoretical resonance enhancement of the Raman scattering cross-section is of the order of  $10^6$ ; this enhancement has been observed in laboratory experiments.

Sensitivity similar to that of resonance Raman is theoretically possible with fluorescence. In this method the laser radiation is absorbed by the molecule which re-radiates over several lines. The lifetime of this phenomenon is relatively long, and collisional quenching

at atmospheric pressures reduces the effective cross-section, but it is still comparable to that of resonance Raman. Fluorescence has been observed in the laboratory, in a closed chamber, and possibly in a stack plume. Quantitative interpretation of fluorescence signals is difficult, and there is considerable interference by aerosol fluorescence.

The laser systems with the greatest potential (both in terms of sensitivity and specificity) appear to be the technique of differential absorption by scattering (DAS) for the single-ended measurement of gaseous pollutants. DAS is also known as DIAL (differential absorption lidar) and DASE (differential absorption via scattered energy). In this method, two signals at frequencies on and off a pollutant absorption line are projected into the atmosphere. The difference in the signals back-scattered from atmospheric molecules and aerosols or solid surfaces is related to the pollutant absorption. This technique has been demonstrated in the field, in both stack emissions and ambient air.

The elastic (Mie) backscattering lidar technique for detecting particulate pollution has long been used semi-quantitatively to map the relative concentrations of particles as a function of time and space. The method has been more recently used in the field to measure the opacity of a smoke plume by comparing the return signal from the near side with that from the far side of the plume.

An overview of the tuning characteristics of known broadly tunable coherent light sources was given recently by Kuhl and Schmidt (1974). Their figure is reproduced here as Figure 4-1a, where the solid lines indicate the regions for which reliable sources are available and have proved their potential, and the dashed lines indicate the regions for which sources are being developed.

More details of the diode laser regime is shown in Figure 4-1b, which is taken from Hinkley and Calawa (1974).

A particular application of both passive and active techniques is the so-called "perimeter monitoring", in which the emission from a stack or a complex of stacks can be determined without direct observation of the plume at the stack. In this technique, an up-looking instrument measures the vertical loading of the pollutant continuously along a closed path around the source. These measurements together with knowledge of the wind velocity allow the mass flow rate of the pollutant from the source to be calculated.

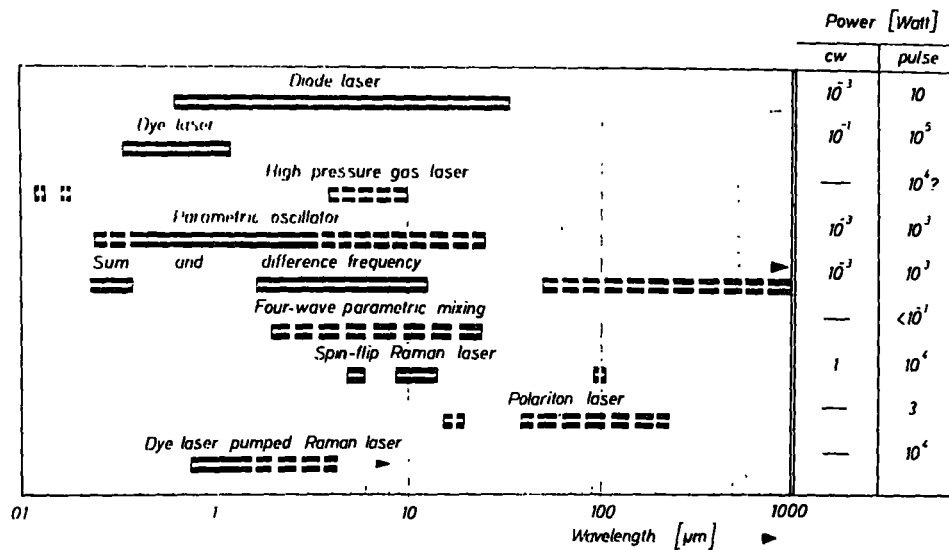


Figure 4-1a. Summary of Tuning Characteristics of Known Laser Sources (Kuhl and Schmidt, 1974)

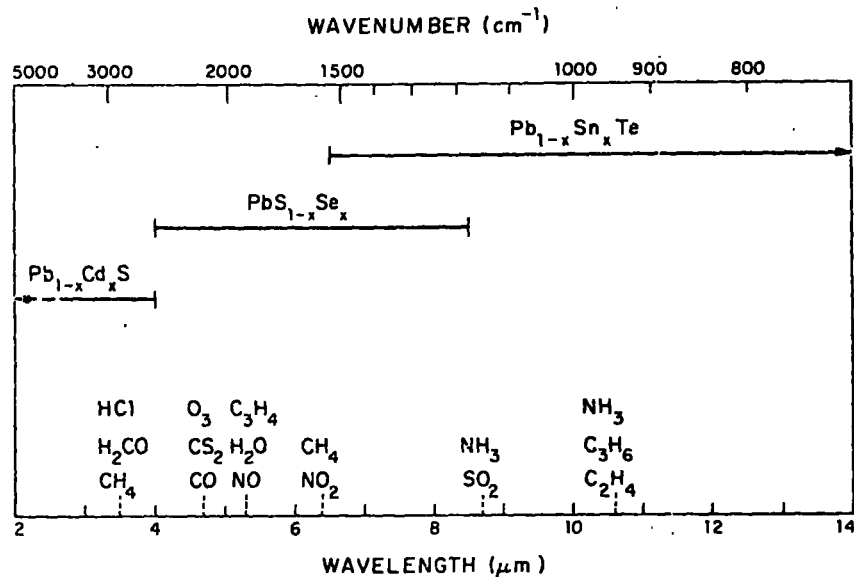


Figure 4-1b. Nominal wavelength regions covered by three Pb-salt semiconductors at 12° K. Strongly-absorbing wavelengths of some common gaseous pollutants are also indicated (Hinkley and Calawa, 1974).



Measurement of the vertical loading may be made with both matched filter correlation (MFC) and gas filter correlation (GFC) instruments mounted in a truck. Another method of measuring the vertical loading from the ground could be with a differential absorption laser system pointed vertically up, with the range being set above the maximum effluent altitude.

Possible airborne methods include the MFC instrument, the GFC instrument, and the differential absorption using laser radiation back-scattered from the earth's surface. The MFC is useful only during the day, and the data interpretation is complicated by aerosols and by the varying surface reflectivity. The GFC method can be used both day and night, but depends on there being a difference in temperature between the pollution and the ground, and thus would be limited in many instances. The best airborne method appears to be the differential absorption using a laser system.

## 4.2 THEORY

### 4.2.1 CW Infrared System

The ability of any detector-noise-limited electro-optical instrument to detect the change in environmental parameters can be quantified generally by the signal-to-noise ratio (SNR)

$$\text{SNR} = \frac{S_{\lambda} d\lambda}{N} = \frac{R_{\lambda} P_{\lambda} d\lambda}{N} \quad (4-1)$$

where  $S_{\lambda}$  is the signal voltage per unit wavelength,  $N$  is the rms-noise voltage,  $R_{\lambda}$  is the instrument responsivity (Volts/Watt) at the wavelength  $\lambda$  and  $P_{\lambda}$  the radiant power per unit wavelength. It is customary in infrared systems to combine the responsivity and the noise voltage into the detectivity:

$$D_{\lambda} = R_{\lambda}/N \quad (4-2)$$

which is equivalent to the inverse of the noise-equivalent-power:

$$D_{\lambda} = 1/(\text{NEP})_{\lambda} = \frac{\sqrt{A_d \Delta f}}{D_{\lambda}^*(f, T_B)} \quad (4-3)$$

where  $A_d$  is the detector area,  $\Delta f$  is the bandpass,  $D_{\lambda}^*(f, T_B)$  is the wavelength-dependent specific detectivity at the chopping frequency  $f$ , and background temperature  $T_B$ .

The available radiant power from an extended source (filling the field-of-view) is proportional to the throughput of the system and the spectral radiance seen by the detector:

$$P_{\lambda} d\lambda = (\eta_{\lambda} A_o \Omega_o) d\lambda \int_x N_{\lambda}^o(T, x) d\tau_{\lambda}(x) \quad (4-4)$$

where  $\eta_{\lambda}$  is the efficiency of the instrument,  $A_o$  is the entrance area,  $\Omega_o$  is the solid angle,  $N_{\lambda}^o(T, x)$  is the blackbody radiance ( $\text{W}/\text{cm}^2\text{sr-}\mu\text{m}$ ) at the temperature  $T(\text{K})$ ,  $\tau_{\lambda}(x)$  is the transmission, and  $x$  is the position along the line-of-sight. The general expression for the transmissivity is given by

$$\tau_{\lambda} = \tau_a \tau_s$$

where  $\tau_a$  is the transmissivity of gases, and  $\tau_s$  is the transmissivity of particles.

Then,

$$\tau_a = \prod_i \tau_{ai}(\lambda) = \exp \left[ - \int_x \sum_i \kappa_i(\lambda) C_i(x) p_t(x) dx \right] \quad (4-5)$$

where  $\kappa_i(\lambda)$  is the spectral absorption coefficient,  $C_i(x)$  is the concentration (mixing ratio) of species  $i$  at location  $x$ , and  $p_t$  is the total pressure, and

$$\tau_s = \exp \left[ - \int_x \sum_i \sigma_i n_i(x) dx \right] \quad (4-6)$$

where  $\sigma_i$  is the sum of the absorption and scattering cross sections, and  $n_i(x)$  is the number density of species  $i$  at location  $x$ .

The Equation (4-4) can be rewritten for the special cases of interest. In Figure 4-2, we show the principal applications of the passive (a and c) and the active CW systems (b and d).

For the case (a), Equation (4-4) is the proper expression, where the integration limits go from  $x = 0$  ( $\tau(0) = 1$ ) to  $x = \infty$ .

For the case (b), Equation (4-4) can be written (in general, assuming a homogeneous atmosphere between the transmitter and receiver) as

$$P_\lambda d\lambda = (\eta_\lambda A_o \Omega_o) d\lambda \left[ \epsilon_\lambda^S N_\lambda^O(T_S) \tau_\lambda + (1 - \tau_\lambda) N_\lambda^O(T_A) \right] \quad (4-7)$$

where  $\epsilon_\lambda^S$  is the spectral emissivity of the source, which has the temperature  $T_S$ ,  $\tau_\lambda$  is the transmission of the atmosphere between source and receiver and  $T_A$  is the atmospheric temperature. The solid angle of the receiver should be larger than  $A_S/R^2$ , where  $A_S$  is the aperture of the transmitter and  $R$  is the distance, in order to reduce scintillation effects. However, the effective throughput is given by  $A_o A_S/R^2$ . By chopping the source, the second term in the square brackets in Equation (4-7) is eliminated. Thus, in this case

$$P_\lambda d\lambda = (\eta_\lambda \frac{A_o A_S}{R^2}) d\lambda \epsilon_\lambda^S N_\lambda^O(T_S) \tau_\lambda \quad (4-8)$$

For the case (c), Equation (4-7) can be written as

$$P_\lambda d\lambda = (\eta_\lambda A_o \Omega_o) d\lambda \left[ \epsilon_\lambda^G N_\lambda^O(T_G) \tau_\lambda + \int_{x=0}^{x=h} N_\lambda^O(T_A(x)) d\tau(x) \right] \quad (4-9)$$

where  $h$  is the altitude of the aircraft [with  $\tau(h) = 1$ ],  $\epsilon_\lambda^G$  is the spectral emissivity of the ground, which has the temperature  $T_G$  and  $\tau_\lambda$  is the integrated atmospheric transmissivity. At the shorter wavelengths ( $\lambda < 5 \mu m$ ), the sun reflection must be accounted for, which is given by

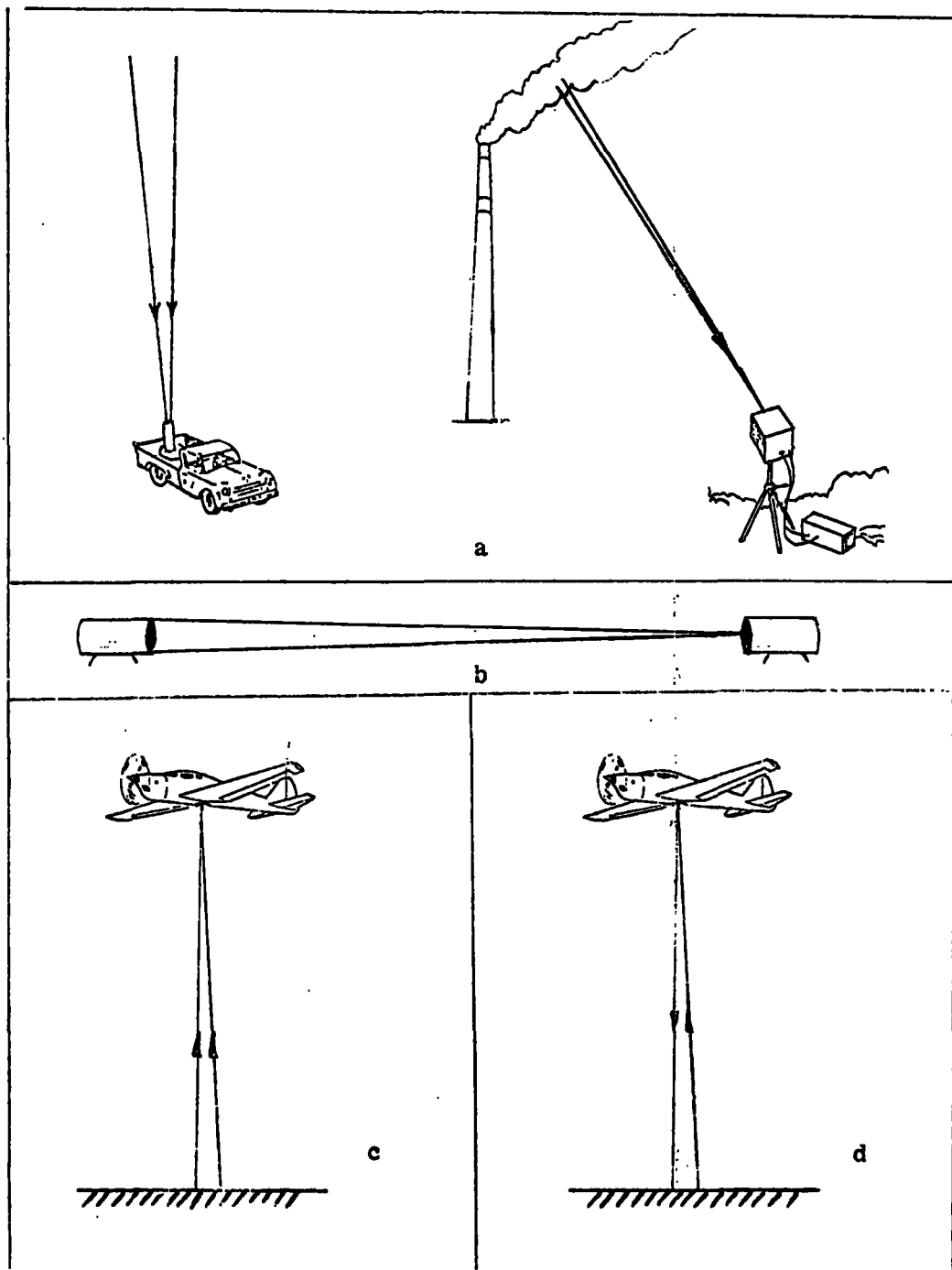


Figure 4-2. The principal CW applications

$$P_{\lambda} d\lambda = (\eta_{\lambda} A_o \Omega_o) d\lambda \rho_{\lambda}^G \frac{\cos \theta}{\pi} H_{\lambda}^S \tau_{\lambda}(h) [\tau_{\lambda}(\infty)]^{\sec \theta} \quad (4-10)$$

where  $\rho_{\lambda}^G$  is the ground diffuse reflectivity,  $\theta$  is the sun zenith angle,  $H_{\lambda}^S$  is the sun irradiance at the top of the atmosphere,  $\tau_{\lambda}(h)$  is the vertical atmospheric transmission from the ground to the height of the aircraft and  $\tau_{\lambda}(\infty)$  is the atmospheric transmission to through the entire atmosphere traversed by the sun rays.

For the case d, Equation (4-7) can be written as

$$P_{\lambda} d\lambda = \eta \frac{1}{\pi} P_{\lambda}^t \rho_{\lambda}^G \frac{A_o}{R^2} \frac{A}{A_L} \tau_{\lambda}^2 d\lambda \quad (4-11)$$

where  $P_{\lambda}^t$  is the spectral radiant power transmitted by the laser source,  $R$  is the height of the aircraft,  $A$  is the surface area viewed by the receiver (thus  $A/R^2 = \Omega_o$ ) and  $A_L$  is the area of the laser beam at the surface. It is assumed that  $A \leq A_L$ ; for optimum signal to background ratio  $A = A_L$ .

A special expression is used for a laser heterodyne radiometer. The thermal radiance  $N_j$  in a spectral channel of bandwidth  $\beta$  centered at frequency  $\nu_j$  is mixed with a laser signal at  $\nu_L$  to provide a signal at the difference frequency  $\nu_D = |\nu_j - \nu_L|$  (Seals 1974). The system responds to the sum of signals in the channels centered at  $\nu_L \pm \nu_D$ . For a quantum-limited system with no excess noise, the SNR becomes

$$SNR = \frac{c^2}{2h\nu^3} N \sqrt{\frac{t}{\beta}}$$

where  $c$  is the velocity of light,  $h$  is the Planck constant,  $\nu$  is the spectral frequency (in Hz),  $t$  is the postdetection integration time, and  $\beta$  is the spectral bandwidth (in Hz).  $N$  is the radiant power per unit emitter area and solid angle for the signal channel and its image.

#### 4.2.2 Pulsed Laser Systems

The basic concept of single-ended laser probing of ambient air and stationary source emissions is illustrated in Figure 4-3 and Figure 4-4 for the case of a Raman system (Inaba and Kobayasi, 1972). The laser is transmitted through a collimating telescope and scattered from mixtures of particulate and molecular scatterers in the atmosphere. The spectrum of the backscattered energy consists of Rayleigh and Mie scattering components of the frequency, centered at  $\nu_0$  identical with the transmitted laser frequency, and the Raman-shifted frequencies at  $\nu_1, \nu_2, \dots, \nu_n$  due to various Raman active gases in the atmosphere. These spectral components are analyzed and detected simultaneously through a spectrum analyzer in conjunction with optical filtering devices (narrow band filters or a monochromator) and an array of sensitive photodetectors. Then, via a data processor, the multichannel information such as location and concentration of gaseous contaminants, and their correlation with the particulate matters may be displayed in real time, and at the same time, if necessary, sent to the pollution alarm/control system.

The systems for the fluorescence, differential absorption and lidar methods are basically the same, but with differences in the frequencies and in the data processing. All these laser systems are sophisticated and expensive, but may be made mobile for enforcement monitoring purposes.

The sensitivity of these techniques, of course, is determined by the design of the system and by the signal strength relative to the system noise and background noise. The latter, due to scattered solar radiation, is generally the dominant noise in daytime operation.

In considering laser systems we can write the basic equation in a form common to all the techniques discussed in the following

$$P(R) = \epsilon P_t L N(R) \beta A R^{-2} \tau_A(R) \tau_G(R) \text{ per pulse} \quad (4-12)$$

where  $P(R)$  is instantaneous received energy from resolution element  $L$  at range  $R$ ,  $P_t$  is transmitted energy (generally given in joules or photons) at  $t_0$ ,  $L$  is effective pulse length, ( $L = c\Delta t/2$ , where  $c$  is the velocity of light and  $\Delta t$  is pulse duration; it is the range interval

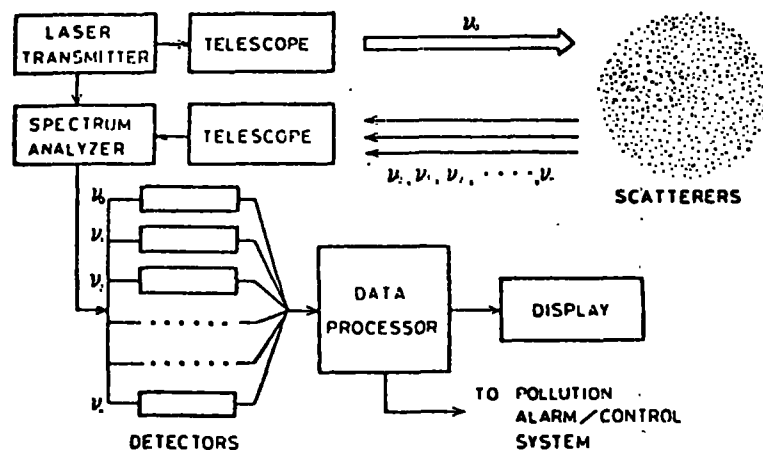


Figure 4-3. System diagram showing the basic concept of the laser-Raman radar as a single-ended and range-resolved probe for constituent analysis of air pollution and ordinary atmosphere in real time (Inaba and Kobayasi, 1972).

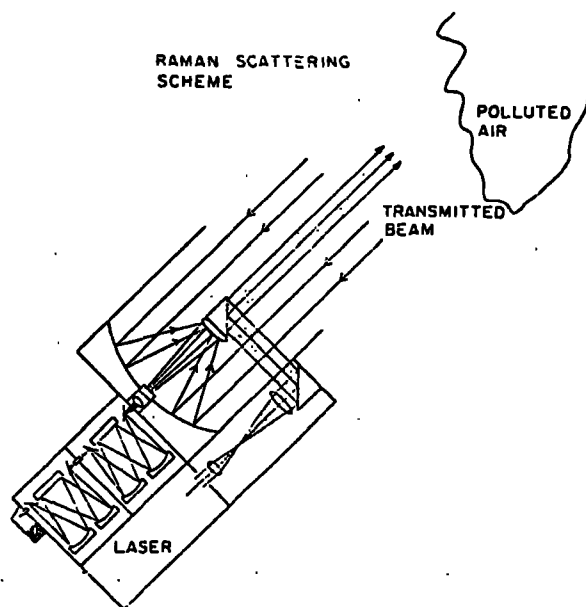


Figure 4-4. Schematic of the Raman scattering scheme showing the transmitting laser, receiving optics, and spectrometer. (Kildal and Byer, 1971).

from which signals are simultaneously received at time  $t$ ),  $R$  is range  $R = c(t-t_0)/2$ , where  $t_0$  is the time of transmission of pulse,  $A$  is the effective receiver aperture,  $\epsilon$  is the optical efficiency of the system,  $N(R)$  is the number density of the relevant pollutant,  $\beta$  is the backscattering cross-section appropriate to the scattering phenomenon under consideration, and  $\tau_A(R)$  is the atmospheric attenuation by interferences along the laser path, and  $\tau_G(R)$  is the pollutant attenuation, both at range  $R$ .

The noise ( $N$ ) in a well-designed laser system should be due only to the photomultiplier current caused by signal photons, background photons and the dark current. Thus

$$N = (\eta P(R) + \eta P_B + N_D)^{1/2} \quad (4-13)$$

where  $\eta$  is the quantum efficiency,  $P(R)$  is the signal photons,  $P_B$  is the background photons, and  $N_D$  is the dark current equivalent noise input. The background radiance collected by the receiver is given by

$$\begin{aligned} W_B &= B A \Omega \Delta \lambda \text{ (watt)} \\ &= \frac{B A \Omega \Delta \lambda}{hc/\lambda} \text{ (photons/second)} \end{aligned} \quad (4-14)$$

where  $B$  is the radiance in  $\text{Wcm}^{-2}\text{\AA}^{-1}\text{sr}^{-1}$ ,  $h$  is the Planck constant, and  $A \Omega$  is the throughput of the receiver in  $\text{sq cm sr}$ .

Thus, at the cathode, the number of background photons in a gated system, with a gate width  $t_g$  sec, is given by

$$P_B = W_B t_g = \epsilon \frac{B A \Omega \Delta \lambda}{hc/\lambda} t_g \quad (4-15)$$

The dark current noise may be neglected in comparison with background noise, particularly when the photomultiplier is cooled. Thus, the signal-to-noise ratio becomes



$$\text{SNR} = \frac{\eta P(R)}{(\eta P(R) + \eta P_B)^{1/2}} \text{ per pulse} \quad (4-16a)$$

For  $n$  pulses,

$$\text{SNR} = \frac{\eta P(R) \cdot n^{1/2}}{(\eta P(R) + \eta P_B)^{1/2}} \quad (4-16b)$$

Assuming that no data processing noise is added to the detector noise, then the ultimate sensitivity of the system is determined by Equation (4-16), and is obtained when  $\text{SNR} = 1$ .

The daytime background noise is typically about  $10^3$  greater than the nighttime noise, i. e.,  $P_B(\text{day}) = 10^6 P_B(\text{night})$ . The significance of this background noise varies with the technique, system, and range, as illustrated in Figure 4-5 and 4-6.

Care must be taken in estimating the atmospheric attenuation since the outgoing and return pulses are at different frequencies for the Raman and fluorescence techniques.

Thus, knowing the system parameters, the atmospheric attenuation, and the relevant scattering cross-section, the number density (concentration) of the pollutant may be determined from the return signal. Typical cross-sections for the different phenomena are given in Table 4-1 (Derr and Little 1970).

TABLE 4-1. Typical Optical Scattering Cross Sections (Per Particle)

Process	Cross section ( $\text{cm}^2/\text{sr}$ )
Mie	$10^{-27}$ to $10^{-8}$
Rayleigh	$10^{-27}$
Raman	$10^{-28}$ to $10^{-31}$
Resonance Raman	$10^{-22}$
Fluorescence *	$10^{-16}$ and smaller (broadband emission)

\* These cross-sections are reduced (a factor of about  $10^5$ ) by collisional quenching.

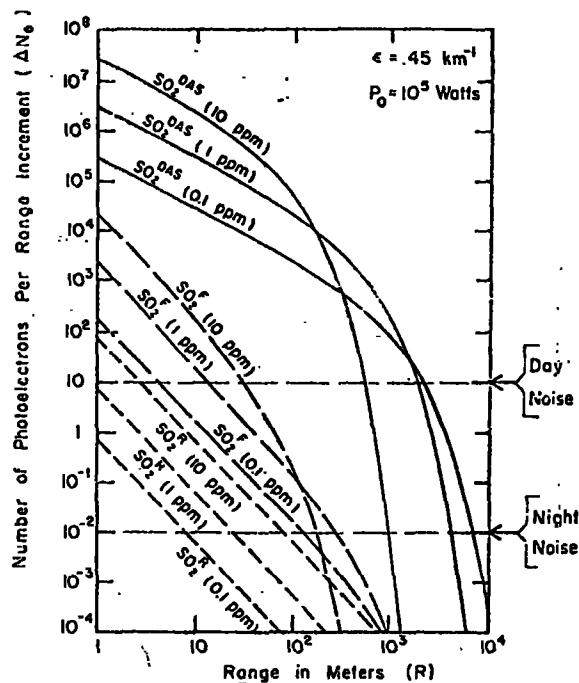


Figure 4-5. Fluorescence, Raman and DAS signals versus range for sulphur dioxide (Measures and Pilon, 1972).

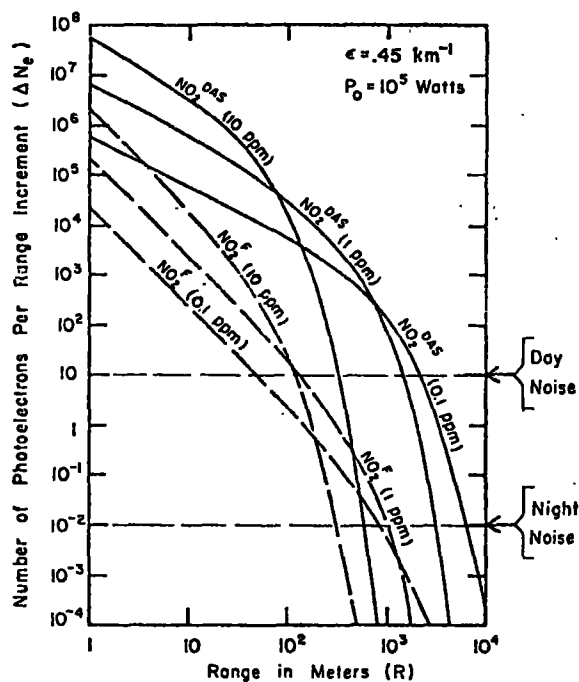


Figure 4-6. Fluorescence and DAS signals versus range for nitrogen dioxide (Measures and Pilon, 1972).

Based on Equation (4-12), a comparison of the techniques may be made for detecting gaseous pollutants. The results of such a comparison for SO<sub>2</sub> and NO<sub>2</sub> in ambient air by Measures and Pilon (1972) are shown in Figures 4-5 and 4-6, where DAS refers to the differential absorption method. There is no Raman calculation for NO<sub>2</sub> since this molecule apparently fluoresces at all visible wavelengths, thus obscuring any Raman effect. It is clear that the differential absorption method shows the highest sensitivity, with fluorescence being better than Raman. Some of the system parameters used in the calculations are given in Table 4-2. These comparisons are strictly on a theoretical basis without considerations of problems such as fluorescence of aerosols and interfering species, imprecise knowledge of quenching effects on the fluorescence cross-section, and the practical problem of optically filtering out unwanted frequencies. A more recent comparison by Byer (1975) also shows DAS to be most sensitive and that future systems should operate in the infrared where more pollutant spectral bands exist, and where eye safety requirements can be more readily met.

TABLE 4-2. System Parameters

Total Output Power	100 kW
Pulse Duration	10 nsec
Collector Diameter	25 cm
Optical Efficiency	75%
Filter Bandwidth	10 Å (NO <sub>2</sub> , SO <sub>2</sub> )
Quantum Efficiency	18%
Resolution ( $\Delta R_{RES}$ )	6 m
$\lambda$ (Diff. Abs.)	3020 Å (SO <sub>2</sub> ); 4480 Å (NO <sub>2</sub> );
$\lambda$ (Fluorescence)	3020 Å (SO <sub>2</sub> ); 4544 Å (NO <sub>2</sub> );

#### 4.2.3 Perimeter Monitoring

Using optical techniques to measure the vertical loading provides a measure of the vertical optical thickness which can be converted to ppm-m, which in turn can be converted to g m<sup>-2</sup>.

The mass flow ( $M \text{ g sec}^{-1}$ ) of pollutant across a line is given by

$$M = \bar{L} \bar{v} s \sin \theta \quad (4-17)$$

where  $s$  is the line length in meters,  $L$  is the mean vertical loading of pollutant in grams per square meter, and  $v$  is the mean wind velocity across the line in meters per sec., and  $\theta$  is the angle between the wind direction and the line.

If this vertical burden is measured continuously along a closed path around a source or a complex of sources, the net mass flow out of this closed path gives the source emission rate ( $M_s$ ), viz.

$$M_s = v \oint L(s) \sin \theta(s) ds. \quad (4-18)$$

If the emitted pollutant is known to be of relatively low concentration in the ambient atmosphere, then a single traverse across the plume,  $90^\circ$  to the wind direction, can be made, and the mass flow rate determined by Equation (4-17). The dimension of the plume(s) can be determined from the shape of the signal recorded by the up-looking sensor (and the sensor's ground speed), and the velocity ( $v$ ) determined by some independent method (laser doppler, UV or IR imagery, or anemometer).

### 4.3 REVIEW OF ACTIVE SYSTEMS

Theoretical comparisons of single-ended active systems for monitoring pollutants have been made by several authors (Kildal and Byer 1971, Measures and Pilon 1972, Ahmed 1973, and Hirschfeld 1974). These studies suggest that differential absorption is the most sensitive, followed by fluorescence and resonance Raman, and finally Raman. However, in reviewing the literature, field measurements appear to have been achieved only with the differential absorption and the Raman methods, and these field measurements were all for  $\text{NO}_2$  and  $\text{SO}_2$ . The fluorescence and resonance Raman methods appear not to have developed beyond the laboratory, and the differential absorption and Raman methods have not been developed for other species of interest in stack emissions.

#### 4.3.1 Differential Absorption

The differential absorption method has been used to measure  $\text{NO}_2$  in urban atmospheres (Rothe et al. 1974a) and in stack emissions (Rothe et al. 1974b). They used a tunable dye laser in the  $4600 \text{ \AA}$  region. For

the urban measurements, a mean concentration of 0.23 ppm of NO<sub>2</sub> was found over the distance 1.73 to 3.74 km. The measurement was made at nighttime and took about 13 minutes; no comparison was made with other data. The same laser system was used to measure NO<sub>2</sub> in stack emissions in a chemical factory. Measurements were made 300 m from the stack exit at a range of 750 m. The distribution across the plume indicates that 1 ppm was detectable. Again the measurement time was long, being about 33 minutes. The same publication shows ambient air contours of NO<sub>2</sub> over the chemical factory, and indicate a measurement sensitivity of 0.5 ppm at a range of 500 m with each data point requiring 20 seconds measurement time. No comparison with other data or a discussion of accuracy is given.

Grant et al. (1974) using a tunable dye laser in the 4500 Å region made nighttime measurements of NO<sub>2</sub> in a closed chamber at a range of 365 m. A sensitivity equivalent to 5 ppm with a 10 m resolution element at this range was determined, but no discussion of the integration time required was given. The results showed good agreement with independent transmissometer readings across the chamber.

Igarashi (1973) reported a differential absorption measurement of NO<sub>2</sub> using the 4480 Å region, and SO<sub>2</sub> using the 3000 Å region. Details of the experiment are not given, but 0.1 ppm of the gases were measured at a range of 300 m, with a resolution element of 100 m, using a 1 mJ laser output.

An interesting variation of this technique due to Zaromb (1974) does not require a tunable laser. It uses the Raman backscattered signals from oxygen and nitrogen, which coincide with absorption bands of NO<sub>2</sub> and SO<sub>2</sub>. A system is presently being built to measure 20-70 ppm of SO<sub>2</sub> and 5-25 ppm of NO<sub>2</sub> at a range of 200 m. The same system will also measure 1000 ppm of CO<sub>2</sub> using the direct Raman signal of CO<sub>2</sub>. No further details are presently available.

Another similar technique (Granatstein et al. 1973) uses the backscatter of laser radiation from droplets (or smoke particles) in a stack effluent. Laboratory measurements of CH<sub>4</sub> and CO<sub>2</sub> were made by tuning a He-Ne laser at either 3.391 μm or 4.217 μm, respectively. Measurements were made using gas concentrations greater than 1000 ppm, and it was concluded that the attenuation properties of the scatterers are needed to interpret the data. It would appear that two adjacent wavelengths are needed for each gas, instead of just one, and then of course, the method is the same as the other differential absorption methods which use the visible/UV.

Feasibility studies have been conducted by Ahmed (1973) and Byer and Garbuny (1973). Ahmed estimates a sensitivity of 0.4 ppm for NO<sub>2</sub> in a 100 m resolution element at a range of 1 km for a 1 mJ laser in the 4000 Å region. Byer and Garbuny, for NO<sub>2</sub>, estimate .85 ppm in 15 m, at 1 km range, using 1 pulse from a 100 mJ laser; they also estimate that .14 ppm of CO can be determined under the same conditions. Schotland (1974) discusses the errors involved in the differential absorption, and using the example of measuring vertical water vapor profiles estimates errors of less than 6% for altitudes below 3 km.

Byer and Garbuny (1973) also considered differential absorption using topographic reflectors. This, of course, does not give range information; it gives only the mean concentration between the laser system and the reflector. They estimate that pollutant concentrations of .01 ppm over a range of 100 m or 10<sup>-4</sup> ppm over 10 km can be measured. The same technique is being developed by Melfi (1974) to measure tropospheric ozone from aircraft using the earth's surface as the reflector. The system uses two tuned CO<sub>2</sub> lasers and will be used to conduct rapid area surveys.

Grant and Hake (1975) have recently made DAS measurements of SO<sub>2</sub> and O<sub>3</sub> at 2900 Å using a 15 mJ dye laser which can meet the Federal eye safety requirements with the addition of a 2 in. diameter beam expander. The gas was contained in a 2.5 m chamber at about 250 m range. Averaging eight pulses, they found an uncertainty of ± 60 ppm-m for SO<sub>2</sub> and ± 130 ppm-m for O<sub>3</sub>. These large errors are attributable to variations in the atmospheric backscatter since the measurements were spread over one hour. They estimate that ± 10 ppm-m for SO<sub>2</sub> and ± 13 ppm-m for O<sub>3</sub> can be achieved by taking all the data within one minute.

Two preliminary reports from the Radio Research Laboratories in Tokyo (Inomata and Igarashi 1974, Asai and Igarashi 1974) discussed the development of two systems suitable for making the two DAS wavelength measurements simultaneously or within 1 msec of each other, to minimize scintillation effects. The simultaneous measurement uses two linearly polarized components (independently tunable) of a dye laser cavity. The results of laboratory NO<sub>2</sub> measurements with this system are discussed in detail in Section 5.3.1. The other report (Asai and Igarashi 1974) concerned the measurement of O<sub>3</sub> using a CO<sub>2</sub> laser and a retroreflector in a long-path measurement. The P(14) and R(14) lines of a single laser were used, and alternately transmitted through the atmosphere at 130 Hz. In controlled tests, they determined a sensitivity of 12.4 ppm-m, but by improving the stability of the laser and by using digital processing, they anticipate a sensitivity of about 5 ppm-m.

Hoell et al. (1975) recently made nighttime measurements of SO<sub>2</sub> downwind using a 0.1 mJ dye laser. They measured the total column of SO<sub>2</sub> as a function of range out to 1.9 km, by averaging over 100 successive pulses for first one wavelength and then the second wavelength, taking a total time of about 15 seconds. The estimated sensitivity of 28 ppb in 900 m could be improved by simultaneous wavelength measurements.

The properties of the various differential absorption systems discussed above are summarized in Table 4-3.

A new approach has been analyzed theoretically by Kobayasi and Inaba (1975), using an infrared heterodyne laser scheme. This approach is of importance because most pollutants have absorption bands in the infrared, while only SO<sub>2</sub> and NO<sub>2</sub> have bands in the UV. The sensitivity in the IR is, of course, lower than in the visible, but the authors state that the heterodyne sensitivity is 10<sup>3</sup> to 10<sup>6</sup> times better than that achieved by the conventional direct detection. They conclude that this method permits the spatially-resolved detection of pollutants (less than ppm) up to several km with an average laser power of 100 W. Heterodyne detection of radiation is discussed in Section 4.4.7.

Murray et al. (1976) recently reported the first measurements with an IR DAS system. This system used a 1 J CO<sub>2</sub> TEA laser to measure water vapor at ranges up to about 1 km. The authors state that the range can be extended by system improvements, and that several other gases, including SO<sub>2</sub>, vinyl chloride, Freon 11 and Freon 12, could be measured in the 10 μm region. Baumgartner et al. (1976) also describe an IR DAS system operating in the 1.4-4.0 μm region. The system consists of a 30 mJ tunable diode source, a 16 in. f/3 Newtonian telescope, an InSb detector, and an on-line minicomputer.

#### 4.3.2 Raman Scattering

The only quantitative measurement of stack emissions using the Raman method appears to be that by Nakahara et al. (1972). They used a frequency doubled Nd: YAG laser at 0.532 μm to obtain a Raman signal from SO<sub>2</sub> in a smokestack plume at a range of 228 m at nighttime. Using 4 mJ pulses, they measured 1850 ppm whereas the actual concentration was 1000 ppm. They attributed the discrepancy to uncertainties in the Raman cross-section for SO<sub>2</sub>, and in the system's parameters. (It could possibly be due to NO<sub>2</sub> fluorescence interfering with the SO<sub>2</sub> Raman signal as reported by three of the authors in the later paper (Nakahara 1973)).

TABLE 4-3. Differential Absorption

Gas	Sensitivity	System Parameters			Range	Resolution	Comments	Ref.
		Laser Energy	pps	Integr. Time				
SO <sub>2</sub>	70 ppm				200 m	not given	} Raman Diff. Abs. } Being assembled in one system. Does not need tunable laser	(a)
NO <sub>2</sub>	5-25 ppm				200 m			
CO <sub>2</sub>	1000 ppm				200 m			
NO <sub>2</sub>	20 ppm	4-8 mJ	8	1 pulse	365 m	100 m	Tunable dye laser - nighttime - controlled sample chamber - claim 10x better possible with 2 Å interf. filter (also same sens. in day)	(b)
NO <sub>2</sub>	.1 ppm	1 mJ			300 m	100 m	No further information.	(c)
SO <sub>2</sub>								
NO <sub>2</sub>	.23 ppm	1 mJ	1	800 s	(1.73-3.74 km) 2.75 km	2 km	Tunable dye laser (nighttime) - actual urban ambient measurements.	(d)
CH <sub>4</sub>	1,000-20,000 ppm	1 mW					Lab test of using backscatter from droplets in plume. Done in IR 3.4 μm and 4.2 μm	(e)
CO <sub>2</sub>								
NO <sub>2</sub>	.4 ppm	1 mJ			1 km	100 m	Feasibility study	(f)
NO <sub>2</sub>	1 ppm	1 mJ	1	2000 s	750 m	100 m	Measurements of stack emission 300 m from exit of stack, plus areal contours over factory	(g)
CO	.14 ppm	100 mJ		1 pulse	1 km	15 m	Feasibility study (daytime)	(h)
NO <sub>2</sub>	.85 ppm							
SO <sub>2</sub>	0.6 ppm	.5 mJ	10	8 pulses	300 m	100 m	Nighttime - controlled sample chamber - 2900 Å - eye safe.	(i)
O <sub>3</sub>	1.2 ppm							
SO <sub>2</sub>	.09 ppm	.1 mJ	15	100 pulses	1.9 km	300 m	Nighttime measurements of stack emission 190 m from exit	(j)

References: (a) Zaromb, 1974; (b) Grant et al. 1974; (c) Igarashi, 1973; (d) Rothe et al. 1974a; (e) Granatstein et al. 1973; (f) Ahmed, 1973; (g) Rothe et al. 1974b; (h) Byer et al. 1973; (i) Grant and Hake 1975; (j) Hoell et al. 1975.



They calculate that 80 ppm of SO<sub>2</sub> can be detected at nighttime with a 10 mJ laser, at a range of 283 m, with a resolution element of 9 m, using an integration time of about 4 minutes. In addition to measuring SO<sub>2</sub>, they use the Raman signal from N<sub>2</sub> to measure the scattering optical thickness (opacity) of the plume, by observations from the same range through and off the plume.

Melfi et al. (1973) made a qualitative nighttime observation of SO<sub>2</sub> in a plume 5 m above the top of the stack using a ruby laser at 6943 Å. Using 1.5 J pulses at a repetition rate of 1 pps averaged over 100 seconds, they detected SO<sub>2</sub> at a range of 210 m with a 3.7 m resolution element. They found good qualitative agreement between the SO<sub>2</sub> Raman intensity and the plant's electrical power output.

Although the two Raman systems discussed above were designed for SO<sub>2</sub>, Inaba and Kobayasi (1972) report on a N<sub>2</sub> laser (3371 Å) demonstration system with a monochromator rather than a filter system. Using this system at a range of 30 m and a resolution of 3 m they analyzed the Raman spectrum from oil smoke and automobile exhaust gas. Using 0.2 mJ pulses with a repetition of 50 pps and a 5 sec integration time, they identified signals from SO<sub>2</sub>, C<sub>2</sub>H<sub>4</sub>, H<sub>2</sub>CO, NO, CO, H<sub>2</sub>S, CH<sub>4</sub>, in addition to the usual CO<sub>2</sub>, O<sub>2</sub>, N<sub>2</sub> and H<sub>2</sub>O.

Poultney et al. (1975) made measurements of SO<sub>2</sub> in a controlled sample chamber at a distance of 300 m at night. Ten percent measurements of  $1.2 \times 10^3$  ppm SO<sub>2</sub> were made in 15 minutes using a 1.5 J ruby laser at 30 pulses/min, interference filters, photon counting detection, and an 8-inch receiver. Certainty of measurement accuracy was checked, by measuring known concentrations of SO<sub>2</sub> in the tank, by tuning the filters on and off the specific Raman line, by varying the SO<sub>2</sub> concentration to very high levels while in SO<sub>2</sub> operation, and by viewing the tank through aerosol veils typical of plumes from stacks with efficient precipitators.

The only other field measurements using the Raman method appear to be those by groups from Block Engineering and Edgewood Arsenal (DeLong 1974). The system uses a frequency doubled ruby laser (0.347 μm) operating with 80 to 160 mJ per pulse at two pulses per second. Daytime field tests have measured controlled amounts of SO<sub>2</sub> (30 ppm), kerosene

(1.7 ppm),  $\text{HNO}_3$  (7 ppm) and organo phosphate (.04 ppm) at a range of 200 m with a resolution length of 10 m, using an integration time of about 1 minute. Based on these measurements and relative Raman cross-sections, DeLong (1974) projected the sensitivity of the present system to other gases, and compared them with calculated values, as shown in Table 4-4. Note that the nighttime sensitivities are about a factor of two better than those in daytime.

TABLE 4-4. Projected and Calculated Sensitivities and System Parameters (DeLong 1974)

Material	Spectral Shift ( $\text{cm}^{-1}$ )	Spectral Position ( $\text{\AA}$ )	Projected Day Sensitivity		Calculated Sensitivity	
			(ppm)	Ref. (21)	Day (ppm)	Night (ppm)
$\text{N}_2$	2331	3777	313		215	124
$\text{O}_2$	1557	3670	262		179	103
CO	2145	3751	317	86	217	125
$\text{CO}_2$	1388	3647	210	62	144	83
$\text{CO}_2$	1288	3634	330		227	130
NO	1877	3713	682		468	269
$\text{N}_2\text{O}$	1290	3634	108		74	43
$\text{H}_2\text{O}$	3652	3976	125	19	86	49
$\text{SO}_2$	1151	3616	58	5	39	23
$\text{CH}_4$	2914	3862	41	9	28	16
$\text{H}_2\text{S}$	2611	3818	57	12	39	22
$\text{NH}_3$	3340	3927	79		54	31
$\text{Cl}_2$	540	3538	91		62	36
$\text{C}_2\text{H}_6$	2650	3823	57		39	22
$\text{H}_2$	530	3536	50		34	20

Present Instrument Parameters	
Collector Diameter, cm	91.4
Transmitter Efficiency	0.9
Receiver Efficiency	0.075
Detector Quantum Efficiency	0.3
Laser Energy @ 3471.5 $\text{\AA}$ , J	0.083
Receiver Bandwidth, u	0.0005
Receiver Field of View, sr	$1 \times 10^{-6}$
Atmospheric Transmission	0.89
Range, cm	$2 \times 10^4$
Range Gate, cm	$10^3$

Smith (1972), Barrett (1974), and Klainer (1974) have suggested a method of enhancing the Raman sensitivity by using a Fabry-Perot interferometer in conjunction with the rotational Raman lines instead of the vibrational lines used in the systems discussed above. The rotational lines are periodically spaced and may be multiplexed by using the Fabry-Perot as a filter with similar periodic transmission peaks. Klainer suggests an increased sensitivity factor over vibrational Raman of 50 for HCl and 150 for CO<sub>2</sub>.

Gelbwachs and Birnbaum (1973) have suggested a problem with the Raman technique due to fluorescence of aerosols which they observed in some in-situ measurements. They estimate that the aerosol fluorescence signal can be equivalent to the Raman signal from 600 ppm of SO<sub>2</sub>, or 6000 ppm of NO, or 3000 ppm of CO. In light of the results reported previously in this section, it appears that these estimated aerosol effects must be much too high. Of course, the discrepancy reported by Nakahara et al. (1972) might be due to aerosol fluorescence, rather than the NO<sub>2</sub> fluorescence suggested by later work (Nakahara et al., 1973).

The properties of the various Raman systems discussed above are summarized in Table 4-5.

#### 4.3.3 Resonance Raman

The resonance Raman method does not appear to have been developed much beyond the theoretical stage. Inaba and Kobayasi (1972) report that the resonance effect has been observed for some gaseous molecules in the laboratory. However, they point out that fluorescence scattering should be expected to be superimposed on the resonance Raman spectrum, since both phenomena require similar exciting frequencies and the emitted frequencies are in the same region. This probable superposition would make accurate determination of the pollutant concentration very difficult, if not impossible. Possibly adjacent frequencies on and off the Raman frequency could be used in a differencing technique to subtract out the fluorescence signal; this method may not be amenable to present filter capabilities.

Fowler and Berger (1974), under EPA sponsorship, investigated the feasibility of measuring SO<sub>2</sub> in stack emissions using fluorescence and resonance Raman methods. In laboratory measurements they found a resonance Raman signal 1.8 times greater than the fluorescence signal around 3000 Å; this ratio could be improved with a narrower spectral

TABLE 4-5. Raman

Gas	Sensitivity	System Parameters				Resolution	Comments	Ref.
		Laser Energy	pps	Integr. Time	Range			
SO <sub>2</sub>	Qualitative	1.5 J	1	100 s	210 m	3.7 m	Nighttime - smokestack	(a)
SO <sub>2</sub>	30 ppm	160 mJ	2	50 s	200 m	10 m	Daylight - controlled source in field.	(b)
Kerosene	1.7 ppm				200 m	10 m		
HCl	x 50	compared with vibrational Raman					Theory of Fabry Perot interferometer to multiplex rotational Raman lines	(c)
CO <sub>2</sub>	x 150							
SO <sub>2</sub>	80 ppm	10 mJ	40	250 s	283	9 m	Theoretical (nighttime) Power plant nighttime measurements: 1850 ppm - Raman (1000 ppm - actual)	(d)
SO <sub>2</sub>	100 ppm	50 mJ	1	100 s	100	10	Calculated (daytime)	(e)
SO <sub>2</sub>	qualitative	0.2 mJ	50	5 s	30	3	Experimental	(e)
C <sub>2</sub> H <sub>4</sub>								
H <sub>2</sub> CO								
NO								
CO								
H <sub>2</sub> S								
CH <sub>4</sub>								
SO <sub>2</sub>	70 ppm	1.5 J	0.5	900 s	300 m	not given	Nighttime - controlled sample chamber	(f)

References: (a) Melfi et al. 1973; (b) DeLong, 1974; (c) Klainer, 1974; (d) Nakahara et al. 1972; (e) Inaba et al. 1972; (f) Poultney et al. 1975.

bandpass (they used 24 Å). The authors also confirm the problems of fluorescence from other species and particles making quantitative measurements unlikely.

Laboratory measurements of the resonance Raman cross-sections have have been reported for SO<sub>2</sub> (Rosen et al. 1975).

#### 4.3.4 Fluorescence

Although there have been several theoretical discussions of the usefulness of fluorescence in the remote sensing of pollutants, there appears to be only one report of actual measurements. These were measurements of NO<sub>2</sub> by Nakahara et al. (1973), who apparently obtained them as a result of NO<sub>2</sub> fluorescence interfering with their Raman measurement of SO<sub>2</sub> in the visible region.

It is clear from this and the preceding discussion on resonance Raman that there are problems in the interpretation of fluorescence (and, of course, Raman) signals. In addition, Kildal and Byer (1971) state that there is no straightforward relationship between the fluorescence intensity and the pollutant concentration, making quantitative measurements very difficult. Presumably this latter problem can be overcome with careful laboratory studies, and, in fact, has been investigated in the infrared by Robinson and Dake (1973). They found that at atmospheric pressure the IR fluorescence intensity is linearly related to the laser power, and to the 6/5 power of the concentration, suggesting that remote monitoring of fluorescence is possible at least in the IR. The same authors (1974) extrapolate some laboratory measurements of ethylene fluorescence using a CO<sub>2</sub> laser to infer that 0.1 ppm of ethylene could be detected at 10 km, or 100 ppm at 1000 km. (Their graphs actually appear to give 0.2 ppm at 10 km and 1000 ppm at 1000 km.) They suggest this latter sensitivity would allow satellite monitoring of stack effluents. However, it appears that they have not considered problems such as the field-of-view being greater than the stack plume dimensions, and background noise.

Pikus et al. (1971) have also considered a satellite-borne system for detecting NO based on fluorescence at 1927 cm<sup>-1</sup>. The calculations assume a 5-joule pulse CO laser and compute a threshold NO concentration sensitivity of  $2 \times 10^{11} \text{cm}^{-3}$  (7.4 ppb) at sea level. Even assuming that a 5-joule laser were available for satellite use, these results may be optimistic since the calculations neglect detector and system noise

sources, 80 cm diameter collecting optics are required, a 50% optical efficiency is assumed, and interferences due to other species are neglected. (At  $1927\text{ cm}^{-1}$ ,  $\text{H}_2\text{O}$  is a strong absorber over the 0.1 micron band pass assumed.)

Another estimate (Menzies 1971) of the capability of remote sensing of NO fluorescence using a 1 mJ pulse CQ laser and sensitive heterodyne detection indicates that 0.1 ppm in a 300 m path can be measured at a 1 km range, if the relative humidity is 50% (quenching by  $\text{H}_2\text{O}$  is faster than that of other constituents for this case).

For fluorescence in the visible/UV region, Kildal and Byer (1971) have estimated that at nighttime about 0.5 ppm of  $\text{NO}_2$  and  $\text{SO}_2$  in a 15 m path can be detected at a range of 100 m using a 0.1 mJ pulse laser. They state that this sensitivity drops by a factor of 200 during the day.

Penney et al. (1973) have made laboratory observations of  $\text{NO}_2$  and  $\text{O}_3$  fluorescence using a  $0.488\text{ }\mu\text{m}$  argon laser, and of  $\text{SO}_2$  fluorescence using a dye laser tuned near  $0.3\text{ }\mu\text{m}$ . They found  $\text{SO}_2$  fluorescence to be strongest, and estimate that it should be feasible to measure  $10^{-3}$  ppm of  $\text{SO}_2$  with a resolution element of 100 m at a range of 1 km.

Gelbwachs et al. (1972, 1973) have also made laboratory observations of  $\text{NO}_2$  fluorescence using laser excitation at 4416 and  $4880\text{ }\text{\AA}$ . They then developed an in-situ fluorescence technique to measure ambient  $\text{NO}_2$ . They do not discuss the possibility of extending the method to remote sensing, except to point out that they observed aerosol fluorescence which may interfere with remote sensing applications.

The sensitivities of the various fluorescence systems discussed in this section are summarized in Table 4-6.

#### 4.3.5 Lidar

Much of the work to date on lidar systems for measuring particulate (Mie) elastic scattering has been done by the group at Stanford Research Institute. Collis and Uthe (1972) discuss the capabilities of lidar systems.

The backscatter from particles is, of course, dependent on the shapes, size distribution and refractive index of the particles, so that return signals will vary from plume to plume. Hence, in order to apply the technique to enforcement monitoring, it will be necessary to make calibrations for the different types of particles.

TABLE 4-6. Fluorescence

Gas	Sensitivity	Range	Resolution	Comments	Ref.
In-situ technique shows that fluorescence from aerosols				$\left. \begin{array}{l} 600 \text{ ppm } \text{SO}_2 \\ 6000 \text{ ppm } \text{NO} \\ 3000 \text{ ppm } \text{CO} \end{array} \right\} \text{Raman}$ $1 \text{ ppm } \text{NO}_2 - \text{fluorescence}$	(a)
NO	0.1 ppm	1 km	300 m	50% R. Humidity. Heterodyne detector Theoretical estimate IR fluorescence	(b)
SO <sub>2</sub> } NO <sub>2</sub> }	~. 5 ppm	100 m	15 m	Theoretical. Nighttime UV. Daytime sensitivity down by 200 x.	(c)
NO	7.4 ppb	Satellite to Surface		Theoretical	(d)
NO <sub>2</sub>	in-situ fluorescence				(e)
C <sub>2</sub> H <sub>4</sub>	.2 ppm	10 km	1 m	CO <sub>2</sub> laser calculations extrapolated from lab tests (0.3 sec time constant)	(f)
NO <sub>2</sub>				Measurements in stack plume - not discussed in abstract	(g)
SO <sub>2</sub>	10 <sup>-3</sup> ppm	1 km	100 m	Theoretical	(h)

References: (a) Gelbwachs et al. 1973; (b) Menzies, 1971; (c) Kildal et al. 1971; (d) Pikus et al. 1971; (e) Gelbwachs, 1972; (f) Robinson et al. 1974; (g) Nakahara et al. 1973; (h) Penney et al. 1973.

Collis and Uthe (1972) summarized the status of lidar systems in 1972 as follows: "Lidar techniques of remote observation of atmospheric particulate concentrations have obvious value in a wide range of air pollution applications where semi-quantitative spatial and temporal data are needed, and are already in regular use in research. For routine operational use, lower cost, eye safe instrumentation must be developed. The degree to which lidar can be used for making objective, remote measurements of significant parameters (i. e., turbidity, opacity or mass concentration) has not been fully established. Considerable progress is being made in this difficult area and already quantitative data can be derived in research applications. For routine use in emission source monitoring however, while work in progress appears promising, the development of a legally acceptable, low cost operational technique is still some way off. "

Progress has been made in the meantime and an operational system was fabricated by GE for EPA, based on the original SRI concept (Evans, 1967). It is shown in its operating configuration at the Barbados Island Station of the Philadelphia Electric Company in Figure 4-7.



Figure 4-7. EPA Mobile Lidar System developed by GE shown in operating configuration at the Barbados Island Station at the Philadelphia Electric Company (Cook et al., 1972)



Cook et al. (1972) report a method in which the plume transmittance is measured by comparing the clear air lidar return from the near side of the plume with that from the far side. They made field measurements on a power plant smoke plume with a van-mounted ruby laser (1 J) system at a range of 487 m. A comparison was made with the passive telephotometer (Conner and Hodkinson 1967), which makes a contrast measurement and relies on having a target with contrast (e.g. sky and hillside) behind the plume. The passive technique is somewhat sensitive to the illumination conditions (e.g. sun position, cloud cover). The lidar accuracy is limited by the PM tube afterpulsing, but within the error limits both methods agreed. The lidar system errors are estimated to be  $< 12\%$  for an opacity of  $< 0.5$ , and  $< 2.5\%$  for opacity  $< 0.2$ .

This system has been recently improved by replacing the PM tube and hence eliminating the afterpulsing. Conner (1975) considers that in good atmospheric conditions the method can now measure the opacity within  $2\%$ . Good atmospheric conditions mean that the atmospheric aerosol content is the same on both sides of the plume. Under poor atmospheric conditions, readings are variable and must be averaged over a period of time.

The technique of Cook et al. is basically the same as that of Nakahara et al. (1972) who used the Raman signal from  $N_2$  in front and through the plume. Nakahara et al. considers their method to be more accurate since the  $N_2$  concentration and Raman backscatter are better known than the atmospheric particle concentration and backscatter. This latter technique appears advantageous since the signal is readily obtained from a Raman system for gases, so that a separate system for particle observations is not required. However, due to the low Raman signals, the range capability would be less, and sky background noise would be more significant.

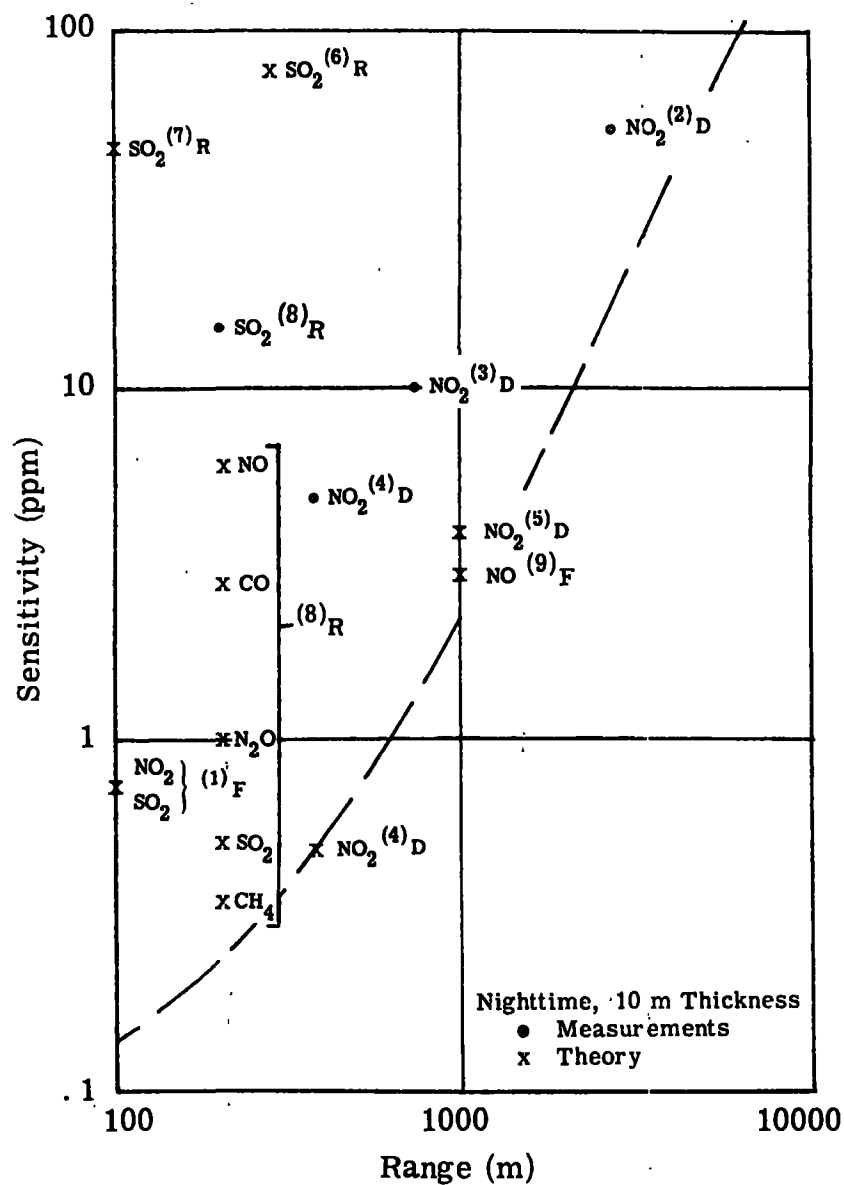
It would appear that the remote laser method could provide observations under certain conditions where the passive observations are not possible. The laser method can give an absolute transmittance, and only requires a clear line-of-sight to the plume. In addition, the laser method is not restricted to daytime observations like the passive one. However, Belanger (1974) discusses a night vision instrument which uses an image intensifier to provide a nighttime image of the scene (including the stack plume) on a phosphor screen. The author considers that the method would be suitable for enforcement of regulations, but does not discuss the possible effects of variations of ambient light.

Conner (1975) considers that the present pulsed laser system may be limited for operational use due to eye safety hazards (see also discussion in Section 5.2). SRI (Saraf and Jackson, 1975), under EPA funding, developed a portable, low power CW laser system, to measure opacity, which would meet safety requirements, and would be smaller and less expensive. Unfortunately the system was not sensitive enough for daytime operation, and the development was redirected (Conner 1976) to a system using a GaAs laser operated at a high pulse repetition frequency (PRF). It is hoped to demonstrate the feasibility of this high PRF system by mid-1976. Conner is hopeful that the price for the system might be less than \$20,000.

It should be noted that optical techniques, as presently known, cannot separate the scattering by particles and by water droplets. The remote sensor will have to examine the plume some distance from the stack exit where visual observation indicates that the droplets have evaporated.

#### 4.3.6 Intercomparison of Measurements of Gases

In order to compare the measurements and predictions for the various methods for remotely measuring gaseous pollutants, the results discussed in Sections 4.3.1 to 4.3.4 are normalized to a certain extent and presented in Figure 4-8. The results are normalized to a pollutant thickness (resolution element) of 10 m. (It should be noted that in an extended source the fluorescence technique cannot achieve 10 m resolution due to the long lifetime of the phenomenon; this lifetime restricts resolution to 100-300 m depending on the molecule.) On the basis of DeLong's (1974) estimate, we assume that at nighttime the Raman method is twice as sensitive as during the day; all other published results are for nighttime. In normalizing for the resolution element, it is assumed that the sensitivity is inversely proportional to the resolution length (see Equation 4-12)). No normalization has been made for the systems parameters such as receiver aperture, laser energy and repetition rate, integration time, wavelength, atmospheric effects, type of detector and assumptions about the relevant scattering cross-section.



References: (1) Kildal et al. 1971 (6) Nakahara et al. 1972  
 (2) Rothe et al. 1974a (7) Inaba et al. 1972  
 (3) Rothe et al. 1974b (8) DeLong, 1974  
 (4) Grant et al. 1974 (9) Menzies, 1971  
 (5) Ahmed, 1973

Figure 4-8. Sensitivity vs. Range. Normalized to 10 m thickness at nighttime. The data points are labeled as [species (reference) technique] where D is differential absorption, R is Raman and F is fluorescence.

The results do show that in general the field measurements are lagging behind the theoretical predictions, which, of course, are all based on reasonable systems parameters. It appears that predictions for the important gases are indicating a lower sensitivity limit shown by the dashed line in Figure 4-8, ranging from about 0.1 ppm at 100 m to about 2.5 ppm at 1000 m.

#### 4.3.7 Stack Effluent Velocity Measurements

Since many emission standards for stationary sources are based on a mass emission rate, a remote measurement of effluent concentration alone is insufficient for determination of non-compliance. The perimeter measurement and area surveys can provide the mass emission rate, but, of course, it will not always be possible to isolate a single source in that type of measurement. Other remote sensing methods provide only a concentration measurement, and a measurement of effluent velocity must be obtained to determine the mass emission rate.

In addition to the two vidicon methods being developed for determining the velocity, EPA and NASA have been supporting the evaluation of a laser-doppler velocimeter (LDV) at the Raytheon Company (Herget et al. 1975, Miller and Sonnenschein, 1975). A comparable LDV system has been built and tested by Lockheed Aircraft Corporation (Lawrence et al. 1975). The Raytheon LDV system consists of a 20-watt CO<sub>2</sub> laser, solid invar interferometer, 30 cm diameter f/8 transmitting and receiving telescope, and a Ge:Cu detector. An elliptically-shaped flat tracking mirror and a bore-sighted telescope are used to aim the laser beam at the stack plume. The difference frequency at the detector produced by the local oscillator (the laser) and the energy backscattered and doppler-shifted by the particles in the plume is monitored visually on a Hewlett-Packard spectrum analyzer. The detector output is recorded on separate magnetic tape channels after processing by the spectrum analyzer and also by a specially built frequency tracker.

The system was tested on a power plant stack (Miller and Sonnenschein, 1975) at a range of 400 m, and showed good agreement with in-situ measurements of the velocity as shown in Table 4-7. The in-situ data were averaged over a 30-minute period, and the LDV velocity is obtained by analyzing a series of 50 msec intervals over a period of 2 seconds. Such data show wide fluctuations in velocity and amplitude. For each velocity determination, the resultant spectrum is a Lorentzian-shaped curve of amplitude versus velocity extending from about zero to 2V. The plume velocity  $V$  is taken as the peak amplitude of the spectrum.

These tests also showed that a linear relationship exists between the intensity of the laser return signal and the in-stack measured opacity of the plume. Since there is probably a relationship (determined empirically by in-situ methods) between opacity and the mass loading for each type of source (Conner 1974), the LDV system has the potential to provide a mass emission rate for particles from a source.

TABLE 4-7. In-Stack and Remote Velocity Data  
(Miller and Sonnenschein 1975)

Load MW	Pitot Velocity Ft/Sec	Doppler Velocity Ft/Sec
83	87.3	80
83	87.3	83
83	100	90
92	110	95
96	107	83
96	107	90
97	102	90
97	102	92
109	118	100
109	118	107
111	118	100
111	118	103
122	129	113
122	129	119
124	136	112
124	136	118
130	136	125
130	142	117
130	142	125
135	146	120
135	146	130
137	146	125
137	146	135

#### 4.4 REVIEW OF PASSIVE SYSTEMS

There seems to be less work on passive methods for source monitoring than on active systems, no doubt due to the data interpretation problems of the passive techniques. However, due to their generally lower cost, it would appear that passive methods would be more attractive for routine monitoring, even though, with their complex data interpretation, they might be more difficult to be introduced in court as admissible evidence. On the other hand, passive methods may be best suited for surveillance monitoring.

Passive methods may be used in either direct observation of the plume, as discussed in this section, or indirect observation by the perimeter monitoring technique, as discussed in Section 4.5.

Two instruments so far developed, the matched-filter spectrometer and the gas filter correlation radiometer, are small, portable and relatively inexpensive, and are thus appealing for enforcement monitoring, whereas other passive systems are larger, more expensive and often require a computer for data processing.

#### 4.4.1 Passive Opacity Techniques

The main passive technique used at the present time is that of the trained visual observer. The observers are trained at EPA smoke schools, using controlled smokestacks, to make the measurements according to Ref. Method 9, taking into account the prevailing illumination conditions. The training method is such that it is generally agreed the observer in the field will underestimate, rather than overestimate, the opacity.

Instrumental techniques for passive opacity measurements have been discussed by Conner and Hodkinson (1967) and include telephotometers, photography, Volz sun photometers, and observers with comparators. In addition, there is the night vision image intensifier for night observations of opacity.

The Volz photometer method requires a direct line-of-sight to the sun through the plume and alongside it; these conditions will not always be available, and so the technique is limited.

The telephotometer and photography method make an observation of a contrast target (e.g. sky and hillside) through and alongside the plume and use the theory of contrast reduction to estimate the plume transmittance; clearly, a suitable target will not always be available.

Comparators may be used by an observer to estimate the plume opacity. The comparator, which contains scattering particles of varying number densities, is viewed in comparison with the plume under the same illumination conditions. Comparators have been developed for both black and white plumes.

The night vision image intensifier is being evaluated by personnel in EPA Region III (Smith 1974), and they consider that it should be suitable for use by observers who take a training course. Of course, it will have the same limitations due to illumination variations.

EPA Region III uses photography, both on the ground and from the air, in their surveillance program. They find that showing a photograph of emissions to the offender usually brings about compliance. Smith (1974) suggests that the contrast reduction of ground features might be measured by densitometry of the aerial photographs. Due to illumination effects and the difficulty of finding constant extensive ground contrast targets, it is doubtful whether this method can be useful. However, Pressman (1976) is working on another aerial photography technique for measuring opacity, illustrated in Figure 4-9. Measurements

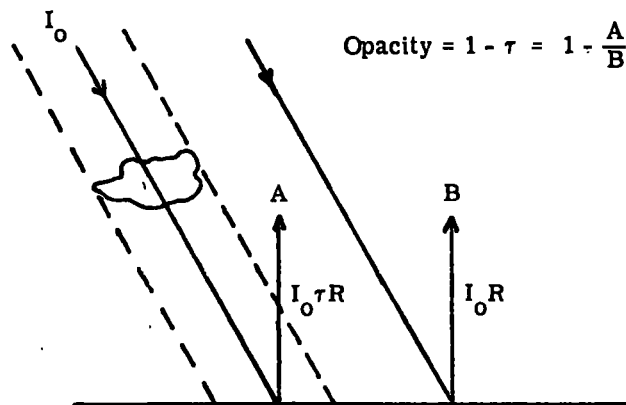


Figure 4-9. Opacity measurement from aircraft

of radiance are made in and alongside the plume shadow on a homogeneous reflecting ground surface. It is clear from Figure 4-9 that the ratio of the radiances gives the transmittance of the plume, assuming that the diffuse radiance over each area is the same, and that there are no other sources of radiation, such as reflected sunlight, illuminating the surface. An analysis of this technique was conducted at EPA-Las Vegas, taking into consideration the film processing requirements, spectral variations of ground features, interference due to sunlight scattered from other structures on to the target surface, and the frequency of suitable targets in photographs of industrial areas. Some preliminary flight tests have been made, indicating that the method works, although no ground-truth measurements have been made yet. Pressman thinks that this method can be more accurate than the visual observer. It can also, of course, check many more stacks per day than the visual observer.

This technique is, of course, limited to daytime operation, and is best used early morning and late afternoon to obtain clear shadows. The wind must also be in the right direction so that the shadow lies over a homogeneous target area. However, within these limitations the technique does appear promising.

#### 4.4.2 Matched-Filter Spectrometer

This technique, in which the spectrum of the incoming radiation is automatically compared with a stored (in the spectrometer) replica of the spectrum of the gas being measured, was pioneered for remote sensing of air pollution by Barringer (1966), and appears to be the first electro-optical instrument for air pollution. It uses scattered sunlight and is restricted to daytime use, and has been developed only for SO<sub>2</sub> (at 3100 Å) and NO<sub>2</sub> (at 4400 Å). The instrument has been refined over the years and is presently marketed as COSPEC II, which is small and portable. The instrument, shown in Figure 4-10, consists of two telescopes to collect light from a distant source (scattered solar radiation), a two-grating

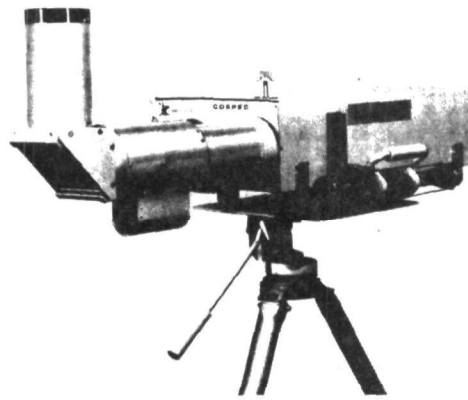


Figure 4-10. The Barringer COSPEC II.



monochromator for light dispersion, a disc-shaped multislit mask, and an electronics system for signal processing. The disc is composed of circular slits photo-etched in aluminum on quartz, and provides a high contrast reference spectrum for matching against the incoming absorption spectra. The arrangement is designed to correlate successively in a positive and a negative sense with the  $\text{SO}_2$  absorption bands via disc rotation in the exit plane on the monochromator. The detector used is the XP 1118 photomultiplier tube. Signal processing results in a voltage output proportional to the optical depth in ppm-m of gas being observed. A schematic of one telescope and associated optics is shown in Figure 4-11.

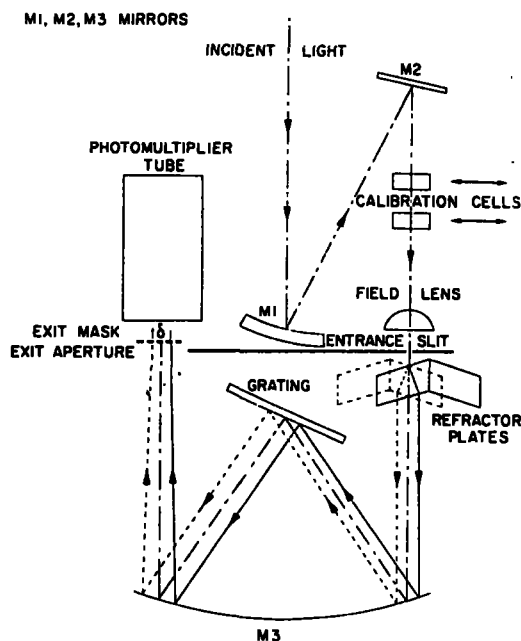


Figure 4-11. Schematic layout of the Barringer remote sensor (Newcomb and Millan, 1970)

The dynamic range of the instrument is 100-10,000 ppm-m. Calibration is effected using four fused-silica cells containing known concentrations of  $\text{SO}_2$  that are incorporated into the instrument. The instrument is 50 x 25 x 37 cm in size, weighs approximately 18 kg and can be operated by either a 12V DC battery or conventional 115V 60 Hz.

The COSPEC II was recently tested by EPA (Barnes et al. 1974) in comparison with in-stack measurements for  $\text{SO}_2$ . The results of the tests are shown in Table 4-8.

TABLE 4-8. Comparison of In-Stack and Remote SO<sub>2</sub> Concentration Measurements

Range (meters)	In-Stack (ppm)	Remote (ppm)	$\frac{(IS) - (REM)}{(IS)} \times 100$
20	500	465	7
20	585	520	10
200	700	240	65
300	460	224	52
300	450	205	54
300	700	275	60

From the table it is seen that agreement with the in-stack readings at the closest range is quite good. However, at greater distances correlation becomes quite poor. The value at 200 m is suspect since it represents only one hour of data taken on one day. On that day the plant experienced an outage terminating further work during the study. At 300 m the results are low, but reasonably consistent (54% to 60%). The authors consider that this consistency could possibly be applicable in using the instrument at extended ranges if the range correction factor is constant under different meteorological conditions, such as rain, haze, and smog, but that much more work would be needed before a firm conclusion could be reached on this matter.

A more serious problem was discussed by Barnes et al. (1974). In their tests they varied the plume opacity by sequentially inactivating the electrostatic precipitators in the stack. When the second bank of precipitators was turned off, resulting in a 20% opacity reading (by in-stack transmissometer), the COSPEC II signal level dropped to an unmeasurable level although the in-stack SO<sub>2</sub> monitors showed no change in SO<sub>2</sub> readings. Since this level (20% opacity) is within federal regulations, it would appear that the COSPEC instrument would not be suitable for enforcement monitoring.

One other problem encountered during the field tests was that of the plume not remaining in the field-of-view of the COSPEC II. This occurred even on moderately windy days. This point should, of course, be noted in the design of any remote sensor. The COSPEC II FOV is 3 mr x 10 mr. Reducing that to 3 mr x 3 mr or perhaps 3 mr x 5 mr should allow operation during moderately windy days when the plume is not reasonably vertical for more than one or two stack diameters.

Barnes et al. (1974), in their summary, state "In conclusion, the COSPEC II in its present design is inadequate for EPA use for routine monitoring purposes. The main limitation, as has been noted, is inadequate AGC compensation for scattering effects by particulates both in the plume and in the intervening atmosphere. The less serious problem of field-of-view is perhaps a more readily rectified one. It should be noted here that EMI, Inc. recommends usage of the COSPEC in two other modes, namely as a mobile perimeter monitor (looking vertically into the sky) and from helicopters (sighting horizontally through plumes)." (See Section 4.5).

#### 4.4.3 Gas Filter Correlation

Another small portable remote sensor is the Gas Filter Correlation (GFC) instrument, for measuring  $\text{SO}_2$ , under development for EPA (Bartle 1974a). It operates in the infrared and can be used both day and night.

GFC is a modification of Non-Dispersive Infra-Red (NDIR) technique that has been known for some time. In contrast to pure radiometry or dispersive spectroscopy, a GFC (non-dispersive) device uses the gas itself to obtain the ultimate high-spectral resolution filter (provided by the line-width of the gas). High spectral resolution is the most important parameter in obtaining specificity and accuracy in pollutant analysis.

GFC combines the high energy throughput feature of radiometers and the high-resolution features of dispersive instruments. It makes use of the contributions of all spectral lines of a band system of a particular species to obtain sensitivity. Specificity is obtained by making use of the correlation between spectra arising from the particular species in the source and in the instrument gas cell. Discrimination for many pollutant species against many interfering species occurring naturally and in polluted atmospheres has been studied previously (Bartle 1972). In addition, a ratioing technique may be employed that minimizes effects of changes in source intensity, background radiation, and continuum absorption due to aerosols, water vapor, or other molecular species. The incoming radiation at the sensor is chopped so that it alternately passes through two optical paths, one through a transparent cell and one containing the specific gas. Thus, the radiation is modulated only at the wavelengths at which the pollutant absorbs and high specificity results.

The JRB instrument operates in the 4  $\mu\text{m}$  combination band of  $\text{SO}_2$  and is designed to minimize the effects of not knowing the plume temperature, and uses a dual split design, shown in Figure 4-12a. It has been shown (Bartle 1972) that the signal generated by chopping between two cells is a non-linear function depending upon the  $\text{SO}_2$  in the plume and fixed instrument parameters and the difference between the radiance emitted by the plume and background atmosphere. By ratioing two GFC signals obtained using different amounts of  $\text{SO}_2$  in the specifying cells, the effects of plume and atmospheric radiance are greatly minimized, so that the plume temperature does not have to be measured. Separate tuning fork choppers are used for each cell pair. The cells are 10 cm in length. The image of the stack plume is focused by an  $f/2.46$  (at 4  $\mu\text{m}$ ) lens on a 1 x 1 mm detector which defines the field-of-view to be 8 milliradians (8 m at 1 km). An ambient temperature operation (ATO) PbSe detector is used; but a single-stage thermoelectric cooler is used to provide temperature control.

---

Section A-A of Figure 4-12a shows the configuration of the dual split cell. The two gas cells contain different partial pressures of  $\text{SO}_2$  and are pressurized to 1 atm with pure  $\text{N}_2$  to pressure-broaden the  $\text{SO}_2$  lines. The reference cells contain relatively low pressures of  $\text{SO}_2$  and are also pressurized to 1 atm with pure  $\text{N}_2$ . The cell areas are the maximum allowed by the tuning fork choppers, about 8 mm wide x 1.9 mm long.

Section B-B of Figure 4-12a shows the dual tuning fork configuration. Fork-1 is shown closed, allowing radiation to pass through the V-1 reference cells; Fork-2 is shown open, allowing radiation to pass through the  $\Delta\text{V}$ -2 gas cell. Fork-1 operates a frequency of 40 Hz and Fork-2 at a frequency of 100 Hz. Because a single lens serves both  $\Delta\text{V}$ -1 and  $\Delta\text{V}$ -2 systems have exactly the same field-of-view at the stack plume, as is essential for proper cancellation of the stack effluent temperature factor. The superimposed image signals of the two  $\Delta\text{V}$  systems are electronically separated by the signal processing. A third tuning fork chopper, operating at 800 Hz, is located immediately ahead of the detector aperture to eliminate the low frequency  $1/f$  detector noise from the PbSe detector. A photograph of the instrument is shown in Figure 4-12b.

---

The JRB instrument was used in a field test conducted by EPA (Bartle 1974b), in which remote measurements were compared with in-situ extractive techniques (DuPont Analyzer and EPA Method 6). The results shown in Table 4-9 show fairly good agreement within the experimental error between the methods. It appears that the errors in Table 4-9 are greater than would be expected from the previously quoted instrument sensitivities, but this may be due to instrument balancing problems experienced

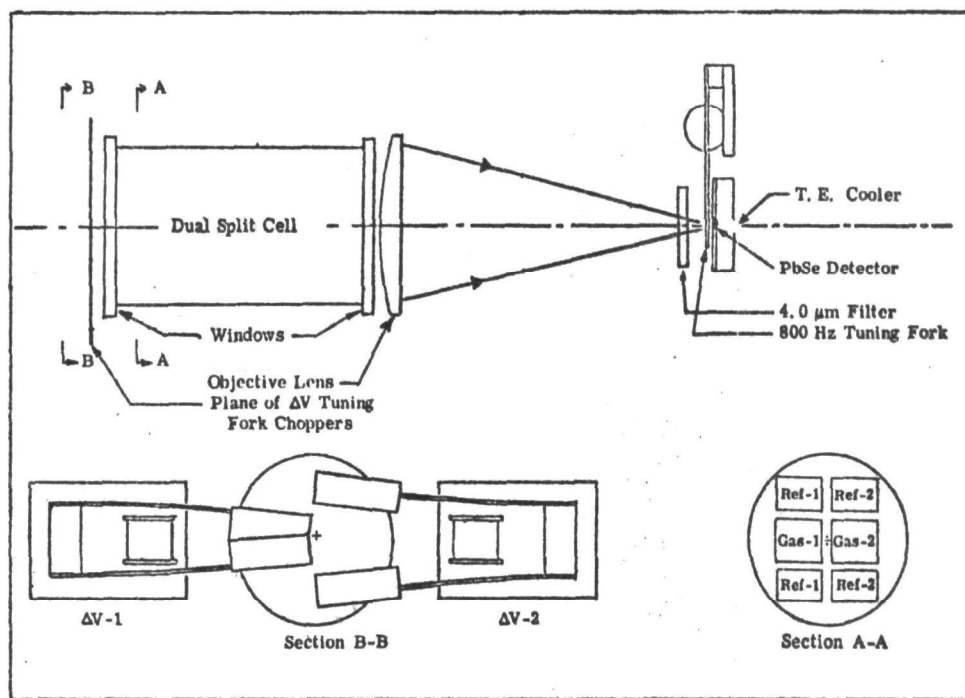


Figure 4-12a. Optical system schematic of the JRB remote SO<sub>2</sub> monitor



Weight: 22 pounds

Size: 38 cm length x 18 cm width x 23 cm height

Field-of-view: 8.0 m rad x 8.0 m rad

Power requirements: 3.3 watts

Power source: 8 Eveready E91 NiCd (1.2 amp-hr, 6.25 V);  
(Batteries) 2 Eveready R6 NiCd (6 amp-hr, 1.25 V)

Battery operating lifetime: >8 hours

Warm-up time: 3 minutes

Time constant (to 1 - 1/e signal level): 1, 3, 10, 30, and  
90 seconds

Attenuation: 1, 5, 10, 50 and 100

Gain selection: 1, 5, 10, 50 and 100

Recording: 1% panel meter; recorder jacks for  
 $\Delta V_1$ ,  $\Delta V_2$  and  $\Delta V_2/\Delta V_1$  signals

Figure 4-12b. Photograph and physical specifications of JRB SO<sub>2</sub> remote sensor

TABLE 4-9. Summary of Average Values of Remote GFC and Extractive Data

Range (m)	Date	Time	[SO <sub>2</sub> ], ppm				% Deviation
			Remote		Extractive*		
			T, °C	Conc.	DuPont Analyzer	EPA Method 6	
160	8-12-74	10:00-11:45	150	540 ± 200	---	---	
390	8-12-74	13:45-16:50	150	630 ± 170	---	525 ± 25	-17
390	8-13-74	09:00-12:00	150	530 ± 120	---	398 ± 23	-25
390	8-13-74	18:45-21:00	150	550 ± 120	412 ± 18	---	-25
390	8-14-74	09:15-12:45	120	490 ± 160	422 ± 28	401 ± 17	-16
390	8-14-74	14:30-16:30	150	440 ± 110	472 ± 32	475 ± 7	+ 7
160	8-15-74	09:30-11:45	110	750 ± 70	519 ± 21	499 ± 11	-32

\* All extractive data taken from plume with a temperature of 150 ± 5 C.

in the field. There does not appear to be any effect of range. The data on 8-14-74 were apparently taken in very hazy conditions, but there was no significant effect due to the haze. On this same day, the stack precipitators were sequentially turned off giving a maximum opacity of about 37%, but there was apparently no effect on the remote SO<sub>2</sub> data. However, these tests and subsequent observations of different smokestacks (Bartle, 1975) and controlled wind tunnel tests (Herget, 1976) revealed that the sensitivity of the instrument is limited. This limitation may be overcome by increasing the sensitivity of the detector through cooling. Bartle (1975) has established the relationship between noise-equivalent optical thickness (in ppm-m) and temperature of the present instrument. His results are shown in Figure 4-13.

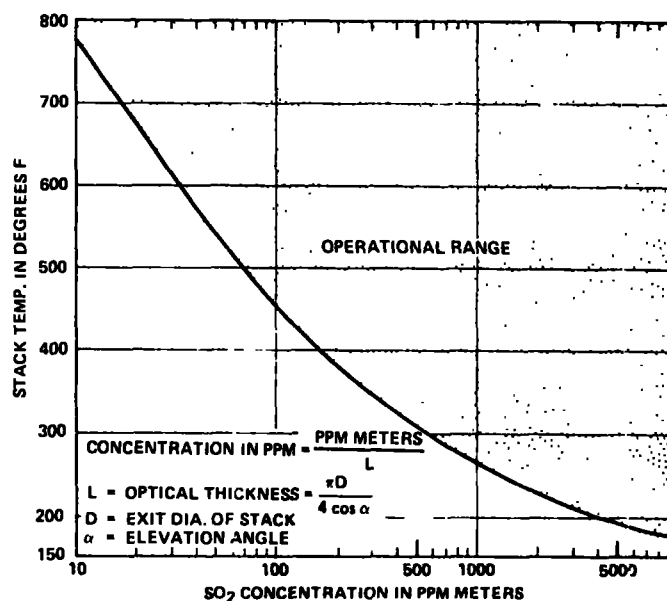


Figure 4-13. Noise-equivalent optical thickness (rms) as a function of source temperature

#### 4.4.4 Medium Resolution Dispersive Spectrometer System

The dispersive spectrometer system, which bears the acronym ROSE (Remote Optical Sensing of Emissions), was designed and fabricated for EPA by General Dynamics/Convair. The basic purpose of the ROSE system is to study the spectra of various stationary source emissions so as to determine which spectral regions are most suitable for measurement of particular species and to verify which species are actually present in the effluent. This information can then be used to assist in the design of simple instruments for specific pollutants. The instrument is generally not considered by EPA for routine monitoring due to its bulk and cost, although it is mounted in a truck like the laser systems. The contractor's final report (Streiff and Claysmith 1972) describes the ROSE system in detail. Figure 4-14 shows the principal parts of the receiver section: Dall-Kirkham telescope optics with a 60-cm diameter primary mirror, Perkin-Elmer Model 210 linear wave number drive monochromator, and detector housing with a portion of a Cryogenic Technology closed-cycle helium refrigeration system. The monochromator contains two gratings that are each used in first order with long-wave pass filters to cover the spectral ranges 2.8-6.5 and 6.5-14 microns. The spectral resolution is variable, depending on the

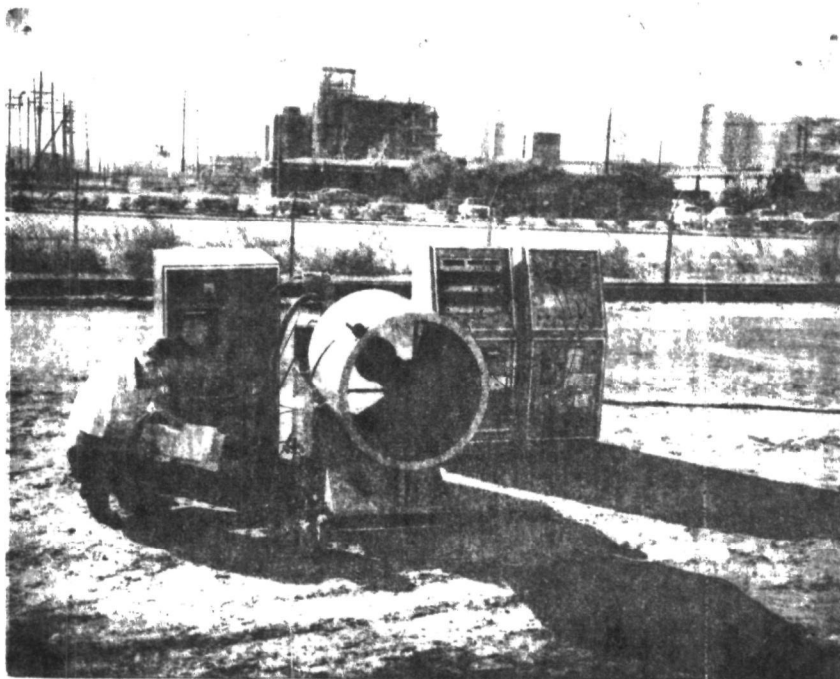


Figure 4-14. The ROSE system receiver section with electronics during field tests

the slit opening, but  $1 \text{ cm}^{-1}$  at  $10 \text{ }\mu\text{m}$  and  $4 \text{ cm}^{-1}$  at  $5 \text{ }\mu\text{m}$  are achievable in the absorption mode. The Ge:Hg detector is operated at  $28^\circ\text{K}$ . The source unit (not shown) contains identical telescopic optics, and a black-body radiation source is located at the telescope focus. The blackbody is operable over the range  $1100\text{--}1800^\circ\text{K}$  and is optically chopped for long-path ( $\leq 2 \text{ km}$ ) absorption measurements. In the remote emission mode, optical chopping occurs just in front of the monochromator entrance slit. For intensity calibration purposes the source unit is placed just in front of the receiver unit so that the blackbody radiation (unchopped) fills the field-of-view of the receiver unit. Both source and receiver units contain bore-sighting attachments to allow visual alignment of the telescopes.

An example of the type of spectra obtained with the ROSE system by EPA in a field test (Barnes et al. 1974) is shown in Figure 4-15.  $\text{SO}_2$  emission bands are readily distinguished, and, if the plume temperature is known, the  $\text{SO}_2$  concentration in the plume may be calculated. The authors calculated 650 ppm for a  $400^\circ\text{K}$  plume, which compared to 710 ppm using an extractive method, and to 680 ppm measured with an in-stack optical method. They show that an uncertainty of 6% in the plume temperature at  $400^\circ\text{K}$  produces an error of about 12% in the concentration.

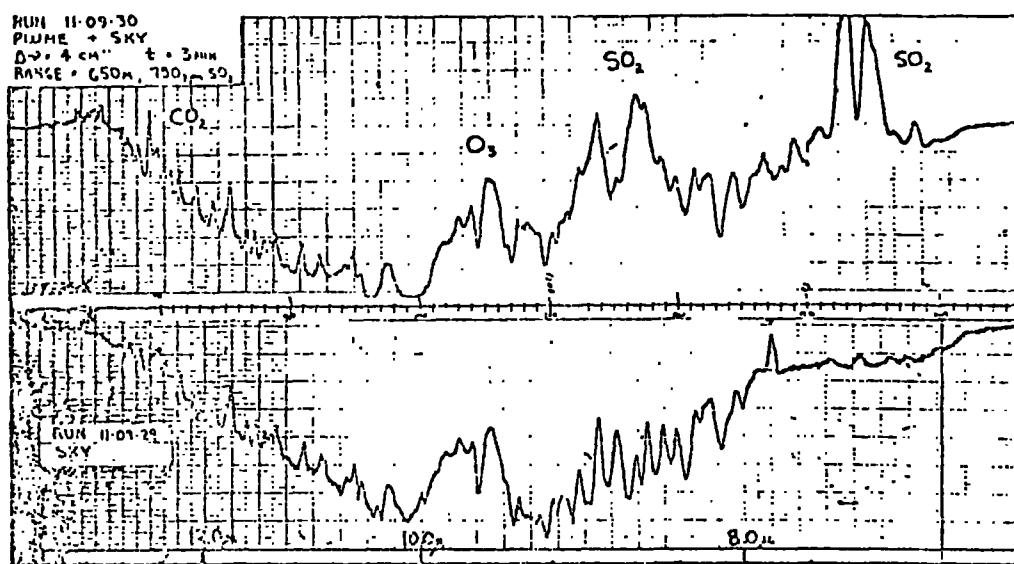


Figure 4-15. Plume and sky spectra from 7-13 microns (Barnes et al. 1974)



The problem with the dispersive technique is the determination of the plume temperature. Barnes et al. (1974) state that spectral resolution better than  $0.5 \text{ cm}^{-1}$  and a computerized data reduction program would be needed to obtain the plume temperature, but they do not elaborate on the method.

Chen et al. (1974) have suggested a method which utilizes the fact that the spectral location of the peak of a vibrational-rotational band of a gas depends on its temperature; the peak of the P or R branch shifts away from its band center as the temperature increases. Assuming that there is a region of no spectral overlap of gases in the plume, they estimate that in the  $8.6 \text{ }\mu\text{m}$   $\text{SO}_2$  band, the P and R branches separation changes by  $0.5 \text{ cm}^{-1}$  per  $10^\circ\text{K}$  change in temperature (over the range  $375^\circ\text{K}$  to  $575^\circ\text{K}$ ). They consider that an interferometer-spectrometer can provide spectra so that the plume temperature can be measured within  $10^\circ\text{K}$ . They also estimate that at  $400^\circ\text{K}$ , a 2% error in temperature results in a 10% error in  $\text{SO}_2$  concentration. They point out that the temperature uncertainty increases in the presence of particles in the plume.

Another method of estimating plume temperatures relies on the use of an interferometer-spectrometer and is discussed in the next section.

#### 4.4.5 Interferometer-Spectrometer

Interferometer-spectrometers have an advantage over conventional scanning spectrometers with their high optical throughput and rapid acquisition of the spectrum (assuming an on-line special purpose computer is available). They have been used to remotely sense stack emissions by Low and Clancy (1967), the General Dynamics/Pomona group (Streiff and Ludwig 1973; Tanabe 1975) and by Prengle et al. (1973).

The GD/Pomona system, which is installed in a van for mobility, was used in comparison with the ROSE system described above. Two Michelson-type interferometer-spectrometers were used to obtain spectral data over the 2 to 14 micron region. One interferometer using an LN2 cooled InSb (PV) detector covered the region from 2-5.4 microns while the second interferometer equipped with an LN2 cooled HgCdTe detector obtained useful data from 3.5-14 microns. The characteristics of both interferometers are tabulated in Table 4-10.

TABLE 4-10. Principal Interferometer Characteristics

Item	Interferometer #1	Interferometer #2
Model Designation (Drive Mechanism)	IF-3	IF-3
Wavenumber Region of Operation	1850 to 5000 $\text{cm}^{-1}$	716 to 2500 $\text{cm}^{-1}$
Optical Resolution	$\sim 2.5 \text{ cm}^{-1}$	$\sim 1 \text{ cm}^{-1}$
Spectrum Recording Rates	1 per 2.5 sec.	1 per 4.5 sec.
Detector	1.0 mm dia. InSb (PV)	2 x 2 mm HgCdTe
Detector Lens	1/4" dia. silicon	1 1/4" dia. Germanium
Detector Cooling	Liquid Nitrogen	Liquid Nitrogen
Foreoptics/Field-of-View (50%)	10" dia. /2 m rad.	12" dia. /6 m rad.
Wavelength Reference	0.63282 $\mu$ HeNe Laser	0.63282 $\mu$ HeNe Laser

The principal element in the interferometer is an optical cube consisting of a GD/Pomona developed beam splitter, a fixed front surfaced mirror and a moving mirror driven by a servo-controlled system developed by Idealab, Incorporated, in a triangular sweep to obtain linear mirror movement.

The optical cube is shown in schematic form in Figure 4-16. As indicated in the schematic, the single cube is used for the information channel, a laser reference and a white light synchronization pulse. The sync pulse is used to locate the exact center of the interferogram for coherent averaging of successive interferograms (when desired). The laser provides the digitizing clock and wavelength reference.

Both instruments were equipped with f/8 collecting optics with the 2-5 micron interferometer having a 10-inch diameter collecting mirror and the 3.5-14 micron interferometer having a 12-inch diameter collecting mirror. The design allows for variations in the field-of-view from a few milliradian to several degrees by means of quick-change foreoptics elements.

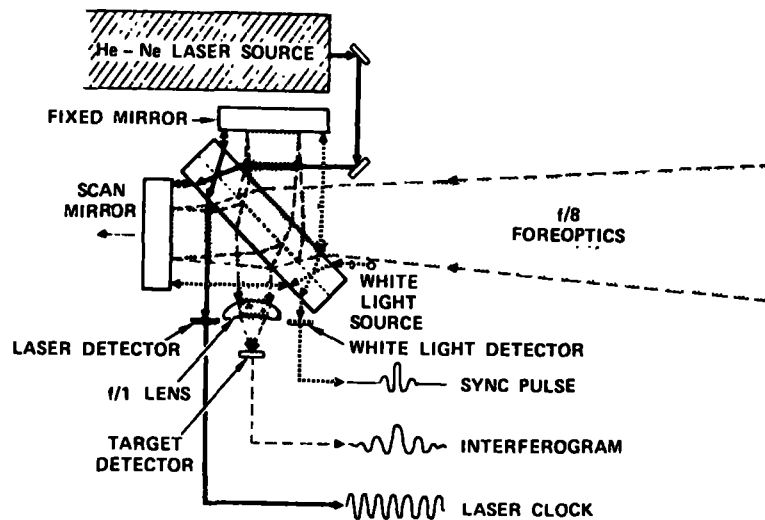
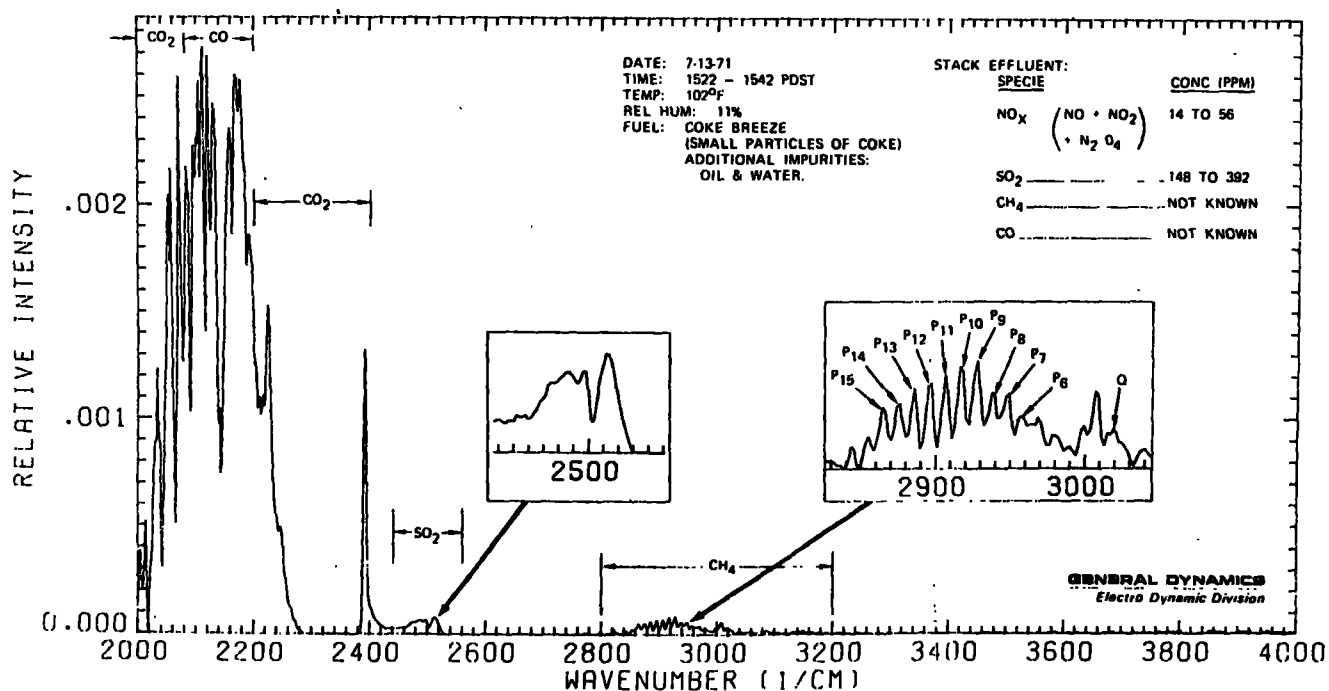
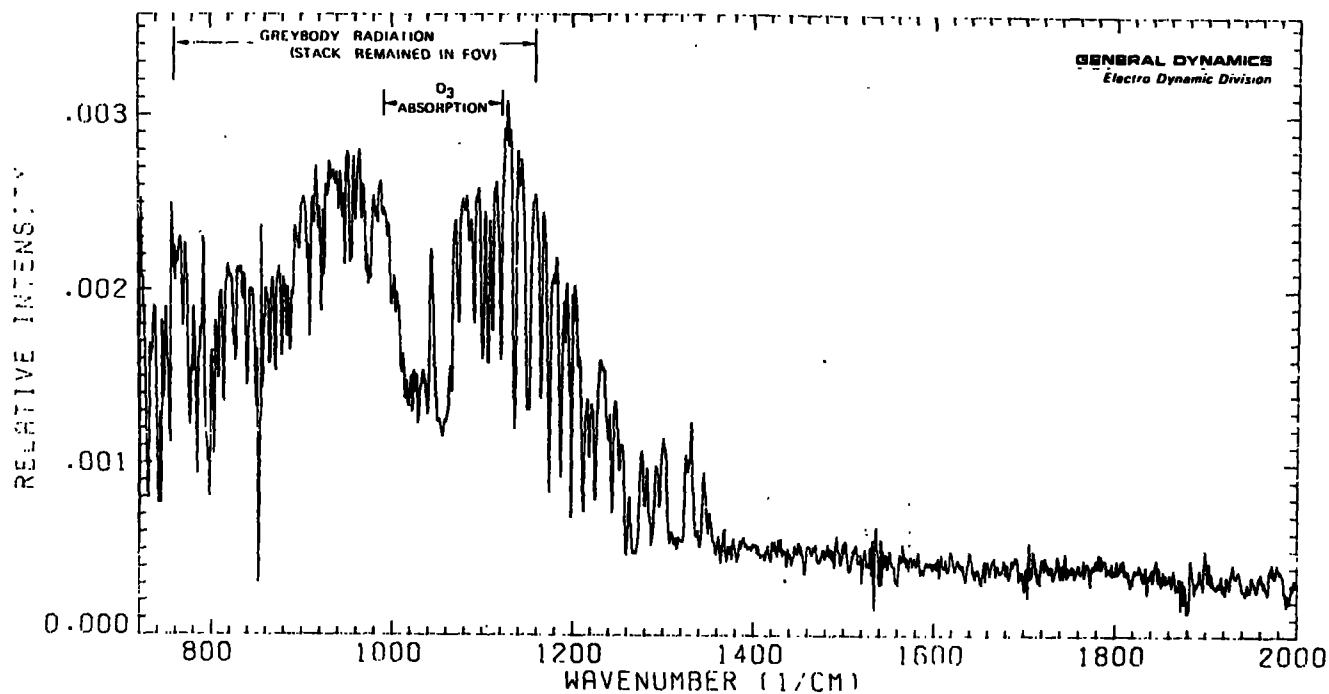


Figure 4-16. Optical layout of Michelson interferometer (Streiff and Ludwig, 1973)

Some typical spectra (Streiff and Ludwig, 1973) of a stack plume, obtained at a range of about 500 m, are shown in Figure 4-17, with the inset giving the plume concentrations of some gases, measured in-stack. The plume temperature was not known, and no attempt was made to determine it from the remote spectra, so no estimate of the gas concentrations were made. It is of interest to compare these spectra with those of the ROSE system, see Figure 4-18, obtained on the same stack. The ROSE system, with its somewhat lower spectral resolution, detects  $\text{SO}_2$  in the  $8.6 \mu\text{m}$  and  $7.6 \mu\text{m}$  regions, whereas these bands are not obvious in the interferometer spectrum. Tanabe (1975) used the  $4.0 \mu\text{m}$  region to estimate the  $\text{SO}_2$  concentration in the plume, but it appears that knowledge of the  $\text{CO}_2$  concentration in the plume is necessary to determine the plume temperature from the measured  $\text{CO}_2$  radiance, and this information cannot be obtained remotely. Tanabe found that the method (Chen et al, 1974) of measuring the separation of the P and R branches to determine the temperature was not accurate enough.

Prengle et al. (1973) have made interferometer spectrometer measurements of stack emissions with a mobile system shown in Figure 4-19. The Cassegrain telescope has a 25 cm diameter primary mirror, and the interferometer is a Block Engineering Co. Model 296, covering the  $2.8\text{--}15 \mu\text{m}$  range with  $0.5 \text{ cm}^{-1}$  resolution.

The authors propose a method to obtain the plume temperature which is applicable only to the interferometer spectrometer sensor. At zero retardation of the interferometer mirrors all frequencies have the same phase and add to give a narrow spike in the interferogram. The



A75738

Figure 4-17. Emission spectra of the gaseous effluents from a sinter plant stack measured at Kaiser Steel Corporation, Fontana (Streiff and Ludwig, 1973)

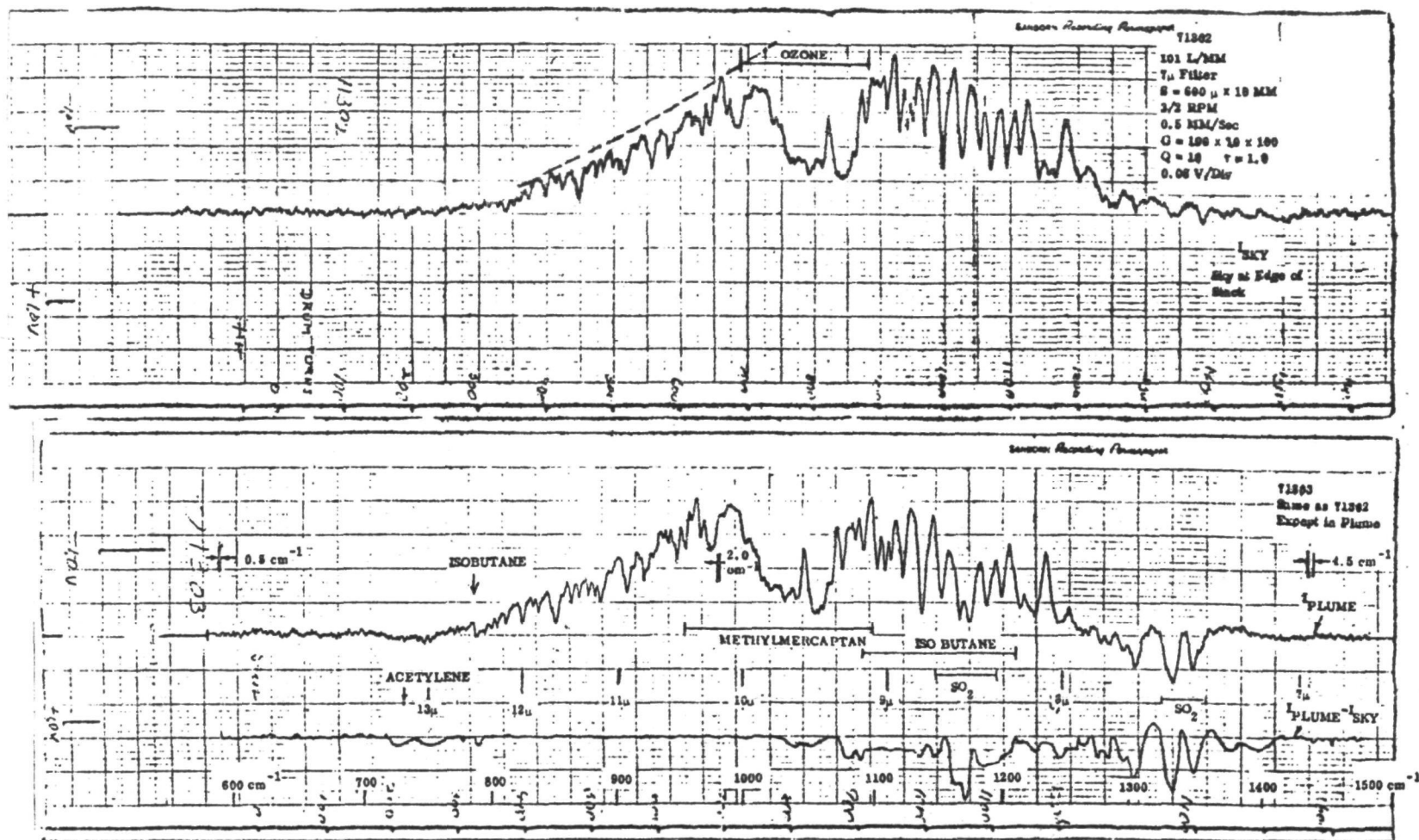


Figure 4-18. Top: Sky Background  
Center: Coke Oven Plume Emission  
Bottom: Difference: Plume-Sky  
(Streiff and Ludwig, 1973)

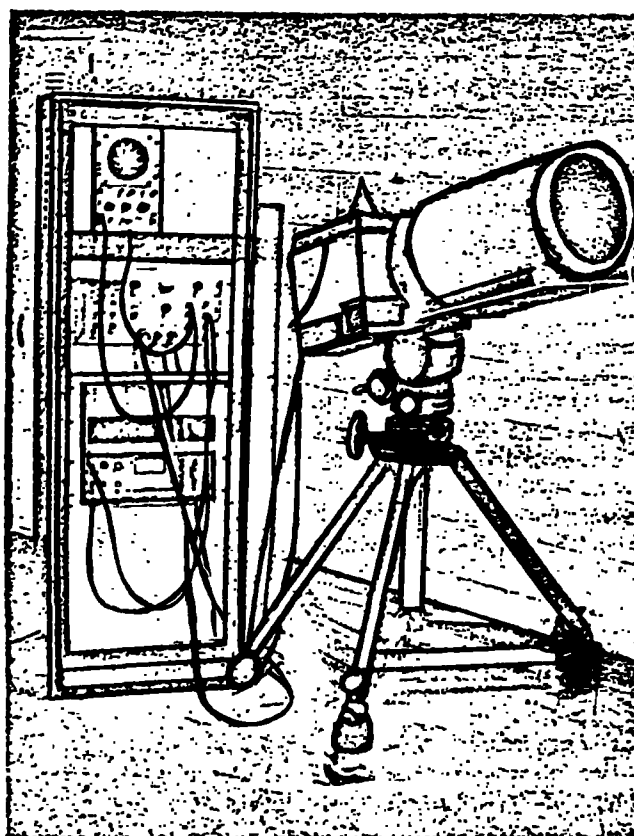


Figure 4-19. Assembled mobile interferometer-spectrometer system (Prengle et al., 1973)

amplitude of this spike represents the total flux incident on the interferometer, integrated over the 2.8-15  $\mu\text{m}$  region. This total flux provides a measure of the plume temperature (this would appear to be true only if the plume emissivity is constant with time and is known). The spike amplitude is calibrated against temperature using a blackbody.

Measurements were made of a power plant stack plume at a range of about 65 m. A single measurement typically consisted of averaging a total of 20 to 100 scans (mirror scans), each scan taking 3 sec. The results, compared with in-stack measurements, are given in Table 4-11.

TABLE 4-11. Interferometer Compared with In-Stack

	Temp(K)	CO(ppm)	NO(ppm)	CH <sub>4</sub> (ppm)	C <sub>2</sub> H <sub>4</sub> (ppm)
Remote	560	5550	324	858	296
In-Stack	561	4130	376	878	292

The agreement is very good; details of the data interpretation are not given, but it appears that some sort of calibration of the system is required using in-stack measurements, i. e., quantitative measurements cannot be made on a plume without prior access to the stack to empirically calibrate the interferometer for that particular stack and its emissions.

It seems that this approach for measuring the temperature of the plume is not suitable for routine monitoring. Hence the interferometer-spectrometer does not appear to have a significant advantage over the dispersive spectrometer. Of course, it does have a greater throughput and makes rapid spectral scans. These advantages must be balanced against the disadvantages of the greater expense and complexity of the interferometer system.

#### 4.4.6 Filter Wheel Sensor

A filter wheel remote sensor was built by Bendix (Prostak and Dye 1970) for EPA, for measuring pollutant spectra in the 7-14  $\mu\text{m}$  region. The wavelength is scanned by rotating a continuously variable filter wheel, which has a resolution of about 1 percent. The radiation is collected by a 28 cm Dall-Kirkham telescope, and passed through the filter wheel on to a mercury-doped germanium detector mechanically cooled to 28°K. An on-line computer is used to analyze the spectra in terms of pollutant concentration using regression analysis based on previous calibration data.

This device is much simpler, optically (see schematic in Figure 4-20), than the scanning spectrometer or interferometer, but due to the poor spectral resolution, the data interpretation is difficult even with help of the on-line computer. The system was also tested in the long-path active mode at the same time as the ROSE and the GD/Pomona interferometer systems, but had problems with its computer. The filter wheel technique does not seem to have been pursued since that time.

#### 4.4.7 Laser Heterodyne Technique

The passive laser heterodyne technique (illustrated in Figure 4-21), discussed by Hinkley (1972), Menzies and Shumate (1974), and Seals (1974) does not appear to have been applied to field measurements of stack emissions.

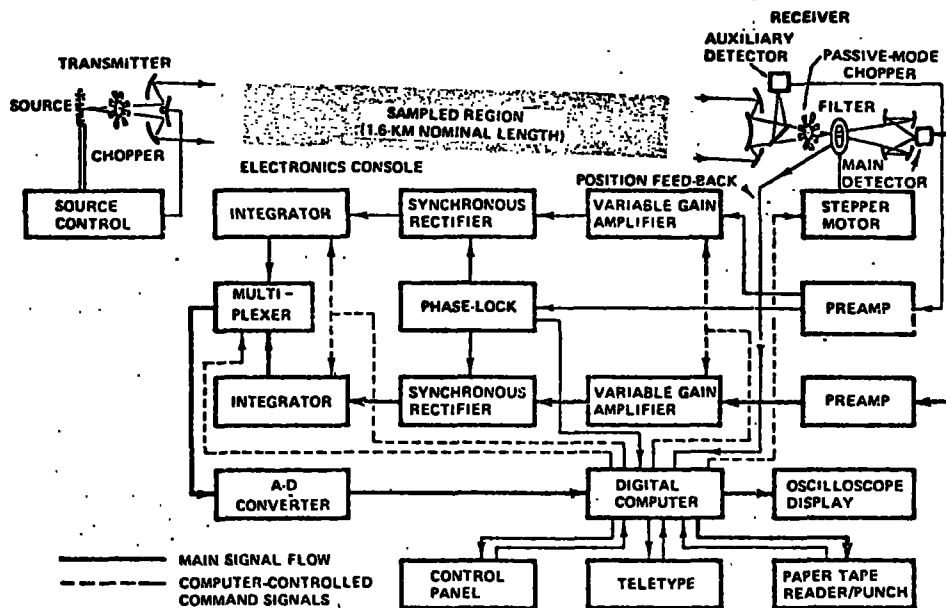


Figure 4-20. Block diagram of Bendix filter wheel sensor (passive mode does not use transmitter) (Prostak and Dye, 1970)

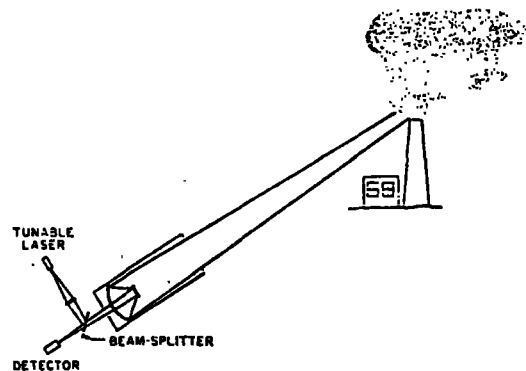


Figure 4-21. Configuration for remote heterodyne detection of pollutant gases from a smokestack using a tunable-diode-laser local oscillator (Hinkley, 1972)



The laser heterodyne technique may be used to selectively detect a pollutant emission line if a local oscillator (laser) frequency is found to coincide with that emission line. If this line is relatively free from interference due to other species, the technique can be better than correlation techniques in certain spectral regions where interference is relatively high, such as in water vapor bands.

The basic detection technique is illustrated in Figure 4-22. The laser can be at a fixed frequency, or it can be tunable so that it scans across the emission line of interest, and a beat frequency is produced whenever the difference frequency is within the bandpass of the electronics.

The sensitive spectral width in this technique can be less than  $0.06 \text{ cm}^{-1}$  (corresponding to an IF bandwidth of  $10^9 \text{ Hz}$ ), and the NEP is typically  $10^{-15} \text{ W}$  in the  $5\text{-}12 \text{ }\mu\text{m}$  region for a 1 sec integration time.

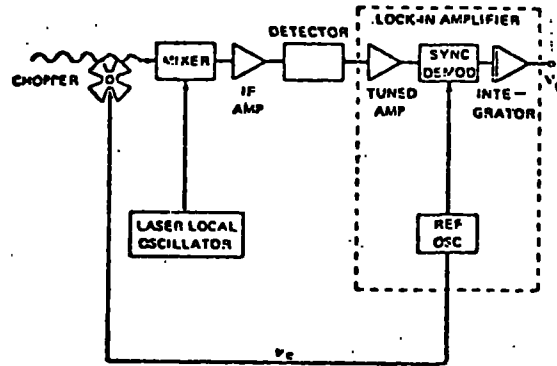


Figure 4-22. Schematic of heterodyne technique (Hinkley, 1972)

Hinkley (1972) shows that by scanning the laser wavelength through that of the pollutant emission line, a beat frequency is produced whenever the difference frequency between the two infra-red signals is within the bandpass of the detector/amplifier system; the amplitude of the signal is related to pollutant concentration. The signal-to-noise ratio is given by

$$\text{SNR} = \frac{1}{4} \eta (\tau/B)^{1/2} \left\{ \left( \exp\left(\frac{h\nu}{kT_g}\right) - 1 \right)^{-1} \int_{\nu_{LO-B}}^{\nu_{LO+B}} \left[ 1 - \exp(-\alpha'_c cL) \right] d\nu \right. \\ \left. - \left( \exp\left(\frac{h\nu}{kT_b}\right) - 1 \right) \int_{\nu_{LO-B}}^{\nu_{LO+B}} \epsilon_b(\nu) d\nu \right\} \quad (4-19)$$

where  $\alpha'_c$  is the absorption coefficient of the line per ppm of gas concentration (c), L the thickness of the plume,  $T_g$  its temperature,  $\epsilon_b$  the emissivity of the background at temperature  $T_b$ ,  $\nu$  is the infra-red frequency, h is Planck's constant, k is Boltzmann's constant, B the system bandwidth, and  $\tau$  the post-detection integration time. Equation (4-19) is also based on the following assumptions: (i) that the IF bandwidth is less than the emission linewidth; (ii) that the emission and absorption due to the pollutant in the ambient atmosphere is not important because of a low concentration there relative to that in the plume; (iii) that the background attenuation from the wings of other molecular absorption lines is negligible; and (iv) that the local oscillator has sufficient power to overcome the other sources of noise. Equation (4-19) holds, regardless of range, as long as the field-of-view of the collecting telescope is filled by the plume; in the infrared, with collection optics only a few centimeters in diameter, it should be possible to detect pollutants 1 kilometer away.

Under these conditions the minimum detectable concentrations for pollutant gases with line strengths of  $1 \times 10^{-5} \text{cm}^{-1}/\text{ppm}$  are shown in Figure 4-23 as a function of wavelength and for different source temperatures and background emissivities. Concentrations of a few ppm of NO and CO at 400 to 600°C can be detected; and similar sensitivities are achievable for  $\text{C}_2\text{H}_4$  and  $\text{NH}_3$  (at longer wavelengths) at a temperature of only 50°C. Since  $\text{SO}_2$  in the 8.7  $\mu\text{m}$  region has a measured absorption strength almost ten times smaller, the minimum detectable concentrations for this gas should be raised accordingly.

The local oscillator power necessary to satisfy assumption (iv) above is given by the equation (Keyes and Quist, 1970)

$$P_{LO} = \frac{(kT_A)(h\nu)}{\eta e^2 G^2 R_L}, \quad (4-20)$$

where  $T_A$  is the noise temperature of the amplifier, G the infra-red detector gain and  $\eta$  its quantum efficiency,  $R_L$  the load resistance, and e the electronic charge. For an amplifier with a noise temperature of 240°K (noise figure of 2.4 dB), and assuming  $\eta = 0.5$ ,  $G = 0.12$ ,  $R_L = 50 \text{ ohms}$ , and  $\lambda = c/\nu = 10 \mu\text{m}$ , we obtain  $P_{LO} = 12 \text{ mW}$ .

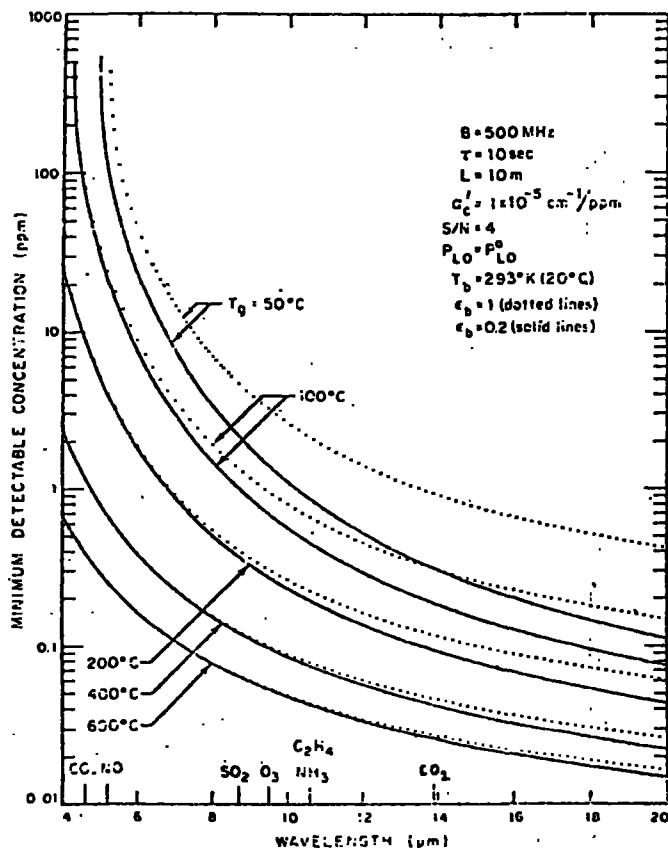


Figure 4-23. Theoretical wavelength dependence for remote heterodyne pollutant monitoring for various gas temperatures, and for background emissivities of 0.2 and 1.0. Useful wavelengths for some pollutant gases are indicated on the abscissa. Other parameters are shown in the figure (Hinkley, 1972).

Using state-of-the-art infra-red detectors and low-noise amplifiers, the local oscillator power of 12 mW is prohibitive, producing not only excessive heating of the detector, but a substantial liquid helium boil-off. When wide band ( $\approx 500$  MHz) photodiodes having nearly unit quantum efficiency become available, the local oscillator power requirement will be less than  $100 \mu\text{W}$ , a more realistic value.

Of course, as with most other passive techniques, knowledge of the plume temperature is required for quantitative measurements of the pollutant.

Shumate and Menzies (1974) have developed a heterodyne radiometer, with a CO<sub>2</sub> laser as a local oscillator, and used it to remotely detect several laboratory samples of gaseous pollutants at ambient temperature. Previous demonstrations of heterodyne radiometer sensitivities to SO<sub>2</sub> and CO<sub>2</sub> were accomplished by heating the gas samples. The sensitivities to O<sub>3</sub>, NH<sub>3</sub>, and C<sub>2</sub>H<sub>4</sub> were found to be adequate for detection of ambient concentrations in the parts per billion (ppb) region. The sensitivities to SO<sub>2</sub> are on the border line for detection of ambient concentrations around 50 ppb, and it may be possible to improve this by a factor of 4 if detection wavelengths near 8.8  $\mu$ m are being used instead of their operating region around 9.0  $\mu$ m. A CO laser, operating near 5.2  $\mu$ m, has also been used as a local oscillator in the detection of nitric oxide (NO) at a temperature of 390°K. The passive heterodyne radiometer does not appear to be capable of detecting ambient NO at normal smog concentrations; however, the authors suggest that it can be used to monitor NO concentrations in stationary source emissions which are at elevated temperatures.

The sensitivities to the various gases are shown in Table 4-12. The minimum detectable amounts in the second column (in units of concentration times path length) give a signal-to-noise ratio of one when a time constant,  $\tau$  of 10 seconds is used. For these measurements, B = 600 MHz. This corresponds to a spectral resolution of 0.04 cm<sup>-1</sup>.

TABLE 4-12. Experimental Sensitivities to Pollutant Gases (Menzies and Shumate 1974). The gases were at 298°K, except for NO, which was at 390°K. The band designations I and II refer to the upper and lower of the two mixed (10°0, 02°0) states.

Gas	Sensitivity (atm cm)	Laser line	Wavelength ( $\mu$ m)
Nitric oxide	10 <sup>-2</sup>	<sup>12</sup> C <sup>18</sup> O: 7-6, P(15)	5.19
Sulfur dioxide	10 <sup>-3</sup>	<sup>18</sup> C <sup>18</sup> O <sub>2</sub> : 00°1-II, R(40)	9.02
Ozone	2 × 10 <sup>-4</sup>	<sup>12</sup> C <sup>18</sup> O <sub>2</sub> : 00°1-II, P(40)	9.50
	2 × 10 <sup>-4</sup>	<sup>12</sup> C <sup>18</sup> O <sub>2</sub> : 00°1-II, P(14)	9.50
Ethylene	5 × 10 <sup>-5</sup>	<sup>12</sup> C <sup>18</sup> O <sub>2</sub> : 00°1-I, P(14)	10.53
Ammonia	10 <sup>-4</sup>	<sup>12</sup> C <sup>18</sup> O <sub>2</sub> : 00°1-I, P(32)	10.72

To date, much of the work in the laboratory on heterodyning has used helium-cooled detectors, and conventional laser sources, as well as helium-cooled tunable laser diodes. For field applications, higher temperatures must be used; developments of both detectors and tunable laser diodes are progressing along these lines. The HgCdTe detector, which operates at a higher temperature, has the added advantage of requiring considerably less local oscillator power than doped germanium and pyroelectric detectors (Koehler 1974).

#### 4.4.8 Dispersive Hadamard Transform Spectrometer

Hadamard transform spectroscopy (HTS), which appears not to have been applied to remote monitoring of air pollution, utilizes the multiplex technique by means of a conventional spectrometer with entrance and exit masks containing many slits. Spectral scanning is achieved by moving the slits rather than the grating. The detector output is decoded by use of Hadamard matrices in a computer. The basic concept is illustrated in Figure 4-24 (Decker 1971). The dispersed radiation is "de-dispersed" by being returned through the spectrometer on to a detector adjacent to the entrance slit.

Although spatial information alone, or spectral information alone, can be Hadamard multiplexed, a combined system (imaging spectrometer) is possible (Swift and Wattson 1974). The object or field of interest is focused onto a field stop at the entrance plane of a dispersion spectrograph by a conventional lens or telescope (a field stop replaces the usual entrance slit). A two-dimensional Hadamard mask is then scanned across the field stop, thus transmitting a time-varying light intensity that contains information about all spatial resolution elements in terms of the mask pattern. In this way, the spatial information is encoded. The transmitted radiation is in turn dispersed, and focused as a spectrum at the exit focal plane of the spectrograph. A one-dimensional Hadamard mask is placed across the spectrum and stepped one element of its cycle for each complete scan of the spatial mask. This, too, produces a temporal modulation which contains encoded spectral information.

A laboratory instrument having a spatial field of 31 x 33 elements (each one typically 0.1 mm x 3.5 mm) and a spectral array of 63 elements, with the detector and gratings covering the 6  $\mu\text{m}$  to 25  $\mu\text{m}$  region with a resolution of 0.02  $\mu\text{m}$  or better has been built (Swift and Wattson 1974).

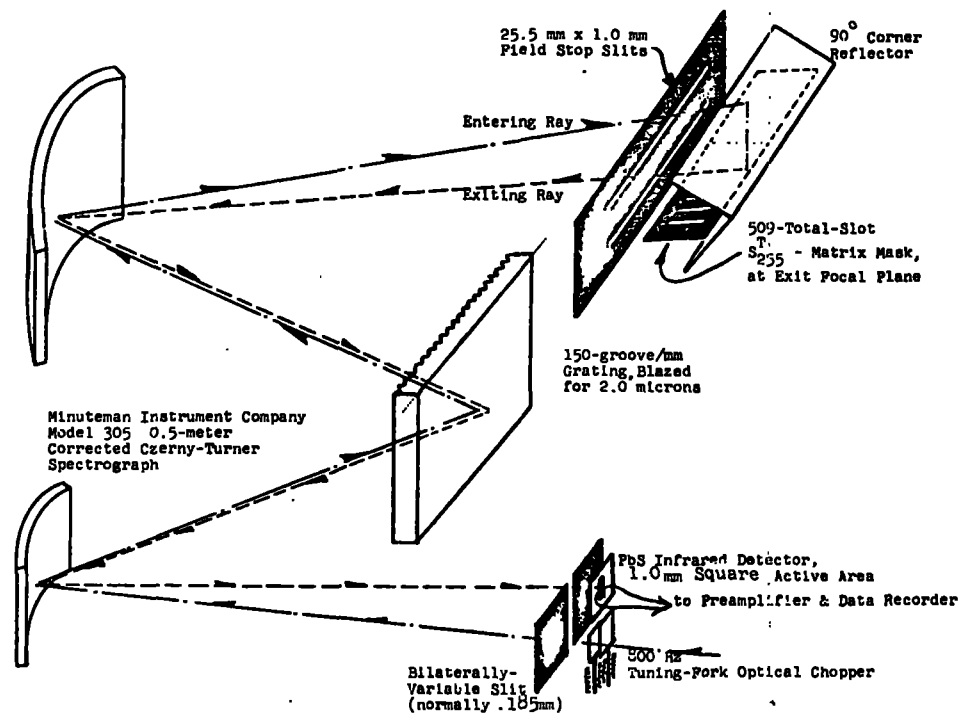


Figure 4-24. Schematic of Hadamard transform spectrometer (Decker 1971)

Theoretical analysis (Larson et al. 1974) shows that HTS is best suited for spectra which are characterized by a few well-defined and intense peaks on a low intensity background. Conversely, for spectra with high backgrounds, for dense spectra, or for weak spectral features, HTS has no advantage over a conventional scanning spectrometer. On the basis of this analysis it would appear that, in general, HTS has no special advantage for remote sensing of pollutants, since their spectra are generally weak and mixed with interfering spectra.

#### 4.4.9 Passive Vidicon Instrumentation

A UV vidicon system for the measurement of SO<sub>2</sub> and plume velocity is being developed at NASA-Langley (Exton 1974). The vidicon is sensitive to a bandpass of 50-100 Å in the SO<sub>2</sub> absorption band at 3100 Å, and detects scattering solar radiation (similar to the COSPEC). Hence the intensity of the plume image on the vidicon screen provides a measure of the SO<sub>2</sub> in the plume. The quoted accuracy is  $\pm 20$ -30 ppm at a concentration of 100 ppm. However, the instrument has been tested only with low opacity (<1%) plumes, and presumably, like the COSPEC, the accuracy will deteriorate with increasing plume opacity, range, and increasing atmospheric haze.

It would appear that this device would be most useful as a qualitative device for imaging the invisible SO<sub>2</sub> plume; it could show the location of the plume with respect to the stack so that other remote sensors could optimize their pointing location. Exton (1974) indicated that on one occasion the device showed downwash of the plume around the stack, which would change the SO<sub>2</sub> path length observed by remote sensors.

This vidicon device has also been used to estimate the effluent velocity. The plume has eddy inhomogeneities which show as "blobs" on the SO<sub>2</sub> image of the plume. The plume velocity is obtained by tracking these eddies as a function of time. However in the tests to date, the device has consistently underestimated the velocity (Herget 1976), and is thought to be due to seeing only the outer edge of the plume which is slower than the inner plume.

Another vidicon device operating in the IR (3-4.5 μm) has been evaluated by Aerospace Corporation under EPA support (Herget 1976). This too provides an image of SO<sub>2</sub> in the plume due to emission in the 4.0 μm SO<sub>2</sub> band, and it is hoped to obtain velocity by tracking the plume inhomogeneities. It does not provide quantitative SO<sub>2</sub> data independently, since the plume temperature is not known, at least not remotely.

#### 4.5 AREA SURVEYS

Area surveys of air pollutants can be useful for episode monitoring, for selecting plant sites, for evaluating environmental degradation, for assisting in the design of contact monitoring networks, and for tracking plumes to study atmospheric dispersion, diffusion and fate of pollutants. Area surveys can be conducted from airborne platforms such as aircraft,

helicopters or blimps; from vehicles driven through and around the area, and from long-path observation networks traversing the area. It would appear that space observations of pollutants will not be suitable for local purposes since the spatial resolution, both horizontal and vertical, is too coarse.

From the point-of-view of enforcement, area surveys of ambient air pollution levels are not relevant except where the area surveyed includes stationary sources. Since the sources of emissions are mostly above ground level, ground level long-path measurements of ambient pollutant amounts will not, in general, provide a measure of the source emissions. However, if a measure of the pollutant in a vertical column can be made continuously around the perimeter of an area source, a knowledge of the mean wind velocity enables the rate of emissions within that area to be estimated. Measurements of the vertical loading may be made with ground-based instruments looking up, or airborne instruments looking down from above the upper altitude limit of the emissions. Considerations of this technique seem to have been limited to gaseous pollutants. Similar measurements for particulate pollutants would be difficult, although qualitative three-dimensional mapping of particle concentrations over an area may be done with an airborne lidar system.

The COSPEC instrument has been used for perimeter monitoring of  $\text{NO}_2$  and  $\text{SO}_2$ , in the vertical up-looking mode in which the scattered (by molecules and aerosols) solar radiation is measured (Langan 1971a). The instrument is periodically calibrated by placing cells containing known amounts of each gas in the line-of-sight within the instrument. The problems of multiple scattering, varying sun angle and varying aerosol amounts and distribution makes quantitative interpretation very difficult. Some measurements (Langan 1971b) of  $\text{SO}_2$  around a single stack gave an emission rate of about 24 metric tons/day (averaged over a 50 minute measurement period), whereas an in-stack chemical method gave 17.3 metric tons/day (averaged over a 60 minute measurement period). The report suggests that some of the discrepancy can be attributed to fluctuating winds. More recent (Sperling 1975) detailed inter-comparisons showed that the COSPEC could measure the  $\text{SO}_2$  mass flux within  $\pm 24\%$  of the in-stack EPA reference method. The errors were again attributed to inaccuracies in the wind velocity. Herget (1976) plans to use an LDV system to measure the wind velocity in conjunction with COSPEC measurements to determine the possible improvement in accuracy.



EPA is currently supporting the development of a GFC instrument by Science Applications, Inc. (1975) for measuring SO<sub>2</sub> at 4.0  $\mu$ m in the up-looking mode. Field tests of this instrument will be conducted in the summer of 1976. Ward and Zwick (1975) describe measurements of CO and CH<sub>4</sub> using a GFC instrument in the up-looking mode.

An up-looking differential absorption laser system installed in a van would seem to be well suited for perimeter monitoring by measuring the return signal from an altitude above the emissions to give the vertical integrated pollutant optical thickness.

This basic technique appears also to be the most suitable for airborne measurements. Two instruments are being developed for aircraft operation, using downward looking laser systems, and utilizing the earth-reflected laser radiation. EPA, Las Vegas (Melfi 1974) is developing a system for measuring O<sub>3</sub>, using two pulsed CO<sub>2</sub> lasers, tuned to different wavelengths. The laser beams must be accurately boresighted so they are illuminating the same ground patch, and it is assumed that the wavelengths are close enough that the ground reflectivity is the same for each. This basic system could be used for other gases as well, such as SO<sub>2</sub>, C<sub>2</sub>H<sub>4</sub> and NH<sub>3</sub>, either by tuning or by using isotopic CO<sub>2</sub> laser.

NASA-Langley (Allerio 1976) is also supporting a similar program at JPL to develop a tunable CO<sub>2</sub> laser heterodyne aircraft system for O<sub>3</sub>. Another aircraft laser system is being developed at NASA-Langley for the measurement of CO. This DAS system uses heterodyne detection of the earth-reflected radiation from a CW tunable diode laser. The shape (due to pressure broadening) of the pollutant line obtained by the spectral tuning apparently can be mathematically analyzed to provide coarse information on the pollutant height distribution.

In all of these differential absorption methods, a careful analysis must be made of possible errors due to the earth/atmosphere fluctuating background; to the effects of the aircraft moving over different targets between pulses or during the laser tuning; and to variations in the laser output.

A summary of on-going programs in perimeter and area monitoring of different agencies is given in Table 4-13.

TABLE 4-13. Area Survey Techniques

<u>SPACE</u>	
NASA/MAPS (Planned)	IR. Uses GFC method. Not suitable for enforcement--area too large--gives integrated tropospheric amount.
NASA/ERTS (Feasibility Shown)	Visible. Radiometer. Not suitable for enforcement--gives vertical burden of aerosols over water surfaces.
NASA (Suggested)	Visible polarimeter. Not suitable. Tropospheric aerosol amounts--data interpretation difficult for quantitative information.
<u>AIRCRAFT - HELICOPTER</u>	
EPA	Airborne lidar system. 3-dimensional mapping of relative particulate distributions.
EPA	IR. 2 wavelength CO <sub>2</sub> laser. Earth reflection giving vertical integrated amount. Looks promising in theory--needs flight demonstration.
NASA	IR. Tunable diode laser. Earth reflection. Same comments as for EPA program above.
POLARIMETER	Visible--same comments as for space application.
NASA	IR. GFC. 2 flight models tested by NASA--gives vertical integrated amount--needs temperature profile--in general, not sensitive to lowest 1 km, so not suitable for enforcement.
BARRINGER RESEARCH	Visible. COSPEC matched filter--severe data interpretation problems due to scattering.
NASA/CIMATS	IR. Correlation interferometer--uses reflected sunlight--data problems due to varying surface reflectance--gives vertical integrated amount, so no good for enforcement.
<u>GROUND - MOBILE</u>	
BARRINGER RESEARCH	Visible. COSPEC looking upward from van--for area emission monitoring--quantitative interpretation is a problem due to scattering.
BARRINGER RESEARCH SAI/EPA	IR. GFC looking upward from van--for perimeter monitoring.
<u>GROUND - FIXED LONG PATH</u>	
BARRINGER RESEARCH	Visible. COSPEC. Xenon source. SO <sub>2</sub> , NO <sub>2</sub> only. Aerosol attenuation may be significant. Present range: 100-930 m.
BENDIX	IR. Filter wheel. Blackbody source--computer problem--not pursued. Present range: 1.6 km.
EPA/ROSE	IR. Scanning spectrometer. Blackbody source. Used as research tool. Present range: 400 m - 4 km.
GD/POMONA	IR. Interferometer spectrometer. Blackbody source. Present range: 2-4 km.
SAI/DOT	IR. GFC. Blackbody source--for highway CO emissions. Present range: 50 m.
GE/EPA	IR. 10.6 $\mu$ m CO <sub>2</sub> laser source for O <sub>3</sub> . Present range: 670m.
LINCOLN LAB/EPA	IR. 4.7 $\mu$ m tuned diode laser source for CO. Present range: 610 m - 2 km.
SAI/EPA	IR. GFC. Blackbody source--H <sub>2</sub> S, VC - for area surveys. Present range: 1 km.
NASA	Visible DAS. SO <sub>2</sub> and O <sub>3</sub> . Present range 1.9 km.

#### **4.6 ON-GOING AND PLANNED RESEARCH PROGRAMS**

In addition to the literature search for remote sensing work relevant to this program, we have learned from various government agencies and laboratories their relevant on-going and planned programs. A listing of these programs is given in Tables 4-14 and 4-15.

**TABLE 4-14. Non-Extractive Electro-Optical Techniques for Air Pollution Measurements, NERC/RTP (Courtesy of W. Herget, EPA)**

**GASES**									
TECHNIQUE	QUANTITY MEASURED	MODE <sup>1</sup>	TYPE STUDY <sup>2</sup>	INVESTIGATOR	STATUS	SPECTRAL REGION	PROJECT OFFICER	COMMENTS	
Fluorescence	SO <sub>2</sub>	I,R	LF	UARL	EPA-650/2-74-020 <sup>3</sup>	UV	Herget	Not promising for R or I	
Vibrational Raman	SO <sub>2</sub> , NO	R	FE	NASA/LRC	co-op	UV	(Herget)	Old Dominion U Report TGS-TR-PM-75-12	
Rotational Raman	NO	R	LF	Princeton	Grant 800805 <sup>4</sup>	UV	Herget	Uses Fabry-Perot; has potential	
DIAL	SO <sub>2</sub> , NO <sub>2</sub>	R	LF	CCNY	Grant 803109	UV	Herget	Joint funding with Army	
DIAL	multi-gas	R	ID	NASA/LRC	IAG	IR	Herget	Includes Army and Air Force Funds	
IR Imagery	SO <sub>2</sub> , Velocity	R	FE	Aerospace	68-02-2242 <sup>5</sup>	IR	Herget	Not promising	
UV Imagery	SO <sub>2</sub> , Velocity	R	FE	NASA/LRC	co-op	UV	(Herget)	(Exton)	
LDV - Reference Beam	Velocity, Mass	R	FE	Raytheon	EPA-650/2-75-062	IR	Herget	Feasibility demonstrated	
Dispersive Correlation	SO <sub>2</sub> , NO <sub>2</sub>	R	IU	EPA	current	UV,VIS	Barnes	} Barringer Correlation Spectrometer	
Dispersive Correlation	SO <sub>2</sub>	R	IU	EMI	68-02-1773	UV	Barnes		
Gas-Filter Correlation	Multi-gas	R,O	ID	SAI	68-02-1798	IR	Herget	Uplooking and long-path instruments	
Gas-Filter Correlation	SO <sub>2</sub>	R	ID	SAI (JRB)	EPA-650/2-75-041	IR	Barnes	Stack exit; evaluation underway	
Gas-Filter Correlation	NO, H <sub>2</sub> S	R	LE	Philco-Ford	68-02-0766	IR	Herget	To be completed late 1976.	
Diode Laser	CO, NO	O	ID	MIT/LL	IAG	IR	McClenny	Report available soon	
Gas Laser	O <sub>3</sub> , NH <sub>3</sub> , C <sub>2</sub> H <sub>4</sub>	O	FE	GE	EPA-650/2-74-046	IR	McClenny		
ROSE System	Multi-gas	R,O	IU	EPA	current	IR	Herget	Field spectrometer; research	

Notes:

- I = Insitu (cross-stack non-extractive)
- O = Open path (long path) double-ended
- R = Remote single-ended

- 2. LF = Laboratory Feasibility Study
- ID = Instrument Development
- FE = Field Evaluation
- IU = Instrument Use

- 3. EPA report number
- 4. EPA grant number
- 5. EPA contract number

TABLE 4-15. Review of Other Agency Programs

<u>NASA/LANGLEY</u>	1.	Evaluation of AAFE instruments for A/C use CIMATS - correlation interferometer MAPS - GFC HSI - interferometer spectrometer
	2.	JPL program--O <sub>3</sub> from A/C looking down at earth reflected signal from tunable CO <sub>2</sub> laser, plus heterodyne detection on A/C October 1976.
	3.	AIL program--passive radiometry using CO <sub>2</sub> laser heterodyne for O <sub>3</sub> and NH <sub>3</sub> . On A/C October 1976.
	4.	Tunable diode laser plus reflector on A/C fuselage for CO. On A/C May 1976.
	5.	Differential absorption for SO <sub>2</sub> using 3000 Å dye laser. Have SO <sub>2</sub> spectrum with 0.2 Å resolution. Tested downstream of stack emission.
	6.	SAI program--GFC with retroreflector on A/C wing for HCl and CO.
	7.	Differential absorption in IR (1.4-4.0 μm) with tunable diode lasers. (Joint NASA, EPA, AF, Army program).
	8.	Differential absorption for SO <sub>2</sub> and O <sub>3</sub> in ambient air with double-pulse dye laser.
	9.	Differential absorption for H <sub>2</sub> O using 7000 Å tunable dye laser. Used in up-looking mode for humidity profiles.
	10.	UV camera for SO <sub>2</sub> and velocity in plumes.
<u>EDGEWOOD ARSENAL</u>	1.	Passive LOPAIR, advanced development. 8-12 μm, 16-channel filter instrument. Looks at sky at low elevation angle. Uses on-line computer using selected channels and weighting functions for Dimethylmethylphosphonate (DMMP).
	2.	Isotopic CO <sub>2</sub> laser using topographic reflector. Exploratory programs.
	3.	Differential absorption program (with EPA)--Ahmed of New York. Visible laser (.09 ppm NO <sub>2</sub> at 1 km).
	4.	Raman. Currently planning on using Ruby laser without doubling to get increased S/N.
<u>NSF</u>	1.	SRL. SO <sub>2</sub> , O <sub>3</sub> , NO <sub>2</sub> --Differential absorption laser system.
<u>EPA-LAS VEGAS</u>	1.	In-house O <sub>3</sub> 2λ CO <sub>2</sub> laser on A/C--area survey.
	2.	Aerial photography for opacity.
<u>USAF</u>	1.	Brooks AFB-JRB -- GFC in-situ for HCl and HF designed for ready adaptation to long-path measurements.
	2.	RADC-Block Engineering -- Remote detection, tracking and quantitative measurement of HCl in the residual effluent plumes of solid booster launches.
<u>DOT</u>	1.	SAL GFC long path (50 m) with retroreflector across highway to monitor CO (car emissions) and SF <sub>6</sub> (released tracer).
<u>NCAR</u>	1.	Transportable system: Lidar for aerosols Doppler velocimeter Can also do Raman scattering.
	2.	Acoustic soundings for inversion height.

# 5

## PRACTICAL CONSIDERATIONS

### 5.1 OVERVIEW

In this section we consider the practical systems constraints due to safety considerations and to instrument and source parameters.

One of the first constraints to consider is the eye safety requirements. Thus, an analysis of the performance standards for laser products as proposed by the DHEW is made and the maximum permissible exposure and minimum safe range are determined. The resulting instrument parameters are then used as an input into the error analysis of the different laser systems. It is obvious that the errors of single-ended pulsed laser systems vary due to the method of data interpretation, the scattering cross sections, and the assumptions made about the pollutant and the atmosphere. A detailed analysis to intercompare techniques is very much dependent on the system design, and on the assumptions made about the atmospheric properties (temporal, spatial and spectral). A true comparison will ultimately be made only by simultaneous field tests on a plume with coincident in-situ measurements of the pollutant. However, when the instrument and atmospheric parameters are made equal for the most promising systems (DAS, Raman and Lidar), operating at 4500 Å, with a minimum eye safe range (MSR) of 50 m, which is probably acceptable for operational use, the calculations show that the Raman system probably does not have an acceptable range and accuracy capability during nighttime use, and is not at all useful for daytime operation. The lidar system and the DAS system appear to have useful accuracies up to at least 1000 m range for the integration times permitted by the existing Federal Regulations (15 seconds for opacity and 15 minutes for gas concentration). The daytime use of DAS may be limited to smaller ranges at large gas concentrations.

In the case of passive remote monitors, a different set of requirements must be met. The source radiation is dependent on pollutant and interfering species concentration, as well as gas temperature for infrared methods, and on the plume and atmospheric particle concentration for UV/visible methods. Hence, knowledge about, or a technique to eliminate, these latter parameters is required in the data interpretation. The degree of accuracy with which the temperature and particle effects can be measured/eliminated is directly reflected in the ability to determine the pollutant concentration. It is found that instruments which utilize optical correlation and ratio techniques are better suited than other spectroscopic instruments. However, the sensitivity of the infrared method is still dependent on the source strength, i. e., blackbody temperature, so that cool exhaust plumes near ambient temperatures will be very difficult to observe. The UV/visible method is considerably hampered by variations in the plume opacity and atmospheric particle amounts. Active systems are not constrained by these limitations.

## 5.2 EYE SAFETY HAZARDS FROM LASER SYSTEMS

A consideration in evaluating remote sensing laser systems for air pollution is the potential safety problem. The most obvious hazard with the laser beam is direct axial viewing, but specular reflections are also a risk, and considerable care must be exercised in the use of laser systems. The skin can be burned by some laser beams, but the main hazard is damage to the eye. The danger varies with wavelength of the laser radiation due to the wavelength dependent optical properties of the eye.

The most sensitive region is the visible region, 4000 to 7000 Å since the cornea, aqueous humor and the lens readily transmit this radiation. Thus, the full laser beam energy is focused on the retina in an image 10-20  $\mu\text{m}$  in diameter resulting in high power densities of kilowatts/cm<sup>2</sup> on the retina even for milliwatt powers incident on the pupil of the eye. These high power densities can cause severe damage to the retina, and the fovea, resulting in loss of visual acuity.

In the UV region, the radiation below about 4000 Å is absorbed by the lens, and below about 3150 Å it is absorbed by the cornea, so that UV hazards are mostly limited to these parts of the eye. The radiation is absorbed over a larger area than is the focused visible light

on the retina, so the power densities are not so high. Exposure to excessive UV results in inflammation of the cornea and conjunctiva at the shorter wavelengths, and cataract formation at the longer wavelengths.

In the IR region, up to 1.4  $\mu\text{m}$ , the ocular transmission is less than that of the visible, and varies with wavelength. From 1.4 to 1.9  $\mu\text{m}$ , essentially all radiation is absorbed by the cornea and the aqueous humor. Beyond 1.9  $\mu\text{m}$  all the radiation is absorbed by the cornea alone. The absorbed energy can be conducted to the interior of the eye, raising the temperature of the lens, and resulting in the formation of cataracts.

#### 5.2.1 The Maximum Permissible Exposure and Minimum Safety Range

The Department of Health, Education, and Welfare proposed (1974) Performance Standards, which were subsequently promulgated (1975), for Laser Products to minimize the hazards of laser systems. The standards are somewhat complex, but may be summarized in terms of a Maximum Permissible Exposure (MPE) which varies with the laser emission duration. The following values are for pulse lengths of about 0.1  $\mu\text{sec}$ . In the visible band from 4010 to 7000  $\text{\AA}$  the MPE is  $5.2 \times 10^{-7} \text{J/cm}^2$ . In the IR, this value increases to  $2.6 \times 10^{-6} \text{J/cm}^2$  at 1.06  $\mu\text{m}$  and remains constant out to 1.4  $\mu\text{m}$ . From 1.5 to 13.0  $\mu\text{m}$  the MPE is  $2.1 \times 10^{-4} \text{J/cm}^2$ . In the UV, the MPE at 4000  $\text{\AA}$  is  $2.1 \times 10^{-2} \text{J/cm}^2$  decreasing to  $6.2 \times 10^{-5} \text{J/cm}^2$  at 3020  $\text{\AA}$ , and remaining constant to 2500  $\text{\AA}$ . It should be noted that there are discontinuities (or, at least, a very rapid change in MPE with wavelength) in the MPE values near 4000  $\text{\AA}$  and near 1.5  $\mu\text{m}$ . For CW lasers the exposure time must be considered, and the DHEW Performance Standards (1975) should be consulted for the details. For exposure times (tsec) between  $2 \times 10^{-5}$  and 10 seconds, which should cover most situations, the MPE, in the visible band (4010 to 7000  $\text{\AA}$ ) is given by  $1.8 \times 10^{-4} t^{3/4} \text{J/cm}^2$ , and in the IR (1.5 to 13  $\mu\text{m}$ ) is given by  $1.1 \times 10^{-2} t^{1/4} \text{J/cm}^2$ . In the UV (2500 to 4000  $\text{\AA}$ ) the MPE is independent of  $t \leq 3 \times 10^4$  seconds.

These standards will have an impact on the choice of laser systems for operational use in the remote sensing of air pollution. The minimum safe range (MSR) beyond which the beam irradiance is less than the MPE may be calculated approximately, without consideration of atmospheric effects (attenuation, scintillation), by assuming that the energy is uniformly distributed across the beam, and by assuming the laser to be a point source (a typical beam might be 1 cm diameter unexpanded, or 10 cm



when a beam expander is used to reduce its divergence). If the laser beam has a divergence solid angle  $\Omega$  and an energy of  $P$  joules, then the radiant exposure (irradiance),  $E$ , at a distance  $R$  cm is given by

$$E = \frac{P}{R^2 \Omega} \quad \text{J/cm}^2 \quad (5-1)$$

When  $E$  is the MPE, then  $R$  is the MSR, i. e.,

$$(\text{MSR})^2 = \frac{P}{(\text{MPE})\Omega} \quad (5-2)$$

When the MSR is computed for the promising laser techniques, Raman, DAS, Lidar and LDV, it appears that the existing Raman and lidar systems cannot safely be used operationally in the visible region, since the beam would present a hazard at great distances. The existing DAS system is possibly acceptable in the visible, and all systems appear acceptable in the near UV and IR. The MSR could be reduced by increasing the laser beam divergence. The present typical system divergence of 0.3 m rad results in a 0.1 m beam width at 300 m. A larger divergence of 3 m rad, (1 m at 300 m) would seem still small enough for use with most stacks.

It is theoretically possible to further reduce the MSR by considering the basic laser system equation, given by Equation (4-12). From this equation it is seen that, for a fixed return power,  $P(R)$ , the transmitted signal,  $P_t$ , can be reduced by increasing the product  $L \times N(R)$ ; this product is proportional to the optical thickness which is the measured parameter in the DAS and lidar techniques. This means the minimum detectable concentration is increased, since increasing  $L$  does not help in the case of a stack plume where  $L >$  plume width. In addition, the integration time of the system may be increased, so that  $n$  pulses are integrated rather than the single pulse represented by Equation (4-12). This enables  $P_t$  to be reduced in proportion to  $n^{1/2}$ .

### 5.2.2 Required Modifications

Sensitivity Change: The minimum detectable optical thickness should not be increased for the Raman system since it is already quite high (~ 300 ppm-m for  $\text{SO}_2$ , see Table 4-5).

The DAS sensitivity is about 1 ppm in a plume at 750 m range (see Table 4-3), and could be relaxed to at least 10 ppm for enforcement monitoring; this would reduce the DAS visible MSR, by a factor of 3.2 to 0.05 km (including the divergence modification).

The accuracy of the present GE lidar system is 2.5% at 0.2 opacity, and could reasonably be relaxed to say 10%, giving a reduction by a factor of 4 in  $P_t$ , resulting in a lidar MSR of about 2.8 km (including the divergence modification).

Integration Time Modification: In evaluating the possibility of increasing the integration time to decrease the MSR, the Proposed Performance Specifications of Continuous Monitoring Systems must be considered. These specifications for opacity monitoring with an in-stack transmissometer call for a 10 second maximum response time, although the visual determination of opacity (Method 9) calls for readings at 15 second intervals. Thus, presumably the integration time for a lidar system should not exceed 15 seconds. For in-stack monitoring of  $\text{SO}_2$  and  $\text{NO}_x$ , a 15 minute maximum response time is required. Hence, the integration time for the DAS and Raman systems should not exceed 15 minutes.

The GE lidar system is a single pulse device and is capable of only 3 pulses per minute, so it can obtain a reading every 20 seconds, slightly exceeding the 15 seconds suggested above. It is clear that the integration time of this system cannot be increased.

The DAS integration time is already long (10-30 min.) so that within the specifications constraints discussed above, no significant improvement of MSR is possible, and, in fact, it would worsen for the system which must reduce its integration time to 15 minutes.

The Raman integration time is typically about 1 min., so lengthening this to the permitted 15 min. allows about a fourfold decrease in  $P_t$ , resulting in a Raman visible MSR of about 1.0 km (including the divergence modification).

### 5.2.3 Final System Parameters

In summary, the present systems might be considered safe for near UV and IR operational use, but some modifications must be made for their use in the visible as discussed above. The suggested simple modifications result in MSR's, for all methods, of 2.5 km and less as shown in Table 5-1.

**TABLE 5-1. Proposed System Parameters  
and Achievable MSR's**

	Divergence	P	Integration Time	Sensitivity	MSR	Safe Beam Diameter
DAS (Visible)	$3 \times 10^{-3}$ rad	$10^{-4}$ J	15 min.	10 ppm	50 m	15 cm
Raman (Visible)	$3 \times 10^{-3}$ rad	$40 \times 10^{-3}$ J	15 min.	300 ppm-m	1000 m	300 cm
Lidar (Visible)	$3 \times 10^{-3}$ rad	$250 \times 10^{-3}$ J	20 sec.	10% accuracy	<del>2500 m</del>	<del>750 cm</del>
LDV (IR)	$3 \times 10^{-3}$ rad	20 W	2 sec.	20% accuracy	150 m*	45 cm*

\* One second exposure

In order to make these systems eye safe at the exit of the transmitter, the beam diameter at the transmitter must be equal to the beam diameter at the MSR. These values are shown in Table 5-1. The values for DAS and LDV are not unreasonable for a practical system, but for the existing Raman and Lidar systems, the beam diameters are impracticable.

It is seen that both the MSR and the safe beam diameter of the Lidar are probably excessive using the present GE approach even with the proposed modifications. However, it would appear that the DAS system, which has reasonable values of MSR and safe beam diameter could be used for opacity measurements since, like the Lidar, it measures the transmittance of a plume. In terms of system sensitivity, it does not matter whether gas or particle transmittance is measured. In fact, due to the four signal measurements required for DAS compared to the two required for the Lidar, the Lidar system is more accurate for a given transmittance, as shown in Section 5.3.4.

It should be noted the MPE is much larger, and hence the MSR and safe beam diameter are much smaller, in the near UV ( $< 4000 \text{ \AA}$ ) and in the IR ( $> 1.4 \text{ }\mu\text{m}$ ). Thus, systems should preferably operate in these regions; they have the additional advantage that the solar radiation background is greatly reduced or is negligible. The use of these regions appears possible for the detection of gases using Raman (in the UV) and DAS (in the UV and IR). However, opacity measurements are traditionally based on observations in the visible, and the Federal Regulations are based on visible measurements, so that opacity measurements in the UV may not be readily accepted. Lidar opacity

measurements below 4000 Å could probably be related to conventional visible measurements on a theoretical or empirical basis for all types of particles.

### 5.3 ERROR ANALYSIS OF ACTIVE SYSTEMS

The errors involved in the various remote sensing techniques can be estimated by consideration of the equations describing the signal and noise of the system, although very little error analysis of systems has appeared in the literature. Of course, the final estimate of the accuracy of a system will be made in controlled tests in comparison with in-situ standard methods.

#### 5.3.1 DAS Systems

In DAS the laser radiation is transmitted (and received) at the line center (wavelength 1) and at the wing (wavelength 2). The values of  $N(R)$  and  $\beta$  here refer to the Rayleigh and Mie scatters behind the plume and are assumed constant during the measurements.

$\tau_A(R)$  may also be assumed constant so that Equation (4-12) may be rewritten:

$$\ln P(R) = \ln C - 2 \ln R + \ln \tau_G(R) \quad (5-3)$$

where  $C = \epsilon P_t L N(R) \beta A \tau_A(R)$  and is assumed to be constant with time and wavelength. Now

$$\tau_G(R) = e^{-2 \int_0^R (\rho(R)k + \sigma) dR}$$

where  $\rho(R)$  is the pollutant density at range  $R$  and  $k$  is the absorption coefficient of the pollutant,  $\sigma$  is the attenuation coefficient of particles in the atmosphere or plume, so we have

$$\ln P(R) = \ln C - 2 \ln R - 2 \int_0^R (\rho(R)k + \sigma) dR \quad (5-4)$$

At range  $(R + \Delta R)$

$$\ln P(R + \Delta R) = \ln C - 2 \ln(R + \Delta R) - 2 \int_0^{R+\Delta R} (\rho(R) k + \sigma) dR \quad (5-5)$$

Differencing (5-4) and (5-5) for wavelengths 1 and 2:

$$\ln P_1(R) - \ln P_1(R + \Delta R) = 2 \ln \frac{(R + \Delta R)}{R} + 2 \bar{\rho}(R) k_1 \Delta R + 2 \sigma_1 \Delta R \quad (5-6)$$

$$\ln P_2(R) - \ln P_2(R + \Delta R) = 2 \ln \frac{(R + \Delta R)}{R} + 2 \bar{\rho}(R) k_2 \Delta R + 2 \sigma_2 \Delta R \quad (5-7)$$

where  $\bar{\rho}(R)$  is the mean pollutant density over the distance  $\Delta R$ .

Assuming  $\sigma_1 = \sigma_2$ , the difference of (5-6) and (5-7) gives

$$\begin{aligned} \bar{\rho}(R) \Delta R &= \frac{1}{2(k_1 - k_2)} \left[ \ln \frac{P_1(R)}{P_2(R)} - \ln \frac{P_1(R + \Delta R)}{P_2(R + \Delta R)} \right] \\ &= \frac{\ln Q}{2(k_1 - k_2)} \quad \text{where } Q = \frac{P_1(R) P_2(R + \Delta R)}{P_2(R) P_1(R + \Delta R)} \end{aligned} \quad (5-8)$$

In deriving Equation (5-8) it was assumed that the atmospheric and pollutant properties are constant while the data are taken at the two wavelengths. This is true if they are taken simultaneously, but if it takes more than 1 msec to tune the laser between wavelengths, then atmospheric scintillation and air motion adds an error term to Equation (5-8). Schotland (1974) discussed these errors but did not provide an estimate of their magnitudes. Ku et al. (1975) experimentally varied the pulse repetition rate in a diode laser system operating in the CO 4.6  $\mu\text{m}$  band, and found that 1.5 msec intervals did indeed "freeze" the atmosphere over a 610 m path using a retroreflector at a range of 305 m. At longer intervals the signals varied significantly. Of course, the effects may be different at shorter wavelengths, and it is clear that simultaneous measurements at the two wavelengths are preferred, if possible. If separate lasers are used for each wavelength, then care must be taken to match the beam divergences and the distribution of energy across the beam. Northam (1976) is investigating the significance of these requirements.

In Equation (5-8) the absorption coefficients may be uncertain by as much as  $\pm 20\%$  (Schotland 1974), but this would be merely a systematic error which could be eliminated by careful calibration. Random errors in the absorption coefficient can arise by variation of pressure and temperature of the pollutant, and by fluctuations in the laser wavelength. The other errors in using Equation (5-8) to estimate  $\bar{\rho}(R)\Delta R$  occur in the measurement of the received power as a function of range and wavelength. The received power can possibly be measured to within 1% (implying a signal-to-noise ratio of 100), but since four power outputs must be measured in Equation (5-8),  $Q$  has an error of 4%, and when  $Q$  is close to unity, then the error in  $\ln Q$ , and hence, in  $\bar{\rho}(R)\Delta R$  is large.

This latter conclusion is verified by Inomata and Igarashi (1975), who have developed a DAS system with simultaneous wavelength oscillation of a dye laser. Two linearly polarized components of a dye laser cavity were independently tuned and used to measure 85 ppm-m of  $\text{NO}_2$  in a test cell. The laser power fluctuates by more than 10%, and it was necessary to monitor the output power at each wavelength. Their results are shown in Figure 5-1 which shows the standard deviation of a series of measurements.  $(V/P)_0$  and  $(V/P)$  correspond to  $P_2(R)/P_1(R)$  and  $P_2(R + \Delta R)/P_1(R + \Delta R)$  respectively, in Equation (5-8). These errors also include those due to wavelength instabilities of the laser, although the authors measured them and found them to be negligible.

The advantage of simultaneous wavelength measurements is demonstrated by the reduction in the fluctuations in (c) and (f) compared with (a), (b), (d) and (e). The error in  $Q$  [Equation (5-8)] for this set of data is only 4% [(c) + (d) errors], but translates strikingly into a 47.5% error in the measurement of pollutant optical thickness. This error will be even larger if the SNR is less than the apparent value 100 for each power measurement, as will occur for increasing range.

Of course, for larger optical thicknesses this error is reduced. For 850 ppm-m, which might be more representative of a plume, and 4% error in  $Q$ , the error in the optical thickness is about 25%. For increasingly larger optical thicknesses, the transmission of the plume will decrease so that the resulting return signal decreases and the measurement errors increase, and finally cannot be measured due to system or background noise.

It should be noted that these measurement errors could be reduced by averaging more pulses [ $\text{SNR} \propto (\text{number of pulses})^{1/2}$ ], but a long averaging time may not always be practicable, particularly if the source and atmosphere are fluctuating.

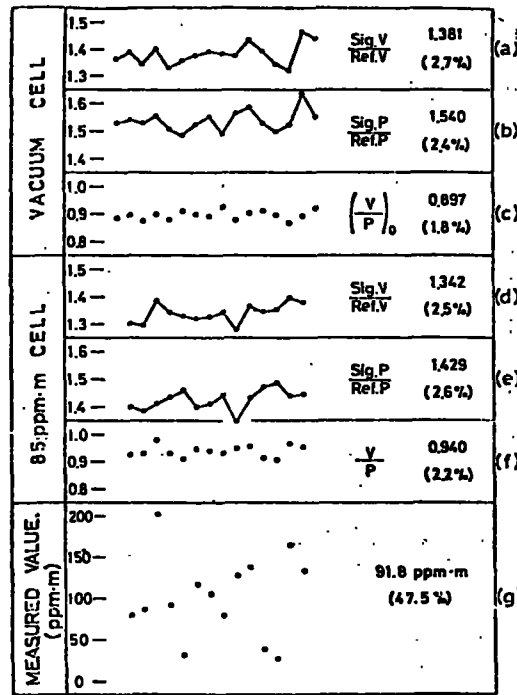


Figure 5-1. DAS experimental errors (after Inomata and Igarashi 1975)

### 5.3.2 Raman Systems

In the Raman technique, the transmitted laser radiation is shifted in wavelength when it is scattered by the pollutant, so that in Equation (4-12) we can consider  $\tau_A(R)$  to be the atmospheric attenuation of the outgoing laser beam, and  $\tau_G(R)$  to be the atmospheric attenuation of the return Raman radiation. If it is assumed that these atmospheric attenuations are constant then

$$P(R) = K N(R) \quad (5-9)$$

where

$$K = \epsilon P_t L \beta A R^{-2} \tau_A(R) \tau_G(R)$$

i. e., the pollutant number density is directly proportional to the measured return signal, so that the precision of the pollutant measurement is the same as that of the power measurement: if  $\text{SNR} = 10$ ,  $N(R)$  is determined within 10%.

There are uncertainties in the value of  $K$  due to instrument uncertainties, due to the value of  $\beta$ , which is uncertain by up to  $\pm 20\%$  (DeLong 1974) and due to the atmospheric attenuation uncertainties. All of these may be considered as systematic errors, although the atmospheric attenuation may fluctuate during a series of pulses being averaged.

A common method to obtain the pollutant concentration in ambient air directly, and to minimize the uncertainties, is to ratio the return signals from the pollutant and from nitrogen, the concentration of which is assumed known and constant in the atmosphere:

$$\frac{P(R)_{\text{gas}}}{P(R)_{N_2}} = \frac{\beta_{\text{gas}} N(R)_{\text{gas}} \tau_{G(R)}_{\text{gas}}}{\beta_{N_2} N(R)_{N_2} \tau_{G(R)}_{N_2}} \quad (5-10)$$

This method must be used with caution for plumes, since they may be oxygen enriched, and at varying exit pressures and temperatures. If the Raman returns of the pollutant and nitrogen are close together so that atmospheric scattering losses can be assumed the same, and do not exhibit different atmospheric absorption losses, then the only random uncertainties in obtaining the pollutant concentration occur in the power measurements, and may be reduced by pulse averaging without concern for atmospheric fluctuations. If  $\text{SNR} = 10$ , then the pollutant concentration error is 20% since two power measurements are needed.

An error source in Raman scattering, not described in the above equations, is that due to overlapping of Raman spectra of different species contained in a pollutant source. The Raman system measures the Q-branch of the vibrational-rotational Raman spectrum, but, as shown in Figure 5-2, the S- and O-branches of strongly scattering, high concentration species may overlap and mask the weaker Q-branch of another species. To retain specificity, narrow band interference filters with high rejection ratios must be used.

Typical Raman signals are small and the SNR is low so that nighttime operation provides greater sensitivity and range. Daytime



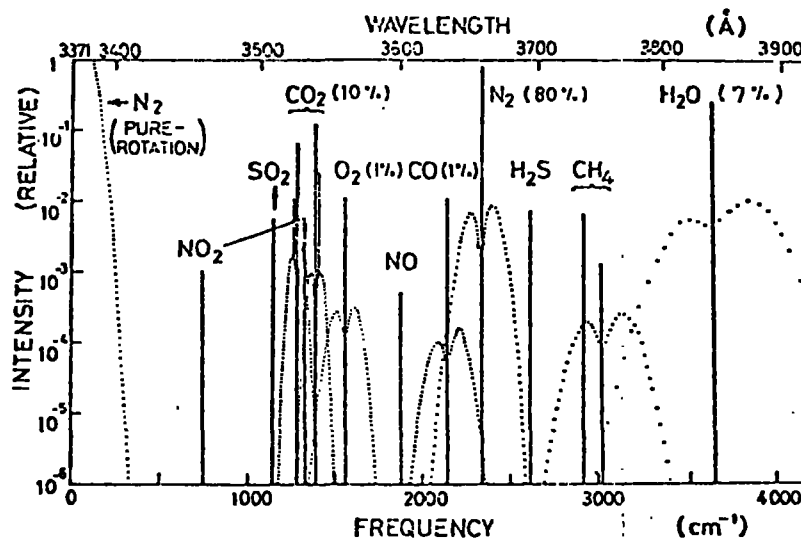


Figure 5-2. Theoretical distribution of Raman volume back-scattering coefficient due to a molecular mixture contained in a typical oil smoke as a function of Raman-shifted frequency. The solid line is the Q-branch and the dotted lines are the O- and S-branches (Inaba and Kobayasi 1972).

operation would be improved if designed for the solar-blind region below about 3000 Å, but at shorter wavelengths the Raman lines are closer, so that the filtering requirements discussed above are greater, and the errors due to interfering gases increase.

### 5.3.3 Lidar Systems

The lidar system for measuring plume opacity makes a measurement of the return signals from in front of the plume and from behind it, so that it is similar to DAS, but uses only one wavelength. Hence, in Equation (4-12),  $\tau_G(R)$  may be written as the scattering losses due to passage of the radiation twice through the plume,  $\tau_p^2$ , where  $(1-\tau_p)$  is the plume opacity. It is assumed that there is no absorption by the plume at the laser wavelength. If it is also assumed that the backscatter from in front and behind the plume is constant, i. e.,  $N(R)/\beta$  is constant, then the signal from in front of the plume is given by

$$P(R_1) = D R_1^{-2} \tau_A(R_1) \quad (5-11)$$

and the signal from behind the plume is given by

$$P(R_2) = D R_2^{-2} \tau_A(R_2) \tau_p^2 \quad (5-12)$$

where

$$D = \epsilon P_t L N(R) \beta A$$

Hence

$$\tau_p = \left[ \frac{P(R_2) R_2^2 \tau_A(R_1)}{P(R_1) R_1^2 \tau_A(R_2)} \right]^{1/2} \quad (5-13)$$

Since  $R_1$  is not greatly different from  $R_2$ , it may be assumed that  $\tau_A(R_1)$  and  $\tau_A(R_2)$  are equal. Hence, the error in  $\tau_p$  is determined by the errors in measuring the powers. Since the square root of the power ratio is involved, the percentage error in  $\tau_p$  is the same as in the power measurement, i. e., if  $SNR = 100$ , then the uncertainty in  $\tau_p$  is 1%. It must be noted that the error in opacity is greater than that in  $\tau_p$ , especially for low opacities. For example, a 1% error in  $\tau_p$  results in 4% and 9% opacity errors when the opacity is 0.2 and 0.1 respectively.

The assumption of the backscatter being the same on both sides of the plume may not be a good one, particularly in an industrial atmosphere where measurements would be made. This error is difficult to estimate, but could be eliminated by using the Raman scatter of nitrogen as the scattering source, but of course, the SNR would decrease and maybe result in uncertainties larger than those eliminated.

Another error source in this lidar technique is that of thermal lensing (Cook et al 1972) by the hot plume gases, which causes some

of the radiation from behind the plume to refract in and out of the receiver field-of-view, and hence causes the return signal to fluctuate; the magnitude of this effect is uncertain. This thermal lensing effect (which is similar to scintillation) does not affect the DAS technique if simultaneous measurements at two wavelengths are made.

#### 5.3.4 Intercomparison of Laser Techniques

A comparison of the promising laser techniques has been made on the basis of the error considerations discussed above. Let us consider the signal-to-noise relationship (Equation 4-16b):

$$SNR = \frac{\eta P(R) \cdot n^{1/2}}{(\eta P(R) + \eta P_B)^{1/2}} \quad (5-14)$$

where the signal  $P(R) = \epsilon P_t L N(R) \beta A R^{-2} \tau_A(R) \tau_G(R)$  photons,\* and the background noise is

$$P_B = \frac{\epsilon B A \Omega \Delta \lambda t_g}{h\nu} \quad (5-15)$$

where  $t_g$  is the gate width in seconds, and  $n$  is the number of pulses integrated.

For this intercomparison we have assumed system parameters common to all techniques; only the parameters  $N(R)$ ,  $\beta$ , and  $\tau_G$  vary with the method. The system parameters in Table 5-2 were assumed as reasonable, based on existing or planned real systems. The wavelength of 4500 Å is chosen since it is one used for NO<sub>2</sub> DAS measurements, it can be used for Raman, and it is not far removed from lidar wavelengths.

---

\* Note that  $\frac{P(R) \text{ Joules}}{h\nu} = P(R) \text{ photons.}$

Table 5-2. System Parameters

$\lambda$	=	4500 Å
$\Delta\lambda$	=	5 Å
$L$	=	10 m
$t_g$	=	$10^{-7}$ sec (> pulse width)
$A$	=	500 cm <sup>2</sup>
$\Omega$	=	$10^{-5}$ sr
$\epsilon$	=	0.1
$P_t$	=	$10^{-4}$ J (based on DAS MPE eye safety requirements)
$\eta$	=	0.2
$n$	=	900 pulses (based on 1 pps and 15 minute integration time permitted by Federal Regulations for gas measurements)
$B$	=	$10^{-6}$ W cm <sup>-2</sup> sr <sup>-1</sup> Å <sup>-1</sup> (daytime) and is negligible at night.

Using these values:

$$P(R) = 1.14 \times 10^{15} N(R) \beta \frac{\tau_A}{R^2} \tau_G \text{ photons (R in m)} \quad (5-16)$$

$$P_B = 5.66 \times 10^2 \text{ photons during the day} \quad (5-17)$$

and

$$SNR = 13.4 \frac{P(R)}{(P(R) + P_B)^{1/2}} \text{ during the day} \quad (5-18)$$

$$SNR = 13.4 (P(R))^{1/2} \text{ during the night} \quad (5-19)$$

The values of  $N(R)$  and  $\beta$  assumed for this comparison are given in Table 5-3.

Table 5-3. Backscatter Parameters

	DAS and Lidar		Raman
	Raleigh	Mie	
$\beta(\text{cm}^2 \text{sr}^{-1})$	$10^{-27}$	$10^{-8}$	$10^{-28}$
$N(R)(\text{cm}^{-3})$	$10^{19}$	$10^2$	$10^{15}$ (100 ppm)
$\beta N(R)(\text{sr}^{-1} \text{cm}^{-1})$	$10^{-8}$	$10^{-6}$	$10^{-13}$

The Mie parameters, given here for a clear day (25 km visibility), will, of course, vary with the particle type and size distribution and with the visibility. The Raman parameters vary with the gas and with the concentration. All of the values of  $\beta$  depend on wavelength.

These values of  $\beta N(R)$  are consistent with independent estimates by Collis and Uthe (1972) for Rayleigh scattering:

$$\beta N(R) = \frac{1.5}{4\pi} \sigma_R$$

where  $\sigma_R$  is the Rayleigh attenuation coefficient ( $\text{cm}^{-1}$ ) and by Measures and Pilon (1972) for Mie scattering:

$$\beta N(R) = 4 \times 10^{-2} \sigma_M$$

where  $\sigma_M$  is the Mie attenuation coefficient ( $\text{cm}^{-1}$ ). The value of  $\tau_A(R)$  is based on the model atmosphere (Elterman 1968) (25 km visibility), and ranges from 1.0 at 10 m to .12 at 5000 m for the 2-way transmission. The parameter  $\tau_G$  does not appear in the Raman equation, and in the lidar equation it represents the 2-way particulate transmittance of the plume. In the DAS equation  $2 \ln \tau_G$  is used, so that the difference in the absorption coefficient on and off an absorption line, is used directly. We have assumed that  $k_1 = 16 (\text{atm-cm})^{-1}$  and

$k_2 = 8 \text{ (atm-cm)}^{-1}$  based on the work of Grant et al (1974) in using DAS for  $\text{NO}_2$  measurements. Thus, the effective value of  $\tau_G$  for 100 ppm with a 1 m stack exit diameter is given by

$$\tau_G = e^{-(16-8) 10^{-2}} = .92$$

for passage once through the plume. This same transmittance for particles in the lidar system represents an opacity of 0.08.

Using the above values of the systems parameters, and Equations (5-18) and (5-19), calculations were made of the SNR of the backscattered signal for DAS, Raman and lidar, both day and night, for 100 ppm of the gas in a 1 m exit diameter (or 0.08 opacity). It is assumed in these calculations that the transmitter and receiver fields-of-view completely overlap at all ranges, and that the effective backscattering cross-sections and system efficiency are constant at all ranges.

Figure 5-3 shows the results for DAS and lidar at a single wavelength. These values are computed for the backscattered signal in front of the plume, and are the same for each DAS wavelength. The SNR is slightly smaller from behind the plume and different for each DAS wavelength. The SNR for the Raman system is not shown in Figure 5-3 since the values are very low: SNR = 13.4 at 10 m and 1.31 at 100 m during the night, and SNR < 1 during the day.

In order to compute the concentration (opacity) measurement errors, the SNR values were used in conjunction with the data analysis procedures developed in Section 5.3. It is assumed that SNR = 100 represents 1% signal error, SNR = 40 represents 2.5% signal error, etc. These error estimates must be considered as optimistic since (a) the value of  $N(R)\beta$  is likely to vary during the measurement period, (b) the value of  $N(R)\beta$  may not be the same on each side of the plume, (c) signal processing errors are not considered, (d) laser wavelength and intensity fluctuations are not considered, (e) thermal lensing effects by the plume are not considered, and (f) spectral interference effects of other species are not considered. There is also a systematic error due to lack of precise knowledge of the absorption coefficient and its variation with temperature, but this can be eliminated by careful laboratory and field calibration.

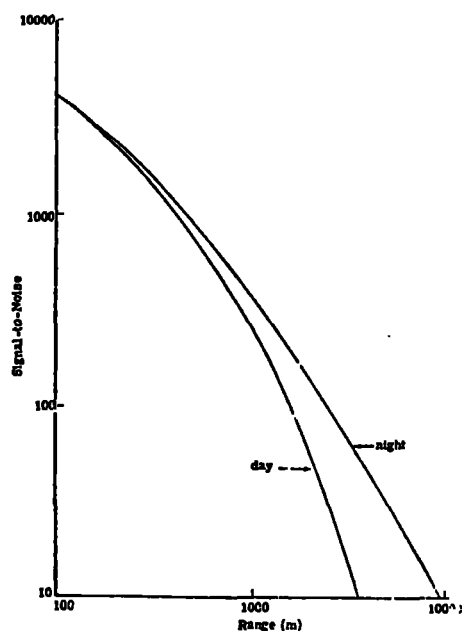


Figure 5-3. SNR calculations for DAS and Lidar (900 pulses at one wavelength) for a 1 m plume (100 ppm) at range R

The calculated measurement errors, shown in Figure 5-4, indicate that DAS and lidar are probably useful (20% error) out to 1 to 3 km, but that Raman does not have a useful range capability. It should be noted that the lidar system, to comply with the present Federal Regulations for opacity, cannot use a 15 minute integration time, but must use 15 seconds. Figure 5-4 is strictly for intercomparison of the techniques and does not represent optimized systems, although it does indicate that a Raman system designed for eye safe operation in the visible does not have a useful range capability. Figure 5-5 shows the effect on the lidar accuracy of reducing the integration time to 15 seconds and indicates a useful (20% error) range of 650 m during the day and 840 m at night. The calculations shown in Figures 5-4 and 5-5 are for 100 ppm in a 1 m stack exit diameter, and for 0.08 opacity in the case of lidar. The 100 ppm-m of gas is probably a lower limit of interest in enforcement monitoring. For opacity, 0.08 is less than the 0.10 and 0.20 limits prescribed for most sources in the Federal Regulations; presumably enforcement personnel will be most concerned with monitoring larger opacities which are exceeding the limits.

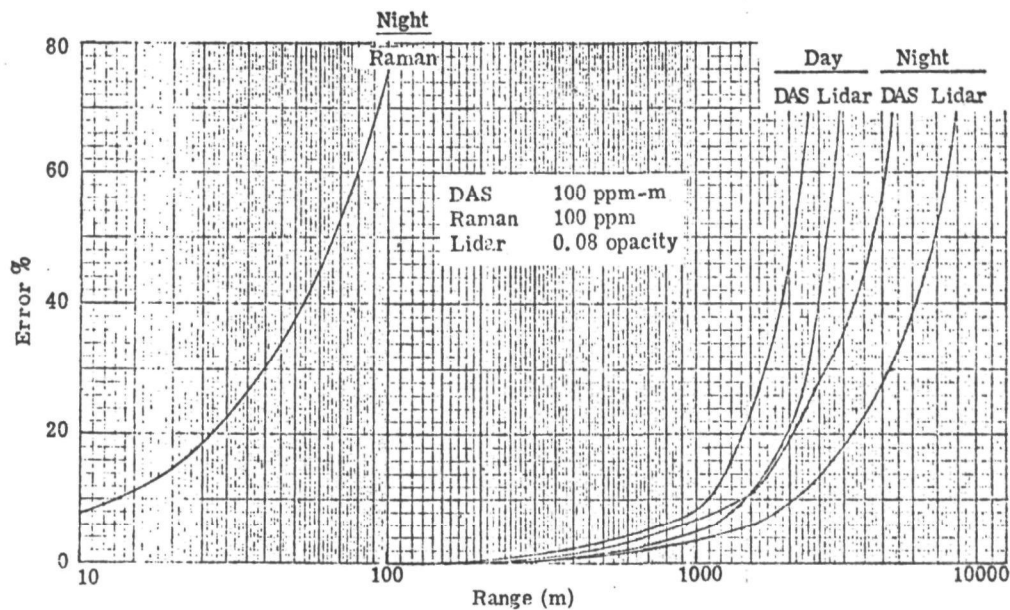


Figure 5-4. Intercomparison of measurement errors for plume at various ranges. These results are not optimized for each system, but are strictly for intercomparison of techniques.

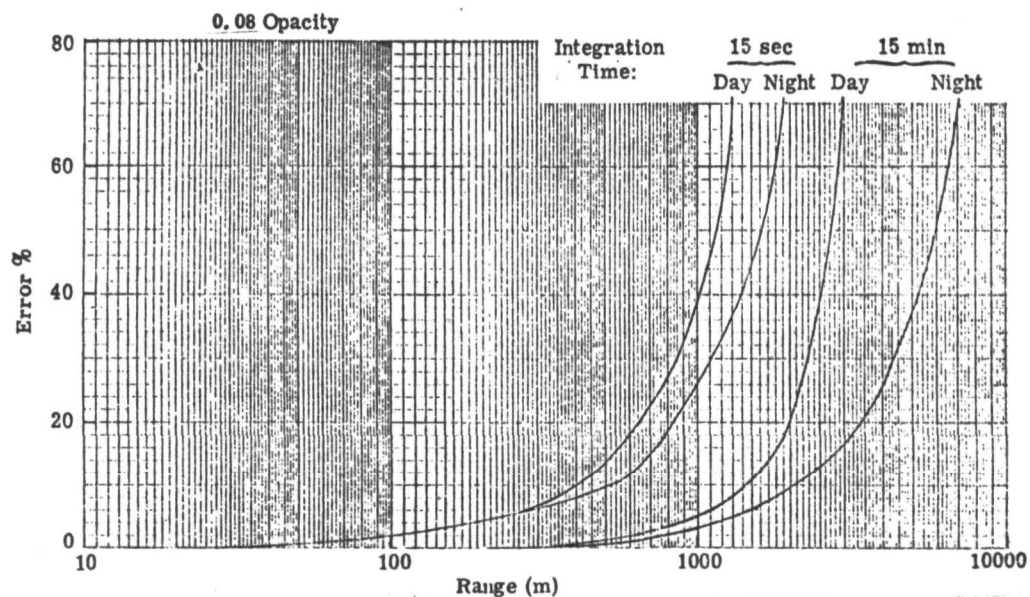


Figure 5-5. Lidar errors as a function of integration time



As the gas concentration in a stack plume increases, so the Raman return signal will increase, and the errors will decrease. However, for DAS and lidar, the transmittance of the plume decreases with increasing gas (particle) amounts, and the errors will decrease at first, and then increase. The signal-to-noise of the measurement behind the plume, of course, decreases continuously with increasing gas (particle) amounts, but this decrease is initially outweighed by the increase in the values of  $Q$  and opacity, so that initially the percentage errors in concentration (opacity) decrease. However, at larger amounts the signal-to-noise decrease outweighs the increase in  $Q$  and opacity, and the errors increase again.

Figure 5-6 shows the increasing range capability of the Raman technique with increasing gas concentration. However, even at very high concentrations (10,000 ppm) the system does not have a useful daytime range capability. Figure 5-7 shows the variation of lidar errors with increasing opacity up to an opacity of 0.8. It is seen that 0.8 opacity is not large enough to increase the errors during nighttime operation, but during the day the errors start to increase between 0.4 and 0.8 opacity values. Figure 5-8 shows that at nighttime the DAS errors decrease

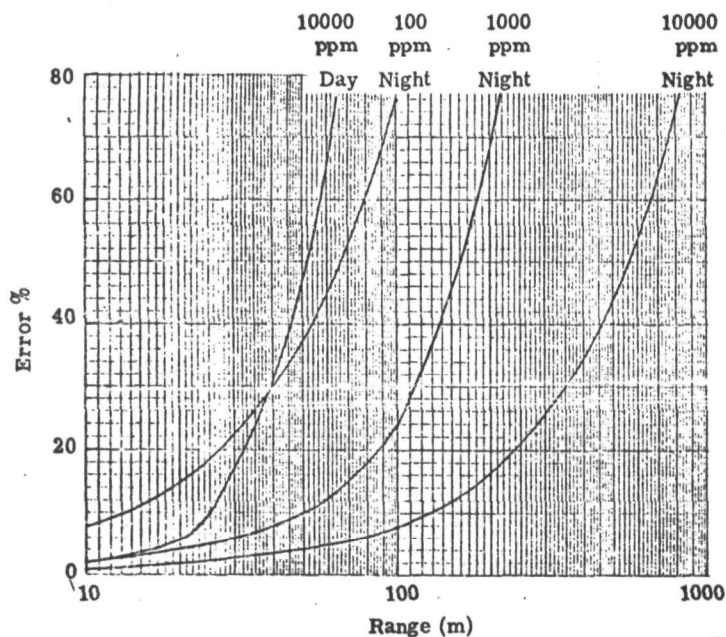


Figure 5-6. Raman errors as a function of gas concentration

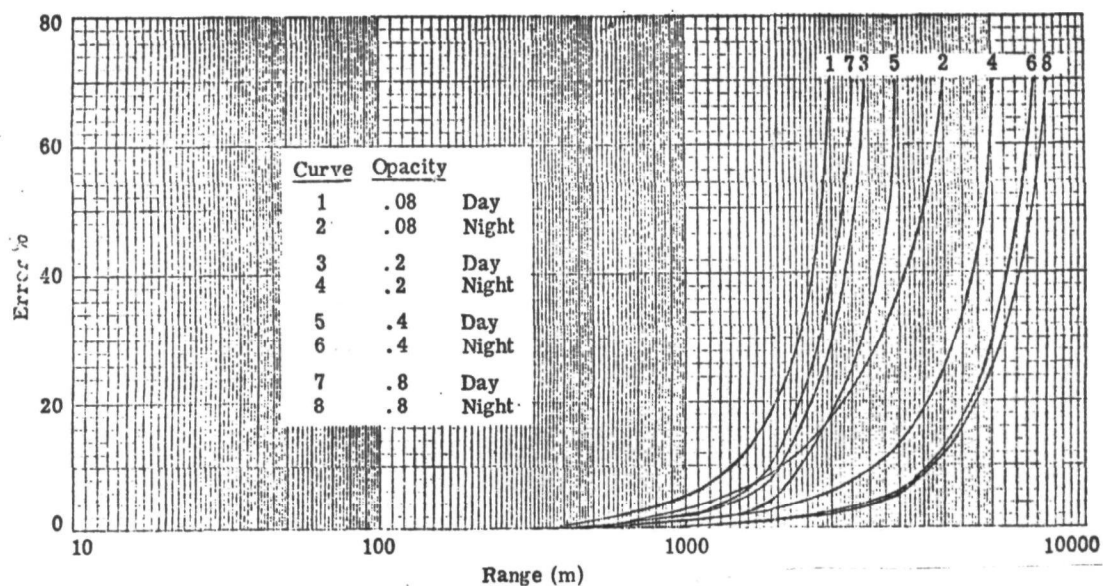


Figure 5-7. Lidar errors as a function of opacity

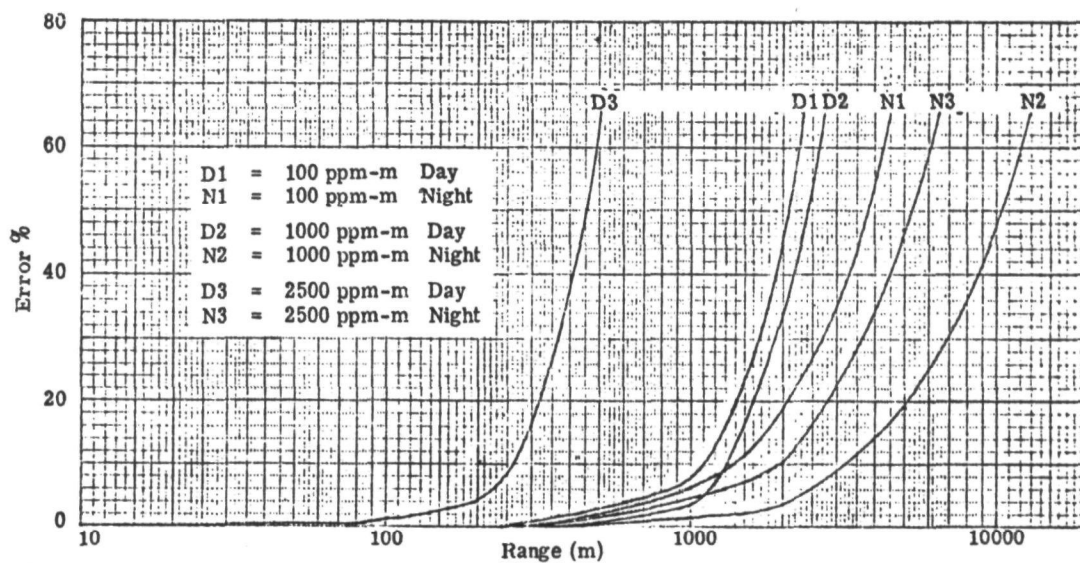


Figure 5-8. DAS errors as a function of gas optical thickness

up to 1000 ppm-m, but increase between 1000 and 2500 ppm-m. During the day the errors decrease slightly going from 100 ppm-m to 1000 ppm-m; however, increasing the gas optical thickness to 2500 ppm-m, dramatically increases the errors and greatly reduces the daytime range capability of this DAS system.

#### 5.4 ERROR ANALYSIS OF PASSIVE INFRARED SYSTEMS

In the following, results of calculations are presented which show that the influence of source and atmospheric parameters is significant in the data interpretation of passive systems. Because of the importance of the pollutant  $\text{SO}_2$ , the calculations were made for this species. Since  $\text{SO}_2$  has several infrared bands, some calculations were made for more than one band in order to show that the proper selection of the infrared spectral region is important, and also that the device is dependent upon many competing parameters and requirements.

##### 5.4.1 Source Strength

In order to assess the plume radiation and the required noise-equivalent-radiance, the radiated energy of  $\text{SO}_2$  in the  $4\text{ }\mu\text{m}$  spectral region was calculated in a line-by-line model. The line parameters (position, shape, strength and lower energy level) were developed previously (Ludwig et al. 1974). The results are shown in Figure 5-9 in which a normalized filter function with a bandwidth of  $60\text{ cm}^{-1}$  at half-height was used ( $2465\text{-}2525\text{ cm}^{-1}$ ).

The influence of other species in the plume and of the atmosphere between the observer and the plume and beyond was found to be negligible. (For a pathlength of 130 m between observer and plume, the atmospheric absorption transmission is 0.998 for 50% relative humidity, 0.3 ppm  $\text{N}_2\text{O}$ , 320 ppm  $\text{CO}_2$ , 1.4 ppm  $\text{CH}_4$ , and 0.01 ppm  $\text{SO}_2$ . The radiance of the clear sky was calculated to be less than 2 percent than that of the plume having 500 ppm-m  $\text{SO}_2$  at  $650^\circ\text{K}$ ). The contribution of scattered sunlight was not considered in these calculations.

From the results shown in Figure 5-9, it is clearly seen that the emitted radiance is a sensitive function of the plume temperature. (An uncertainty of  $\pm 10\%$  in temperature at  $500^\circ\text{K}$  results in an uncertainty of over  $\pm 100\%$  in  $\text{SO}_2$  concentration). Thus, in order to determine

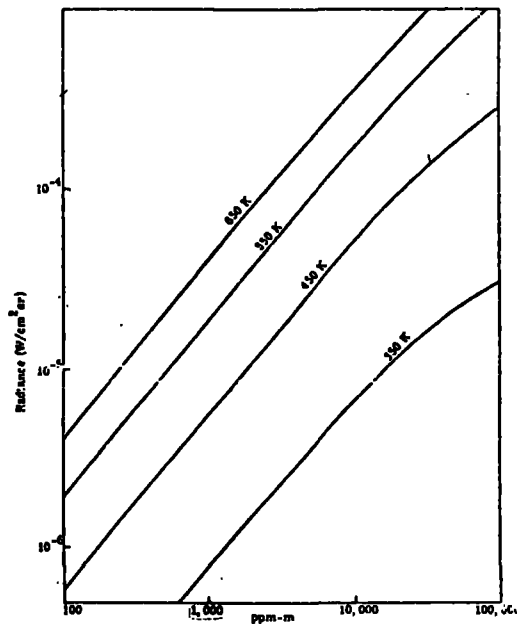


Figure 5-9. Emitted radiance as a function of SO<sub>2</sub> optical thickness

the SO<sub>2</sub> concentration in the plume, a method must be found to either eliminate the temperature dependency or to determine the plume temperature accurately by an independent measurement. (One such method is the SAI-GFC analyzer that was described in Section 4.4.3 and whose field test results indicated an uncertainty of about  $\pm 25\%$  in the determination of SO<sub>2</sub> concentration.)

For the case of perimeter monitoring in the up-looking mode, which was schematically shown in Figure 2-1, line-by-line calculations were made for measuring SO<sub>2</sub> at 4  $\mu\text{m}$  and 8.6  $\mu\text{m}$ . The results for the received radiance at 4  $\mu\text{m}$  as a function of SO<sub>2</sub> loading (ppm-m) are shown in Figure 5-10 with a given filter function. The atmosphere has no significant influence in this spectral region and different amounts of water vapor would not give significantly different radiance values. However, the influence of the atmospheric temperature is significant, as shown in Figure 5-11, where the mean atmospheric temperature was varied between 270 and 300°K. It is easily seen that a pure radiometer measurement would not be very sensitive to the SO<sub>2</sub> vertical loading, but much more to the atmospheric temperature.

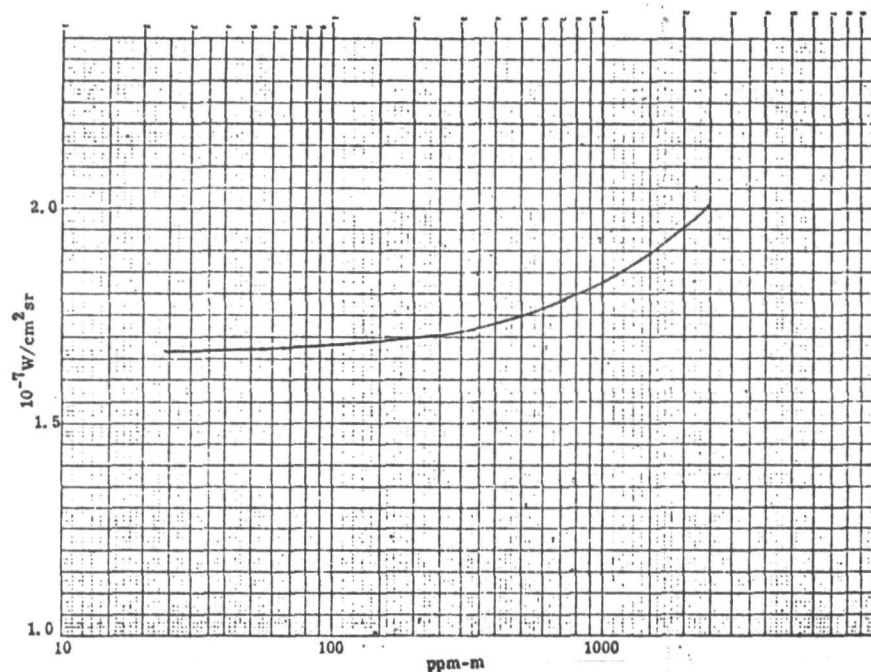


Figure 5-10. Radiance versus SO<sub>2</sub> vertical loading in 4 μm band

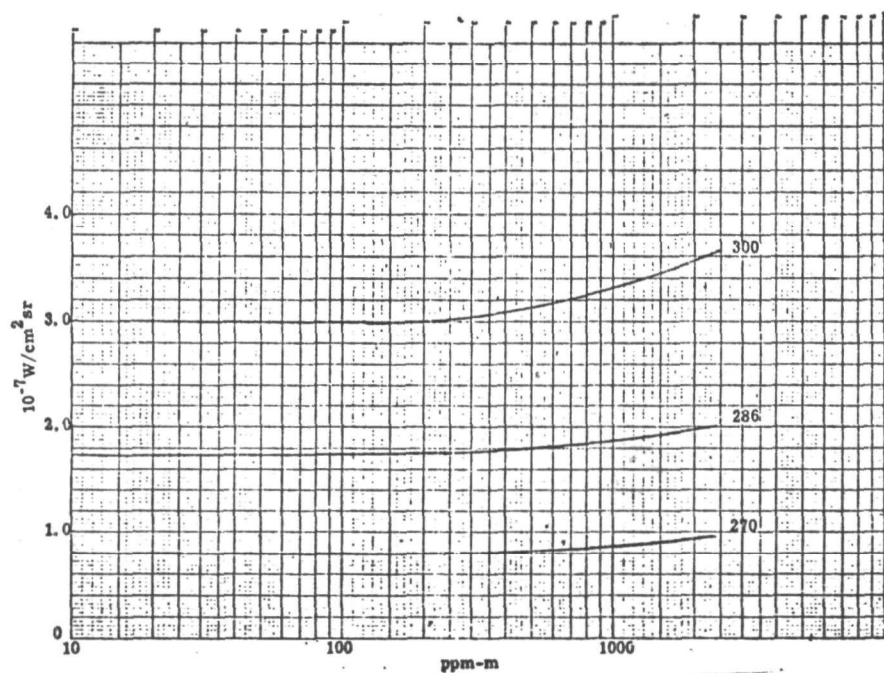


Figure 5-11. Radiance as a function of SO<sub>2</sub> vertical loading in the 4 μm band for three different average atmospheric temperatures

This situation is reversed for the  $8.6 \mu\text{m}$  region, where  $\text{SO}_2$  has a fundamental band. Here, the influence of the mean atmospheric temperature is somewhat reduced, as shown in the comparison between the Figures 5-11 and 5-12, even though an accurate radiometer measurement of the  $\text{SO}_2$  vertical loading remains impossible. The influence of three different water vapor concentrations (0.5, 1.0 and 1.5 normal Gutnick corresponding to about 30, 60 and 90 percent relative humidity) on the effect of the observed radiance is shown in Figure 5-13.

#### 5.4.2 The Measurements of Signal Differences:

The influence of the atmospheric temperature and the water vapor can be reduced by using the signal differencing method, as is being done in the gas filter correlation instruments. In this case, the instrument measures the difference of the incoming energy as it passes through the gas channel, containing  $\text{SO}_2$ , and the reference channel, containing  $\text{N}_2$ .

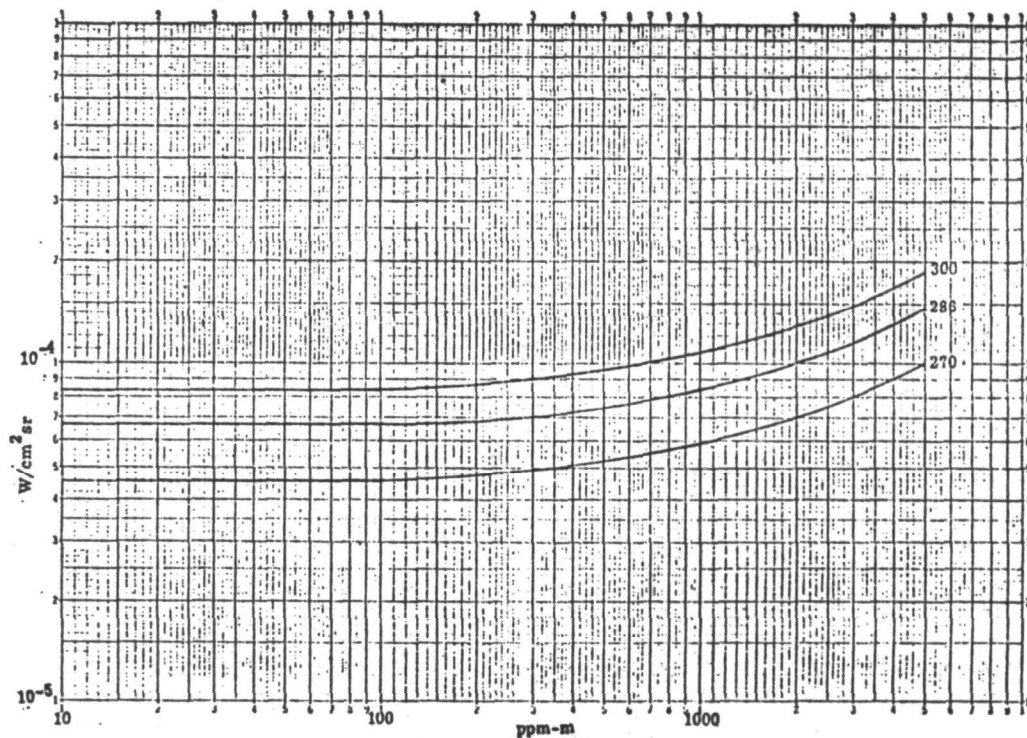


Figure 5-12. Radiance versus vertical  $\text{SO}_2$  loading in the  $8.6 \mu\text{m}$  region for three different mean atmospheric temperatures



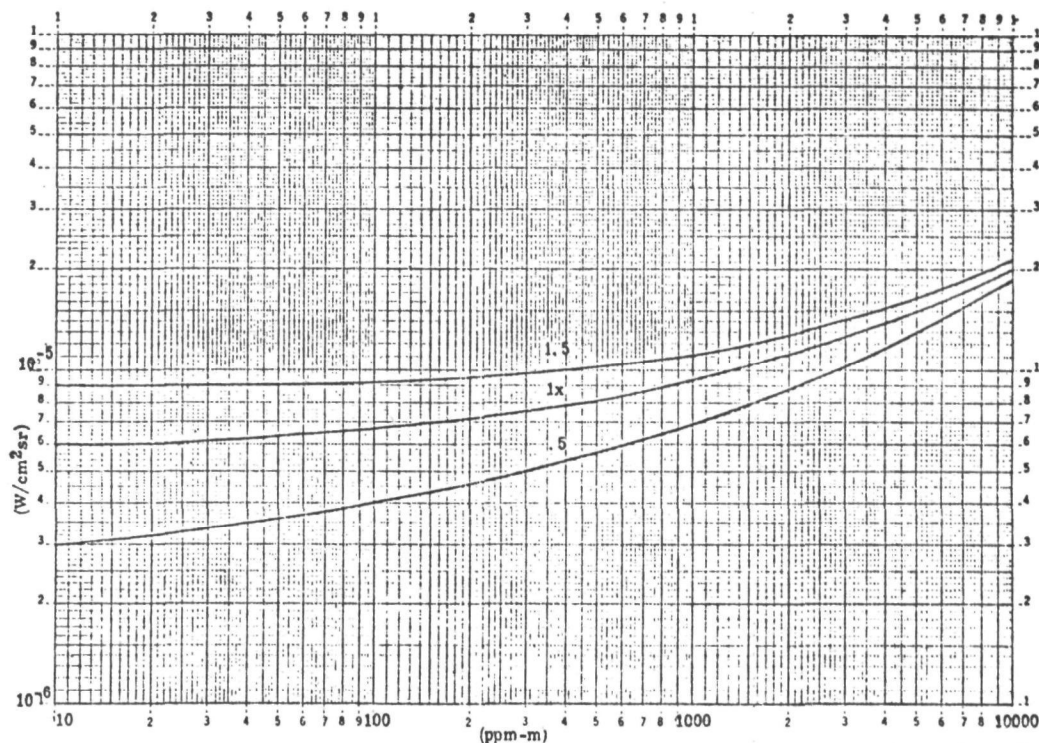


Figure 5-13. Radiance versus vertical  $\text{SO}_2$  loading in the  $8.6 \mu\text{m}$  band for three different water concentrations

We have calculated the correlation term  $\Delta V$  for several atmospheric conditions with different  $\text{SO}_2$  vertical loadings in the two infrared rotation-vibration bands at  $4 \mu\text{m}$  and  $8.6 \mu\text{m}$ . The  $4 \mu\text{m}$  band is essentially free of interfering species, whereas the  $8.6 \mu\text{m}$  band has many interfering water vapor lines. It is apparent from the following analysis that although the signal in the  $8.6 \mu\text{m}$  is stronger, its uncertainty, due to water vapor interference, is significantly greater than in the  $4 \mu\text{m}$  band. The GFC signal in the  $4 \mu\text{m}$  band for  $\text{SO}_2$  amounts from 10 ppm-m to 5000 ppm-m for the effective atmospheric temperatures of 275, 286 and  $300^\circ\text{K}$  is shown in Figure 5-14.

The results show that the  $\Delta V$  signal is a strong function of the  $\text{SO}_2$  concentration, but that its dependence on the atmospheric temperature is relatively small; an uncertainty in temperature of  $\pm 2^\circ\text{K}$  results in an uncertainty of only about  $\pm 10$  ppm-m at 100 ppm-m. The influence of the normal atmosphere was also considered. It was found

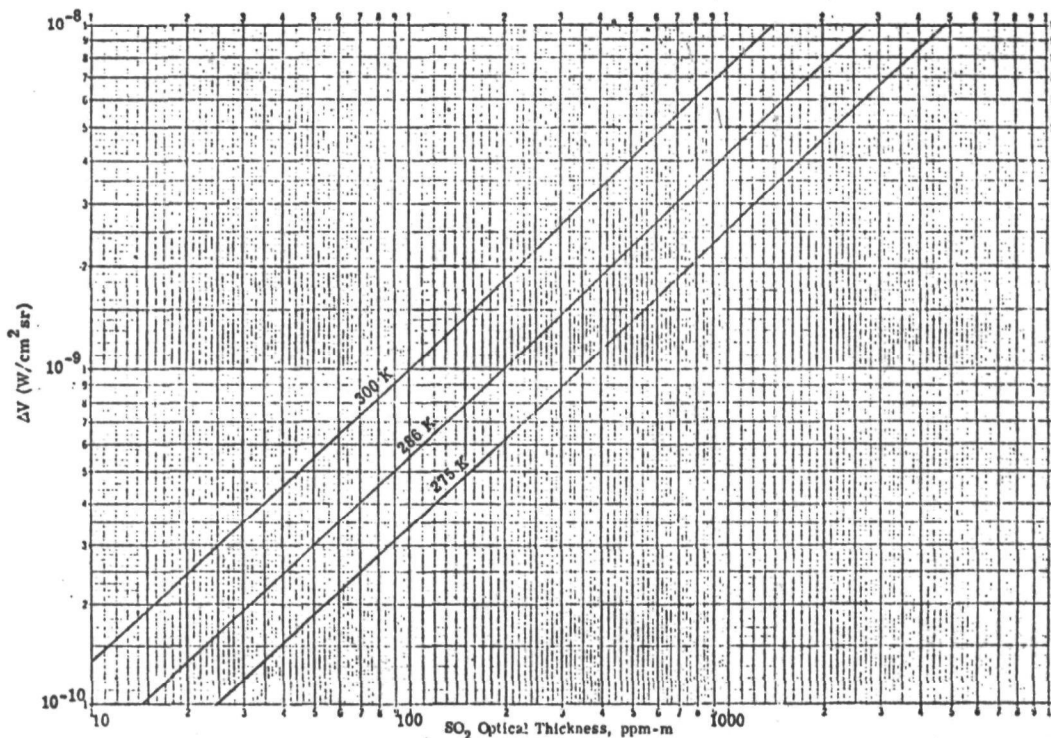


Figure 5-14. GFC signal as a function of  $\text{SO}_2$  loading at  $4 \mu\text{m}$  for three temperatures

that about 1000 very weak lines of  $\text{N}_2\text{O}$ , 10 lines of  $\text{CO}_2$ , 53 lines of  $\text{CH}_4$  and the water vapor continuum contribute in this spectral interval. The influence of these species was found to be negligible. The effect of clouds in the field-of-view was also investigated. It was found that stratus clouds decrease the  $\Delta V$  signal. High clouds will, of course, have less influence.

The results of the calculations as a function of the vertical loading of  $\text{SO}_2$  at  $8.6 \mu\text{m}$  are shown in Figure 5-15. The results show that the  $\Delta V$  signal is stronger than in the case for the  $4 \mu\text{m}$  due to the higher radiance values in the blackbody function and the somewhat larger band strength. Because the slope of the Planck function is much less in this spectral region than in the  $4 \mu\text{m}$  region, the error due to  $\pm 2^\circ\text{C}$  in atmospheric temperature is only  $\pm 2 \text{ ppm-m}$  at  $100 \text{ ppm-m}$ . However, the influence of the other atmospheric species, especially that of water vapor, is considerably greater than in the  $4 \mu\text{m}$  region. There



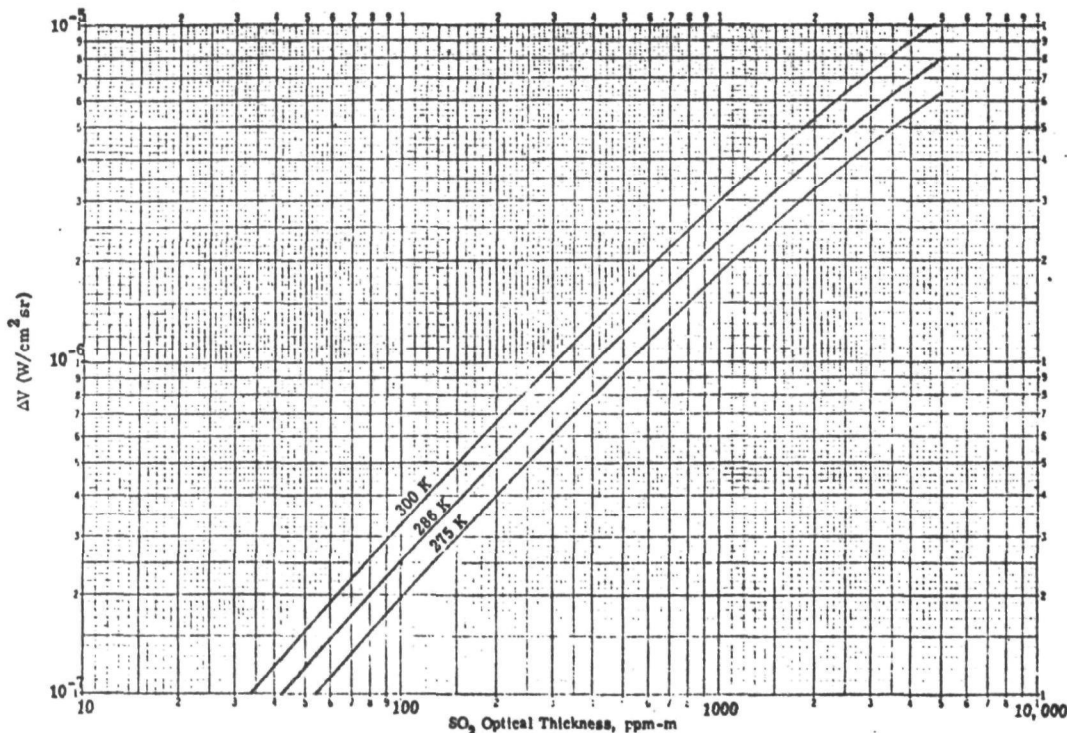


Figure 5-15. GFC signal as a function of  $\text{SO}_2$  loading at  $8.6 \mu\text{m}$  for three temperatures without interfering atmosphere

are 262 lines of  $\text{CO}_2$ , 2518 lines of  $\text{O}_3$ , 1078 lines of  $\text{N}_2\text{O}$ , 89 lines of  $\text{CH}_4$  and 497 lines of water vapor plus its continuum radiation in this spectral region. A change in concentration of any of these species will influence the determination of  $\text{SO}_2$  vertical loading.

The influence of water vapor variation was investigated in greater detail. The effect manifests itself both in terms of a "correlation signal" (water lines on  $\text{SO}_2$  lines) as well as an "uncorrelated emission signal". Representative results are shown in Figure 5-16 for the  $\Delta V$  signal as a function of  $\text{SO}_2$  loading at three different water vapor concentrations. The water vapor concentrations chosen correspond to the 0.5, 1.0 and 1.5 normal Gutnick distribution. They correspond to about 30%, 60% and 90% relative humidity at 286°K.

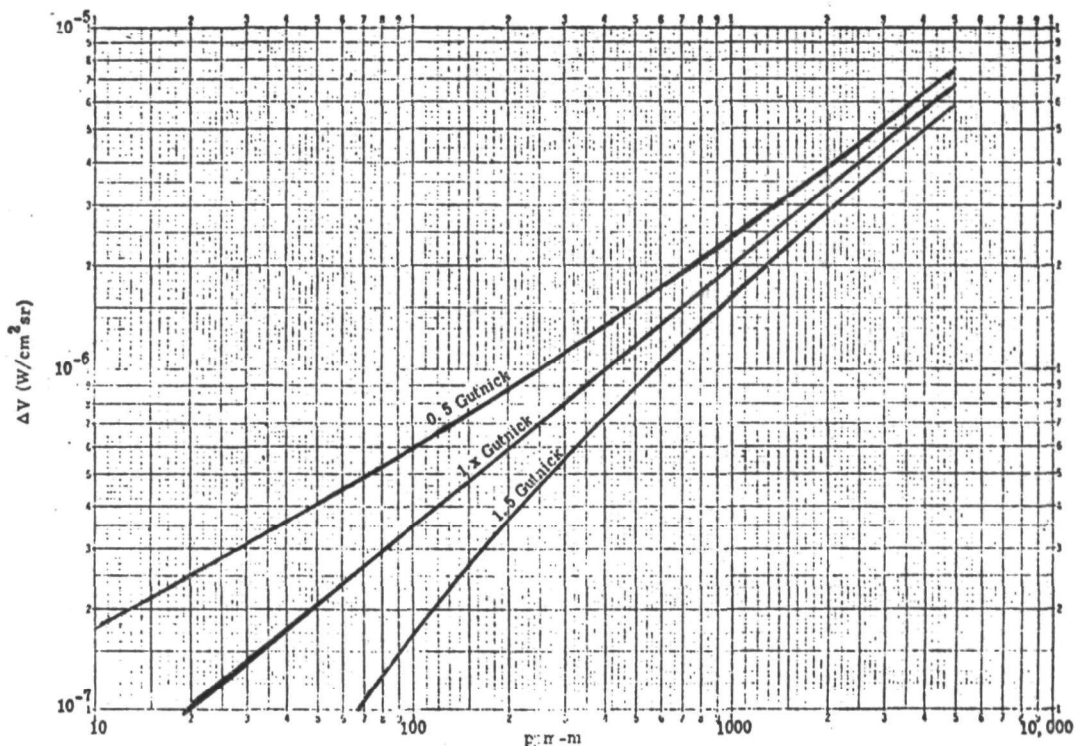


Figure 5-16. GFC signal as a function of SO<sub>2</sub> loading for three water vapor concentration (8.6 μm)

If the water vapor profile were known, it would be possible to correct the  $\Delta V$  signal for the interference. However, it can be shown that a single measurement of the relative humidity near the surface is not representative of the total water vapor content in the atmosphere. A single surface measurement can result in great errors and the uncertainty is estimated as much as  $\pm 50\%$  in total H<sub>2</sub>O loading in the atmosphere, which results in an uncertainty of almost 100% in SO<sub>2</sub> vertical loading at 100 ppm-m (see Figure 5-16). This error becomes somewhat smaller at higher levels of SO<sub>2</sub> loading, but is significantly larger at lower levels. In order to reduce these errors, it would be necessary to include additional channels into the instrument which would permit a better estimate of the water vapor content. However, one single measurement, giving the total amount in precipitable centimeters would not be sufficient, since the radiance signal is both a function of the water vapor vertical distribution and the atmospheric temperature profile.

### 5.4.3 Perimeter Monitoring Data Analysis (Infrared)

The radiative transfer equation shows that the downwelling radiance depends on the atmospheric temperature profile and on the vertical distribution of the pollutant and other species. However, in perimeter monitoring the pollutant is confined to the lowest layers of the atmosphere, probably below 500 m. Since the temperature lapse rate is typically about  $6^{\circ}\text{C km}^{-1}$ , the mean temperature of the 500 m layer is only  $1.5^{\circ}\text{C}$  different from the values at the top and bottom. Hence, assuming the pollutant temperature has equilibrated with that of the atmosphere, the radiance from the layer may be approximated closely by a single slab model, i. e. ,

$$R_{\lambda} = N(\lambda, T) (1 - \tau_{\lambda})$$

Of course, the lapse rate will vary with the meteorological conditions, but it is believed that the mean temperature of the 500 m layer can be estimated within  $\pm 2^{\circ}\text{C}$  by measuring the surface temperature, and by knowing the typical diurnal meteorological variations for the location. Of course, a measured temperature at altitude may be available by other means, such as a radiosonde, a tower or tethered balloon, in which case the mean layer temperature would be known more accurately.

In using the perimeter monitoring technique, the pollutant may be dispersed uniformly (or non-uniformly) through the lowest layers, or it may be confined to a relatively thin layer, depending on the meteorological conditions and the distance from the source. These variations of distribution mean that the pollutant mean temperature and pressure varies, so that the GFC signal is expected to vary. However, since the vertical variation of temperature and pressure is small within the anticipated vertical extent of the pollutant, the effect of the pollutant vertical distribution is small.

In our computer simulations for the GFC instrument, we found that the single slab model  $\Delta V$  signal at  $8.6\text{ }\mu\text{m}$ , in the range 100 ppm-m to 10,000 ppm-m  $\text{SO}_2$ , varies from the model using a profile by less than 1%, and that the maximum effect of the variations in the  $\text{SO}_2$  vertical distribution is an additional 1%. These uncertainties are small compared with the uncertainties in the  $8.6\text{ }\mu\text{m}$  water vapor effects. These single slab effects are approximately twice as great in the  $4\text{ }\mu\text{m}$   $\text{SO}_2$  band due to the greater change of blackbody radiance with temperature, so that at  $4\text{ }\mu\text{m}$  there is a 4% uncertainty in addition to the approximately  $\pm 10\%$  uncertainty due to the  $\pm 2^{\circ}\text{C}$  temperature uncertainty.

# 6

## ADVANTAGES AND DISADVANTAGES OF REMOTE MONITORING TECHNIQUES

### 6.1 OVERVIEW

In this section we summarize the advantages and limitations of remote monitoring techniques in EPA's enforcement and R&D programs.

In general, one of the advantages of "remote sensing" from elevated platforms, namely the coverage of large areas, has been recognized for some time since the advent of Landsat 1 (previously known as ERTS 1). Many interesting features of land and water areas could be recognized, which would otherwise have remained undetected. Some Landsat programs were even concerned with measurements of air pollution (Griggs 1974), and others provided evidence in legal cases. For example, spectral data taken by the Multi-Spectral-Scanner (MSS) on-board the spacecraft were used to determine that a major city water intake pipe had been placed directly into a large pool of pollutants in Lake Superior. The image was used in a court suit by the city against a firm that was paid about \$8 million, before the Landsat program, to position the intake pipe in a clean water area. The suit was settled out of court, according to the NASA official (AWST 1975). In the same article it was stated that Landsat 1 has been used in cases involving the violation of pollution laws. In addition, the spacecraft has been actively involved in enforcing water impoundment laws governing the safety of damming facilities at about 50,000 sites. Inadequate damming was involved in at least one major fatal accident in recent years involving the water containment areas now under Landsat observation.

Besides the advantage of wide area coverage from elevated platforms, there are several other advantages of either stationary or mobile ground-based as well as airborne remote monitors, which can be realized in enforcement and regulatory programs. These include cost effectiveness, direct measurement of mass emission rates, and rapid response in air pollution episodes.

There are, of course, certain disadvantages to remote monitoring, which include the greater initial capital outlay of the instruments, the effect of atmospheric interference on the measurements, the increased requirements in calibration procedures of the instruments, and lastly, the possible eye safety hazard of the more powerful lasers operating in the visible spectrum.

In balance, however, we found that the advantages outweigh the disadvantages.

## 6.2 COST EFFECTIVENESS

We have attempted to estimate the costs involved in remote monitoring and to compare them with present in-stack costs. We have chosen the monitoring of 100 stacks as a basis. Basically, there are three types of costs: research and development, purchase price of the operational field instrument, and operating costs, which include the man hours needed for maintenance, calibration and operation. Obviously, cost estimates for the remote monitors must be regarded as very tentative at this stage. EPA has published cost figures for the continuous monitors (40FR46254, Oct. 6, 1975). For opacity monitoring alone, investment costs including data reduction equipment and performance tests are approximately \$20,000, and annual operating costs are approximately \$8,500. For power plants that are required to install opacity, nitrogen oxides, sulfur dioxide, and diluent (O<sub>3</sub> or CO<sub>2</sub>) monitoring systems, the investment cost is approximately \$55,000, and the operating cost is approximately \$30,000.

The cost estimates given in the following are based on evidentiary monitoring for case development. It is obvious that surveillance monitoring requires less effort, and that greater effort is required for compliance monitoring. This is true for both point sampling as well as remote monitoring. In fact, the development of portable in-stack monitors will make it possible to spend relatively short time for surveillance, and possibly even for enforcement at the stack(s) in question (Nader 1975). Nevertheless, indications are that significantly more time will be required for case development because of the number of samples and the extent of documentation needed. In any case, our studies show that more time will be needed using the in-situ and extractive sampling techniques than the remote ones.

### 6.2.1 Opacity

In this case, we consider as the present methods, both the visual observations of trained observers and the in-stack monitoring by transmissometers. An overview is given in Table 6-1. For the visual observations, we have assumed that approximately one-half day is used for observing each stack and one-half day to record and analyze the data. For 100 stacks this amounts to about 0.4 man year. The initial cost of \$1K is assumed to be needed for the smoke school.

TABLE 6-1. Initial and Operational Costs for Monitoring the Opacity of 100 Stacks

Monitoring Mode	Initial Cost	Man Years Per 100 Stacks	Remarks
Present (visual)	1 K	0.4	Initial Cost: Smoke School
Present (in-stack)	5-10 K	2.5	Initial Cost is per instrument
Remote Monitor	20-80 K	0.4	

The cost figures are drastically different for in-stack transmissometers. New stationary sources are required to have continuous monitors installed and the results have to be reported to the appropriate agencies. Thus, it is difficult to assign any additional cost figures, because the analysis of the company reports demand an uncertain amount of man hours. However, if a state agency is compelled to conduct in-stack monitoring for evidentiary purposes, the cost for 100 stacks increases significantly. The cost of an in-situ transmissometer is estimated to 5-10 K, and the additional effort to monitor is estimated to be about 5 man days per stack (Smith 1974). Thus, for 100 stacks, 4000 man hours or about 2.0 man years will be needed. In contrast, the remote Lidar instrument is estimated to be in the price range from about \$20 K to \$80 K, which is several times higher than the in-stack instrumentation. However, the operational costs are lower, and are judged to be the same as for the visual observations.

The estimate of the cost for enforcement monitoring with a telephotometer shows a low initial purchase price, but comparable operational costs.

The cost estimates for aerial surveillance from aircraft are relatively low because of the large area coverage, assuming automatic data analysis. Of course, the cost of operating the aircraft must be added.

#### 6.2.2 Gas Concentration

An overview for gas instrumentation to measure gases is given in Table 6-2. The present monitoring is conducted by analyzing the company reports, required for new stationary sources. If in-stack monitoring is required, for case development, the reference method costs about \$1.5 K, and takes about 10 man days to collect the data. Thus, for 100 stacks, 8000 man hours or 4 man years would be required. However, if portable in-stack monitors were to be used, the operational time would probably be reduced.

As in the case for opacity monitoring, the initial price of the remote sensors is higher than the in-stack monitor, but the operational costs are considerably less. We have assumed that the operational laser systems will be about \$20-\$80 K; the passive instruments are less expensive and will be in the range from about \$10-\$40 K. The operational costs are assumed to be similar to the ones used for the remote opacity measurements.

**TABLE 6-2. Initial and Operational Costs for  
Monitoring Gases in 100 Stacks**

Monitoring Mode	Initial Cost	Man Years Per 100 Stacks	Remarks
Present (in-stack)	1.5 K	8.0	Initial Cost is per instrument
<hr/>			
Active Remote Sensor	20-80 K	0.4	
Passive Remote Sensor	10-40 K	0.4	Limited in concentration and temperature range

\* Velocimeter (50 K) needed for mass flow.

The price for other spectroscopic instruments such as multi-spectral photometers, interferometer-spectrometers, and monochromators can vary widely, depending on the complexity.

### 6.3 MEASUREMENTS OF MASS EMISSION RATES

The signals of the laser Doppler velocimeter (LDV) are not only related to the particle velocity, but also to the opacity of the plume. When the relationship between the opacity and mass loading for each type of source has been established, the LDV will provide the particulate mass emission rate from a source.

### 6.4 UNANNOUNCED AND NON-INTERFERING MONITORING

The requirements to install continuous monitors in new stacks keeping the records and making them available to enforcement personnel does not appear to alleviate the need for "unannounced" enforcement monitoring, including night observations. The remote techniques discussed in this report are the possible tools for this kind of monitoring. In addition, remote techniques do not interfere with the normal operation of the plant, by the requirement of installing temporary in-stack monitors by the enforcement personnel.



## 6.5 SURVEY OF WIDE GEOGRAPHICAL AREAS

Surveys of wide geographical areas are required for the design of contact monitoring networks, assessment of site selection and in the evaluation of environmental degradation.

For the design of contact monitoring networks are based upon extensive measurements of "dispersion meteorology" data. The term "dispersion meteorology" used here refers to the air mass transport, speed and wind direction, frequency distribution, and to the vertical dimension available for dilution of contaminants. In addition, stream-flow or streamline maps are useful in understanding how the air moves from one area to another, and is influenced by the topography. The complexity in the streamline flow patterns is reflected in the convergence and divergence of the streamlines and in the deflection by elevated terrains. As a general rule, experience has shown that complex flow patterns have more turbulent mixing associated with them than do less complex flow patterns.

Based on these results the location of contact monitoring for area sources should be concentrated in areas of convergence. In areas where similar data are not available, remote monitors will be of great assistance in setting up contact networks.

Also the knowledge of point sources in relationship to the "dispersion meteorology" will influence the location of a contact monitor network. The assessment of the impact to be encountered on the site selection of a new industrial/power plant involves a great number of aspects. Beside the aspects of the water and land requirements, the most difficult ones are the requirements for minimum impact on air quality. This involves a preliminary analysis of available meteorological and background air quality data; plume simulation utilizing aerial smoke techniques under a variety of adverse pollution weather conditions; installation of a meteorological and background air quality monitoring system to obtain routinely ambient data and using tracer systems. The releases of tracers are made in various combinations of time periods depending upon the prevailing weather conditions. To follow the trace gases, an extensive sampling network must be established of radial lines and concentric arcs in the downwind sector on ground level and elevated terrain consisting of numerous individual bag samples and sequential samplers. It is obvious that remote monitors mounted in vans/aircraft would be of great assistance in these programs.

## 6.6 RAPID RESPONSE IN POLLUTION EPISODES

The mobility and near real-time analysis of remote sensed data make it possible to monitor the sources and ambient air in pollution episodes, where it is vital to determine early, whether or not the emergency measures are effective.

For example, many local Air Pollution Control Districts have defined alert stages. The ones given in the Los Angeles APCD have been listed in Table 3-5. When any one of these alert stages is readied, the LAAPCD prescribes certain actions that are to be undertaken to prevent further increase of pollutant levels and to effect a decrease in the pollutant levels. The public at large is to be informed about the alert stages by public announcements, and through announcements of the L. A. County Sheriff to its sub-stations, all city police departments and California Highway Patrol as well as local public safety personnel, air polluting industrial plants and processes which require "alert" data in order to effect pre-arranged plans, are designed to reduce the output of air contaminants.

In the LAAPCD, the pollution levels are monitored by twelve (12) widely separated local sampling stations (see Figure 6-1). In addition, inspectors in radio-equipped cars are utilized to spot "excessive visible" emissions and odors. However, they are not equipped to measure the ambient air in real time, and cannot determine, the air pollution levels in alert episodes, when it is of vital importance. Again, remote sensors mounted either in vans or on airborne platforms would fulfill this aspect of monitoring tasks.

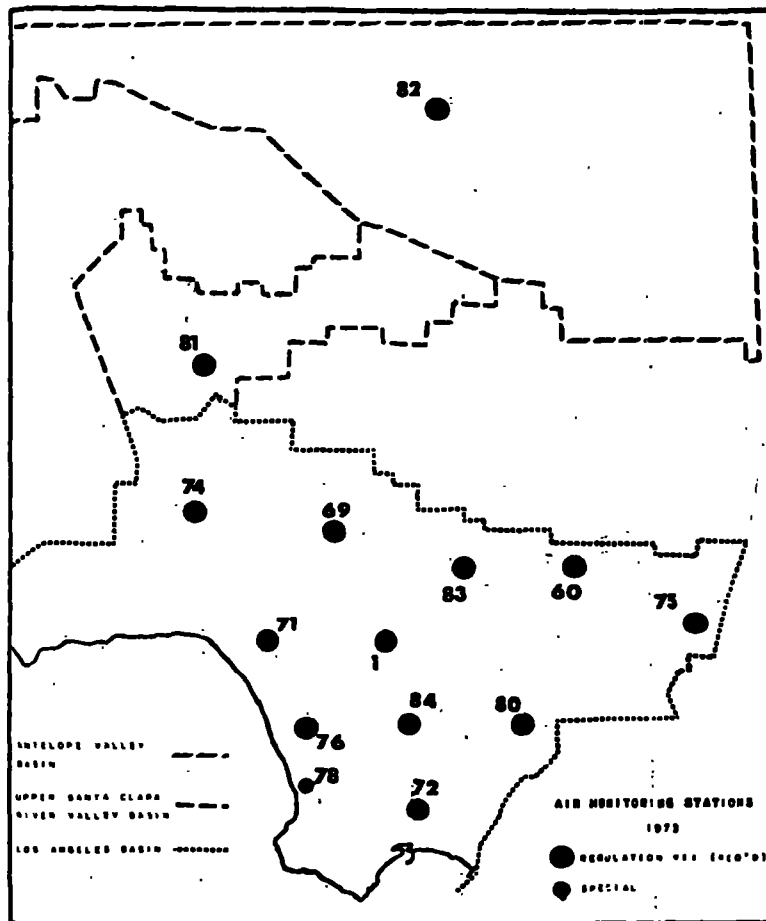


Figure 6-1. Los Angeles County Air Pollution Control District Air Monitoring Network

## 6.7 LIMITATION UNDER CERTAIN ATMOSPHERIC CONDITIONS

Remotely sensed data are influenced by the intervening atmosphere, and extreme conditions such as fog and rain will limit the usefulness of those data. Although in many cases the direct influence is accounted for (for example, by using multiple wavelength detection), the transmission is, in general, reduced, thus reducing the signal levels. In the limit of opaque atmospheres, no signals from the remote source are obtained while extractive and in-situ samples continue to function.

## 6.8 INCREASED REQUIREMENTS IN CALIBRATION

As pointed out in Section 3.4, the calibration procedures for remote monitors are quite different than for point samplers because of the significant influence of the intervening atmosphere and background. Large calibration cells to simulate long atmospheric path must be provided. Test ranges with a calibrated stack emission generator must be provided.

## 6.9 SAFETY HAZARD

The potential health hazard for eye safety has been discussed in Section 5.2. It was pointed out that the most obvious hazard with the laser beam is direct axial viewing, but specular reflections are also a risk, and considerable care must be exercised in the use of laser systems.

The most sensitive region is the visible region, since the cornea, aqueous humor and the lens readily transmit this radiation. Thus, the full laser beam energy is focused on the retina in an image 10-20  $\mu\text{m}$  in diameter resulting in high power densities of kilowatts/cm<sup>2</sup> on the retina even for milliwatt powers incident on the pupil of the eye.

In the spectral regions outside the visible one, the dangers are reduced since the radiation is absorbed by the lens, cornea, and/or aqueous humor. However, inflammation of the cornea and conjunctive can result and cataracts may be formed.

Thus, performance standards for laser products have been promulgated to minimize these hazards. Any operational laser system utilized in remote monitoring must conform to these standards. The analysis made in Section 5.2 showed that the Minimum Safe Range and safe beam diameter for existing laser systems vary widely. While the present laser systems used in the differential absorption by scattering method, in the visible, and the laser Doppler velocimeter method, in the infrared, appear safe, with certain slight modifications, the existing Raman and Lidar systems do not appear safe for operational use in the visible regions.

# 7

## CONCLUSIONS AND RECOMMENDATIONS

### 7.1 GENERAL CONCLUSIONS

Based upon the material presented in the body of this report, the following conclusions are drawn:

Certain remote monitoring techniques can be successfully applied to

- Surveillance and compliance monitoring of smoke-stacks and extended sources;
- Monitoring to support EPA's research studies for the evaluation of control equipment and development of performance standards;
- Surveys of emissions for validation of dispersion models;
- Surveys to determine the representativeness of ambient air point measurements and to assist in developing optimum contact monitoring networks; and
- Quick response in air pollution episodes.

The results of the present survey of the published literature on remote instruments/techniques are summarized in Tables 7-2 and 7-3 for the active and passive systems, respectively. In these tables, only the generic terms of the techniques and/or instruments are given and no specific instruments by manufacturer or model are identified, except for two instruments that are commercially available. The column entitled "Development Status" distinguishes between "commercially available", "advanced prototypes" and "prototypes". The

TABLE 7-1. Pollutant Amenable to Remote Monitoring

IMMEDIATE/NEAR TERM	LONG TERM
Particles (Opacity)*	
SO <sub>2</sub> * NO <sub>2</sub> * CO* Light HC	Heavy HC Oxides of Sulfur Certain Specific Elements Chlorinated HC
HF* HCl NH <sub>3</sub> NO <sub>x</sub> * H <sub>2</sub> S* HNO <sub>3</sub> O <sub>3</sub> Vinyl chloride	
O <sub>2</sub> , N <sub>2</sub> CO <sub>2</sub>	..

\* Standards of Performance for New Stationary Sources  
Proposed or Promulgated

\*\* Species used for determining excess air flow

latter two designations refer to the fact that more "product engineering" has yet to be done before the instruments could be marketed; the "advanced" ones less so that "non-advanced prototypes". Most of them have been field tested. The last column contains also the section or table number(s) where more details are given.

In general, we believe that the active systems appear to have a larger applicability in terms of range in plume temperature and pollutant concentrations. This is because measurements made with passive systems are more influenced by source and background parameters than the active systems. The measurements made by infrared passive systems are particularly dependent upon the plume temperature. Thus, either multiwavelength and/or ratio techniques are required to minimize the temperature dependence. In addition, relatively cool plumes will have lower signal strength. Thus, pollutant measurements in these cool plumes will be more difficult to achieve with passive systems. On the other hand, passive systems tend to be less expensive than active systems, and appear therefore more attractive for the application of surveillance monitoring, where the data are not used in case development. The laser systems that are most

TABLE 7-2. Active Systems

Technique/ Instrument	Spectral Region	Species/ Parameter	Mode	Development Status	Remarks
Differential Absorption	Vis/UV	SO <sub>2</sub> , NO <sub>2</sub> O <sub>3</sub>	Stack/Area	Prototype Field Tested	Ground-based - Present instrumentation as used not eye-safe (Section 4.3.1)
		SO <sub>2</sub> , NO <sub>2</sub> O <sub>3</sub>	Perimeter/ Area	Prototype Field Tested	Has been done for SO <sub>2</sub> (Section 4.3.1)
	IR	Many Gases	Stack	Prototype Under Development	Development is primarily for ambient air (see Table 4-15)
			Perimeter/ Area	Under Development for Aircraft Application	See Table 4-15, at present for ozone
Lidar	Vis	Opacity	Stack	Prototype Field Tested	Not eye safe yet, (Section 4.3.5) eye- safe system being developed
		Particles	Area	Prototype on Air- craft Field Tested	Gives 3-dimensional mapping of relative concentrations (Section 4.5)
Laser Doppler Velocimeter	IR	Velocity	Stack/ Perimeter	Advanced Prototype Field Tested	Necessary for some emission standards (Section 4.3.7 and Table 3-1)
		Mass Flow	Stack	Demonstrated in Field Tests	Relates opacity and mass concentration (Section 4.3.7)
Long-Path	Vis/UV /IR	Many Gases	Area	Several Techniques Field Tested, Some Prototypes Developed; COSPEC Commer- cially Available	Using remote transmitter or retro- reflector; can be laser, dispersive or non-dispersive systems (Table 3-16); useful mainly for ambient air monitoring
Raman	Vis/UV	SO <sub>2</sub>	Stack	Field Tests Not Encouraging	Limited in range, especially during day (Sections 4.3.2 and 5.3.2)
		Many Gases	Stack/ Area	Theoretical	Usefulness limited (Section 4.3.2 and 5.3.2)
Resonance Raman	Vis/UV	Many Gases	Stack/ Area	Laboratory Study	Needs to be demonstrated in field; possible interference due to fluorescence by gases and other species (Section 4.3.3)
Fluorescence	Vis/UV	Many Gases	Stack/ Area	Laboratory Study	Looks doubtful in terms of sensitivity and specificity; (Section 4.3.4)
Fabry-Perot Raman	Vis/UV	Some Gases	Stack/ Area	Laboratory Study	Provides increased sensitivity over vibrational Raman; still limited in range, especially during day (Section 4.3.2)



TABLE 7-3. Passive Systems

Technique/ Instrument	Spectral Region	Species/ Parameter	Mode	Development Status	Remarks
Matched Filter Correlation	UV/Vis	SO <sub>2</sub> , NO <sub>2</sub>	Stack/ Perimeter	COSPEC Commercially Available, Field Tested, Not Encouraging for Stacks; Main Emphasis on Perimeter Monitoring	Quantitative interpretation difficult due to varying aerosols (Section 4.4.2 and 4.5)
Gas Filter Correlation	IR	SO <sub>2</sub>	Stack	JRB Sensor Commercially Available, Being Field Tested	Limited in concentration and tempera- ture range (Section 4.4.3), but tem- perature effect reduced
		CO	Perimeter	Prototype Field Tested	No quantitative data reported as yet (Section 4.5)
		SO <sub>2</sub>	Perimeter	Prototype Under Development	See Table 4-14
Photography	Vis	Opacity	Stack	Being Field Tested on Ground and From Aircraft	Needs further development for quantita- tive analysis; nighttime observations feasible with image intensifier (Section 4.4.1)
Vidicon	UV	SO <sub>2</sub>	Stack	Prototype Field Tested	Quantitative interpretation difficult due to varying aerosols; has potential as a velocimeter (Section 4.4.8)
	IR	SO <sub>2</sub>	Stack	Prototype Field Tested	Independent knowledge of plume tempera- ture required for quantitative analysis; has potential as a velocimeter (Section 4.4.9)
Heterodyne Radiometer	IR	Many Gases	Stack/ Perimeter/ Area	Laboratory Study and Aircraft Based Proto- type Under Develop- ment	Achieves high specificity; has yet to be demonstrated in field (Section 4.4.7)
Dispersive Spectrometer	IR	Many Gases	Stack	Several Techniques Field Tested, Some Prototypes Developed	Includes scanning spectrometer and in- terferometer-spectrometer; requires high spectral resolution for specificity and requires knowledge of plume tem- perature (Section 4.4.4 and 4.4.5)

promising for near-term operational use are differential absorption, Lidar and laser Doppler velocimeter. The most promising passive systems are correlation instruments, vidicons and photographic techniques. Of course, for area surveys, both active and passive systems (ground-based and airborne) have application.

## 7.2 RECOMMENDATIONS

Based upon the general conclusions and, in particular, upon Table 7-2 and 7-3, we recommend that EPA continues, initiates and/or participates in the development of several instruments discussed below. Many agencies, in particular NASA, have been involved in the development of remote sensing techniques for air pollutants. It would appear cost-effective for EPA to coordinate (as is already done in some developments), its research programs with these agencies.

### Laser Doppler Velocimeter

- Stack Emission Monitoring
  - Make system operational in a van, together with the DAS system
  - Make it available to field enforcement personnel
  - Continue the development of the LDV system to relate its output to opacity, and to mass flow.

### Lidar

- Stack Emission Monitoring
  - Make the lidar system operational in a van for the measurement of opacity;
  - Make it available to field enforcement personnel.
- Perimeter and Area Monitoring
  - Adapt lidar to airborne operations for the measurement of mixing height, dispersion of plumes and air quality assessment over wide geographical areas.

## Differential Absorption

- Stack Emission Monitoring
  - Make the DAS system operational in a van for the measurement of SO<sub>2</sub> and NO<sub>2</sub>;
  - Make it available for field enforcement personnel;
  - Develop the DAS system for the measurement of other species, using the infrared spectrum.
- Perimeter and Area Monitoring
  - Continue to develop the DAS system to airborne operation to measure O<sub>3</sub> between the aircraft and the ground for air quality assessment over wide areas;
  - Initiate the development of the DAS system for van and aircraft based operations to measure all gases for perimeter and area monitoring.

## Correlation Techniques

- Stack Emission Monitoring
  - Continue the field testing of the passive GFC instrument for the measurement of SO<sub>2</sub> and make it available to field enforcement personnel;
  - Extend the techniques to other species, such as NO<sub>2</sub>, CO, HCl, and light hydrocarbons.
- Perimeter and Area Monitoring
  - Make available to field enforcement personnel the passive MFC instrument, van based, for SO<sub>2</sub> and NO<sub>2</sub>;
  - Develop the correlation techniques in the IR for SO<sub>2</sub> and other pollutants, van based.

### Vidicons

- Stack Emission Monitoring
  - Make vidicon system for SO<sub>2</sub> operational;
  - Make it available to field enforcement personnel;
  - Develop system to NO<sub>2</sub> in the UV;
  - Investigate possibility further to use vidicon as velocimeter.

### Photographic Techniques

- Stack Emission Monitoring
  - Develop aircraft based photographic techniques for daytime opacity measurements.

### Long-Path Systems

- Perimeter/Area/Ambient Air Monitors
  - Continue to develop laser systems;
  - Continue to develop non-dispersive techniques.

### Resonance Raman

- Conduct field tests to verify feasibility of resonance Raman technique to measure SO<sub>2</sub> in stack emissions.

### Heterodyne Radiometry

- Continue the development of passive/active heterodyne radiometry for measuring gaseous pollutants in smoke-stack plumes.

Based on the specifications which EPA have proposed or promulgated for continuous in-stack and ambient air monitors, we recommend that performance specifications for remote monitors be developed as more experience is gained in the field with existing monitors.

The important instrument parameters specified by EPA for continuous in-stack and ambient air monitors, which will also apply to remote techniques when used in enforcement monitoring, include:

- Span (lower detectable limit to upper level which must be than the emission standard by a given factor)
- Noise (usually 0.5 of the lower detectable limits)
- Accuracy (percentage difference between values measured by the sensor and the applicable reference method)
- Calibration error (absolute mean value plus 95 percent confidence interval)
- Zero and calibration drift (absolute mean value plus 95 percent confidence interval)
- Response time (rise and fall time to 95 percent)
- Interference equivalent (influence on pollutant signal by interfering gases in plume)

Additional parameters that will have to be specified for remote techniques will include, but may not be limited to the following:

- Range (minimum and maximum distance between source and observer, in which the instrument must give data with the specified accuracy)
- Field-of-view (should be small enough for the source plume to fill the fov)
- Interference equivalent (influence on pollutant signal by the intervening atmosphere as well as sky radiation beyond the plume)
- Supporting plume data (velocity, temperature, etc.)

**The information recorded during field observations should include those given in Method 9 for the visual observation:**

- **Time**
- **Observer location (distance, direction, height)**
- **Background description**
- **Weather conditions (wind direction and speed, ambient temperature)**
- **Sky conditions**
- **Plume description (if visible)**

# 8

## REFERENCES

- Ahmed, S. A. (1973) Appl. Opt. 12, 901.
- Allerio, F. (1976) private communication.
- Acton, L. L. et al. (1973) AIAA J. 11, 899
- Asai, K. and Igarashi, T. (1974) Preprint, private communication.
- AWST (Aviation Week and Space Technology) (1975) February 3.
- Barnes, H. M., Herget, W. F. and Robbins, R. (1974) "Analytical Methods Applied to Air Pollution Measurements", p. 245, Ann Arbor Science Publishers, Inc., August.
- Barrett, J. J. (1974) "Laser Raman Gas Diagnostics", Ed. M. Lapp and C. M. Penney, Plenum Press, New York.
- Barringer, A. R. et al. (1966) 4th Symposium on Remote Sensing, Ann Arbor.
- Bartle, E. R. et al., (1972) J. Spacecraft and Rockets 11, 836.
- Bartle, E. R. (1974a) EPA Contract 68-02-1208, JRB Assoc. Inc., La Jolla, CA, April.
- Bartle, E. R. (1974b) EPA Contract 68-02-1481, Final Report, October.
- Bartle, E. R. (1975) private communication.
- Baumgartner, R., Warshaw, S., Wolfe, D. and Byer, R. L. (1976) Mtg. Abstract, J. Opt. Soc. Am. 66, 386.
- Byer, R. L. (1975) Optical and Quantum Electr. 7, 147.
- Byer, R. L. and Garbuny, M. (1973) Appl. Opt. 12, 1497.

- Chen, S. H. , Lin, C. C. and Low, M. J. D. (1974) Environ, Sci. and Techn. 7, 424.
- Collis, R. T. H. and Uthe, E. E. (1972) Opto-electronics 4, 87.
- Conner, W. (1974) EPA-650/2-74-128.
- Conner, W. (1975) EPA, private communication.
- Conner, W. (1976) EPA, private communication.
- Conner, W. D. and Hodgkinson, J. R. (1967) P. H. S. Publ. 999-AP-30.
- Cook, C. S. , Bethke, G. W. and Conner, W. D. (1972) Appl. Opt. 11, 1742.
- Decker, J. A. , Jr. (1971) Appl. Opt. 10, 510.
- Derr, V. E. , and Little, C. G. (1970) Appl. Opt. 9, 1976.
- DHEW (1974) 39 FR 32094.
- DHEW (1975) 40 FR 32257.
- DeLong, H. P. (1974) Opt. Eng. 13, 5.
- Ellison, A. H. (1974) EPA-650/2-74-015.
- Elterman, L. (1966) Appl. Opt. 5, 1769.
- Elterman, L. (1968) AFCRL-68-0153, April.
- Emission Monitoring Requirements and Performance Testing Methods (1974) 39 FR 32852.
- Exton, R. (1974) NASA-Langley, private communication.
- Evans, W. E. (1967) "Development of Lidar for Stack Effluents Opacity Measurements" SRI Project No. 6529 for Edison Electric Inst. (NTIS PB No. 233-135/AS)
- Fowler, M. C. and Berger, P. J. (1974) EPA Report No. EPA-650/2-74-020, January.



- Gelbwachs, J. A., Birnbarm, M., Tucker, A. W. and Finder, C. L. (1972) *Opto-electronics* 4, 155.
- Gelbwachs, J. A. and Birnbarm, M. (1973) *Appl. Opt.* 12, 2442.
- Granatstein, V. L., Rhinewine, M. and Fitch, A. H. (1973) *Appl. Opt.* 12, 1511.
- Grant, W. B., Hake, R. D., Jr., Liston, E. M., Robbins, R. C. and Proctor, E. K., Jr. (1974) *Appl. Phys. Lett.* 24, 550.
- Grant, W. B. and Hake, R. D., Jr. (1975) *J. Appl. Phys.* 46, 3019.
- Griggs, M. (1975) "Measurements of Atmospheric Aerosol Optical Thickness over Water Using ERTS-1 Data, J. Air Poll. Control Assoc. 25, 622.
- Herget, W. F. (1976) EPA, private communication
- Herget, W. F., Miller, C. R., and Sonnenschein, C. M. (1975) Paper WA7, Spring Conf. OSA, Anaheim, CA, March 19-21.
- Hess, R. V. and Seals, R. K., Jr. (1974) "Applications of Tunable High Energy/Pressure Pulsed Lasers to Atmospheric Transmission and Remote Sensing", NASA TM X-72010.
- Hinkley, E. D. (1972) *Opto-electronics* 4, 69.
- Hinkley, E. D. and Calawa, A. R. (1974) "Analytical Methods Applied to Air Pollution Measurements", Ed. R. K. Stevens and W. F. Herget, Ann Arbor Science Publishers, Inc.
- Hirschfeld, T. B. (1974) *Opt. Eng.* 13, 15.
- Hoell, J. M., Jr., Wade, W. R. and Thompson, R. T., Jr. (1975) Int. Conf. on Environ. Sensing and Assessment, Las Vegas, Nevada, Sept. 14-19.
- Hoffman, A. J., Curran, T. C., McMullen, T. B., Cox, W. M. and Hunt, W. F., Jr. (1975) "EPA's Role in Ambient Air Quality Monitoring", *Science* 190, 243.
- Hulburt, E. O. (1946) *J. Opt. Soc. Am.* 27, 377.

Igarashi, T. (1973) 5th Conference on Laser Radar Studies, Williamsburg, Virginia, June.

Inaba, H. and Kobayasi, T. (1972) Opto-electronics 4, 101.

Inomata, H. and Igarashi, T. (1974) Radio Research Laboratories, Tokyo, Preprint, private communication.

Keyes, R. J. and Quist, T. M. (1970) "Semiconductors and Semimetals", Eds. R. K. Willardson and A. C. Beer (Academic Press, New York, Chapter 8).

Kildal, H. and Byer, R. L. (1971) Proc. IEEE 59, 1644.

Klainer, S. M. (1974) SPIE Meeting, San Diego, August.

Kobayasi, T. and Inaba, H. (1975) Optical and Quantum Electronics 7, 319.

Koehler, T. (1974) Electro-Opt. Systems Design, page 24, October.

Ku, R. T., Hinkley, E. D. and Sample, J. O. (1975) Appl. Opt. 14, 854.

Kuhl, J. and Schmidt, W. (1974) Appl. Phys. 3, 251.

Langan, L. (1971a) AIAA Meeting, Palo Alto, November.

Langan, L. (1971b) Environmental Measurement Inc., San Francisco, Report EPA Contract No. 6H-02-0124.

Larson, N. M., Crosmun, R., and Talmi, Y. (1974) Appl. Opt. 13, 2662.

Lawrence, T. R., Krause, M. C., Craven, C. E. and Herget, W. F. (1975) AIAA Mtg. Paper 75-684, May.

Low, M. J. D. and Clancy, F. K. (1967) Environ. Sci. and Techn. 1, 73.

Ludwig, C. B., Griggs, M., Malkmus, W. and Bartle, E. R. (1974) Appl. Opt. 13, 1494.

Measures, R. M. and Pilon, G. (1972) Opto-electronics 4, 141.

Menzies, R. T. (1971) Appl. Opt. 10, 1532.

- Menzies, R. T. and Shumate, M. S. (1974) Science 184, 570.
- Melfi, S. H., Brumfield, M. L. and Storey, R. W., Jr., (1973) Appl. Phys. Lett. 22, 402.
- Melfi, S. H. (1974) EPA, Las Vegas, private communication.
- Miller, C. R. and Sonnenschein, C. M. (1975) Contractor Report EPA-650/2-75-062.
- Murray, E. R., Hake, R. D., Jr., van der Laan, J. E. and Hawley, J. G. (1976) Appl. Phys. Lett., May.
- Nader, J. (1975) EPA-Research Triangle Park, private communication.
- Nakahara, S. et al. (1972), Opto-electr. 4, 169-177
- Nakahara, S., Ito, K., and Ito, S. (1973) Abstract from 5th Conference on Laser Radar Studies, Williamsburg, Virginia, June.
- Newcomb, G. S. and Millan, M. M. (1970) IEEE Trans. Geosci. Electronics GE-8, 149.
- Northam, G. B. (1976) NASA, Langley Research Center, private communication.
- Pikus, I. M., Goldstein, H. W. and Reithof, T. R. (1971) AIAA Meeting, Palo Alto, November.
- Penney, C. M., Morey, W. W., St. Peters, R. L., Silverstein, S. D., Lapp, M., and White, D. R. (1973) NASA CR-132363, September.
- Poultney, S.K., Brumfield, M.L. and Siviter, J.H. (1975), 7th Intern. Laser Radar Conf., SRI, Nov. 4-7
- Prengle, H. W., Jr., Morgan, C. A., Fang, Cheng-Shen, Huang, Ling-Kim, Campani, P., and Wu, W. W. (1973) Environ. Sci. and Techn. 7, 417.
- Pressman, A. (1976) EPA-Las Vegas, private communication.
- Prostak, A. and Dye, R. H. (1970) Bendix Final Report, Contract CPA 22-69-55, October.

- Robinson, J. W. and Dake, J. D. (1973) Spectr. Lett. 6, 685.
- Robinson, J. W. and Dake, J. D. (1974) Anal. Chem. Acta. 71, 277.
- Rosen, H., Robrish, P. and Chamberlain, O. (1975) Appl. Opt. 14, 2703.
- Ross, R. D. (1972) Air Pollution and Industry, Van Norstrand Reinhold Co., New York.
- Rothe, K. W., Brinkmann, U. and Walther, H. (1974a) Appl. Phys. 3, 115.
- Rothe, K. W., Brinkmann, U. and Walther, H. (1974b) Appl. Phys. 4, 181.
- Saraf, D. G. and Jackson, D. W. (1975) 7th Int. Laser Radar Conf., Menlo Park.
- Schotland, R. M. (1974) J. Appl. Meteorol. 13, 71.
- Science Applications, Inc. (1975) EPA Contract 68-02-1798.
- Seals, R. K., Jr., "Analysis of Tunable Laser Heterodyne Radiometry: Remote Sensing of Atmospheric Gases", AIAA J. 12, 1118.
- Smith, W. (1972) Opto-electronics 4, 161.
- Smith, H. (1975) EPA, private communication.
- Sperling, R. B. (1975) Contractor Report EPA-600/2-75-077.
- Streiff, M. L. and Claysmith, C. L. (1972) Contractor Report EPA-R2-72-052.
- Streiff, M. L. and Ludwig C. B. (1973) Contractor Report EPA-650/2-73-026.
- Swift, R. D. and Wattson, R. B. (1974) 9th Rem. Sens. Symp. Abstracts, Ann Arbor, April.
- Tanabe, L. H. (1975) "Determination of SO<sub>2</sub> Concentrations by Remote Sensing in the Infrared", General Dynamics/Pomona Report No. TM/6-125PH-430 on EPA Contract 68-02-1804.
- Ward, T. V. and Zwick, H. H. (1975) Appl. Opt. 14, 2896.
- Zaromb, S. (1974) Pittsburg Conference, Cleveland, March.

<b>TECHNICAL REPORT DATA</b> <i>(Please read Instructions on the reverse before completing)</i>		
1. REPORT NO. <b>EPA 340/1-76-005</b>	2.	3. RECIPIENT'S ACCESSION NO.
4. TITLE AND SUBTITLE <b>Application of Remote Techniques in Stationary Source Air Emission Monitoring</b>		5. REPORT DATE <b>June 1976</b>
		6. PERFORMING ORGANIZATION CODE
7. AUTHOR(S) <b>C. B. Ludwig and M. Griggs</b>		8. PERFORMING ORGANIZATION REPORT NO. <b>SAI-76-687-LJ</b>
9. PERFORMING ORGANIZATION NAME AND ADDRESS <b>Science Applications, Inc. P. O. Box 2351 La Jolla, California 92038</b>		10. PROGRAM ELEMENT NO.
		11. CONTRACT/GRANT NO. <b>68-03-2137</b>
12. SPONSORING AGENCY NAME AND ADDRESS <b>Environmental Protection Agency Stationary Source Enforcement 401 M Street, S. W., Washington, D. C. 20460</b>		13. TYPE OF REPORT AND PERIOD COVERED
		14. SPONSORING AGENCY CODE
15. SUPPLEMENTARY NOTES  replaces EPA 340/1 - 75- 009		
16. ABSTRACT  The usefulness of remote sensing techniques for monitoring the gaseous and particulate emissions from stationary sources is analyzed. The present status of active and passive remote monitoring instruments is evaluated. This study confirms that the technique of differential absorption has the best sensitivity for the single-ended measurement of gaseous and particulate pollutants. In general, data interpretation problems of the passive techniques make them less accurate than the active methods.		
17. KEY WORDS AND DOCUMENT ANALYSIS		
a. DESCRIPTORS	b. IDENTIFIERS/OPEN ENDED TERMS	c. COSATI Field/Group
<b>Air Pollution Observations</b>	<b>Remote Monitoring</b>	<b>13B 14D</b>
18. DISTRIBUTION STATEMENT  <b>Unlimited</b>	19. SECURITY CLASS (This Report) <b>Unclassified</b>	21. NO. OF PAGES <b>178</b>
	20. SECURITY CLASS (This page) <b>Unclassified</b>	22. PRICE

## INSTRUCTIONS

1. **REPORT NUMBER**  
Insert the EPA report number as it appears on the cover of the publication.
2. **LEAVE BLANK**
3. **RECIPIENTS ACCESSION NUMBER**  
Reserved for use by each report recipient.
4. **TITLE AND SUBTITLE**  
Title should indicate clearly and briefly the subject coverage of the report, and be displayed prominently. Set subtitle, if used, in smaller type or otherwise subordinate it to main title. When a report is prepared in more than one volume, repeat the primary title, add volume number and include subtitle for the specific title.
5. **REPORT DATE**  
Each report shall carry a date indicating at least month and year. Indicate the basis on which it was selected (*e.g., date of issue, date of approval, date of preparation, etc.*).
6. **PERFORMING ORGANIZATION CODE**  
Leave blank.
7. **AUTHOR(S)**  
Give name(s) in conventional order (*John R. Doe, J. Robert Doe, etc.*). List author's affiliation if it differs from the performing organization.
8. **PERFORMING ORGANIZATION REPORT NUMBER**  
Insert if performing organization wishes to assign this number.
9. **PERFORMING ORGANIZATION NAME AND ADDRESS**  
Give name, street, city, state, and ZIP code. List no more than two levels of an organizational hierarchy.
10. **PROGRAM ELEMENT NUMBER**  
Use the program element number under which the report was prepared. Subordinate numbers may be included in parentheses.
11. **CONTRACT/GRANT NUMBER**  
Insert contract or grant number under which report was prepared.
12. **SPONSORING AGENCY NAME AND ADDRESS**  
Include ZIP code.
13. **TYPE OF REPORT AND PERIOD COVERED**  
Indicate interim final, etc., and if applicable, dates covered.
14. **SPONSORING AGENCY CODE**  
Leave blank.
15. **SUPPLEMENTARY NOTES**  
Enter information not included elsewhere but useful, such as: Prepared in cooperation with, Translation of, Presented at conference of, To be published in, Supersedes, Supplements, etc.
16. **ABSTRACT**  
Include a brief (*200 words or less*) factual summary of the most significant information contained in the report. If the report contains a significant bibliography or literature survey, mention it here.
17. **KEY WORDS AND DOCUMENT ANALYSIS**
  - (a) **DESCRIPTORS** - Select from the Thesaurus of Engineering and Scientific Terms the proper authorized terms that identify the major concept of the research and are sufficiently specific and precise to be used as index entries for cataloging.
  - (b) **IDENTIFIERS AND OPEN-ENDED TERMS** - Use identifiers for project names, code names, equipment designators, etc. Use open-ended terms written in descriptor form for those subjects for which no descriptor exists.
  - (c) **COSATI FIELD GROUP** - Field and group assignments are to be taken from the 1965 COSATI Subject Category List. Since the majority of documents are multidisciplinary in nature, the Primary Field/Group assignment(s) will be specific discipline, area of human endeavor, or type of physical object. The application(s) will be cross-referenced with secondary Field/Group assignments that will follow the primary posting(s).
18. **DISTRIBUTION STATEMENT**  
Denote releasability to the public or limitation for reasons other than security for example "Release Unlimited." Cite any availability to the public, with address and price.
19. & 20. **SECURITY CLASSIFICATION**  
DO NOT submit classified reports to the National Technical Information service.
21. **NUMBER OF PAGES**  
Insert the total number of pages, including this one and unnumbered pages, but exclude distribution list, if any.
22. **PRICE**  
Insert the price set by the National Technical Information Service or the Government Printing Office, if known.